

ANL-95/43

ARGONNE NATIONAL LABORATORY
9700 South Cass Avenue
Argonne, IL 60439

SEPARATION SCIENCE AND TECHNOLOGY
SEMIANNUAL PROGRESS REPORT

April–September 1993

by

G. F. Vandegrift, D. B. Chamberlain, C. Conner, J. M. Copple,
K. Foltz,* B. Gebby,† J. C. Hutter, R. A. Leonard, L. Nuñez, M. C. Regalbuto,
A. Rozeveld, J. Sedlet, B. Srinivasan, D. Taylor, and D. G. Wygmans

Chemical Technology Division

January 1996

Previous Reports in this Series

October 1992–March 1993 ANL-95/4
April 1992–September 1992 ANL-94/29
October 1991–March 1992 ANL-93/38
April 1991–September 1991 ANL-93/21

DISTRIBUTION OF THIS DOCUMENT IS UNLIMITED

MASTER

* University of Illinois, Champaign-Urbana, IL.

† Ohio State University, Columbus, OH.

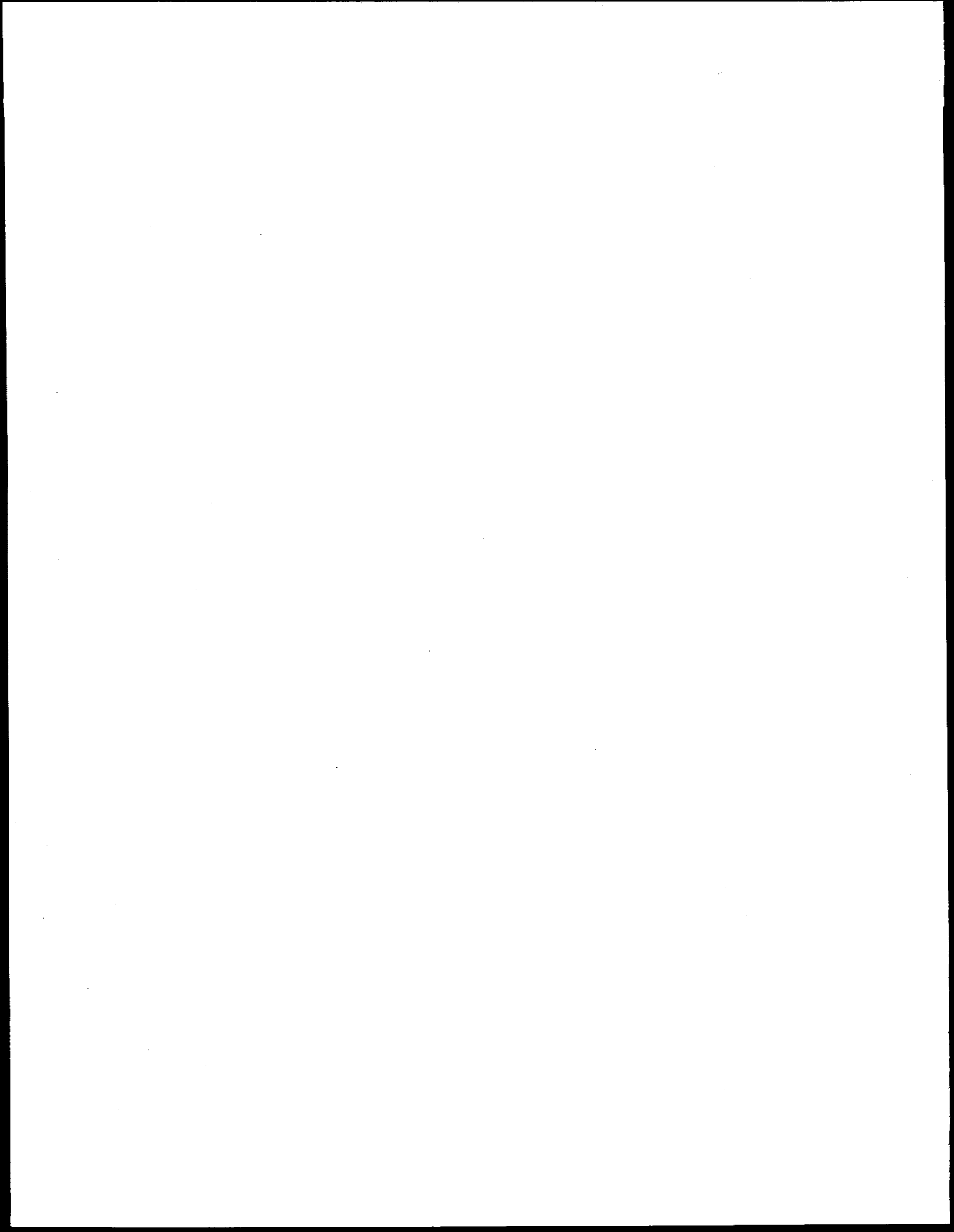


TABLE OF CONTENTS

	<u>Page</u>
ABSTRACT.....	1
SUMMARY.....	1
I. INTRODUCTION	4
II. THE GENERIC TRUEX MODEL.....	5
A. Summary of Recent Improvements.....	5
B. Development of Loading Module.....	6
1. Algorithm for CMPO-TBP Loading.....	7
2. Material Balance Equations	9
3. Solution Method.....	12
4. Excel Implementation	16
C. Use of GTM to Calculate Effects of Batch Contacts	17
1. Clean Aqueous-Phase Contacts	18
2. Clean Organic-Phase Contacts.....	20
3. Combination Contacts.....	21
D. Modeling Studies of Zr and F Behavior.....	31
E. Database Enhancement	32
1. Reductive Stripping of Plutonium.....	32
2. Behavior of Bismuth.....	34
III. CENTRIFUGAL CONTACTOR DEVELOPMENT.....	36
A. Combined TRUEX-SREX Processing.....	36
B. Solvent Properties	36
1. Density and Viscosity	37
2. Dispersion Number	37
3. Hydraulic Tests	40
4. Stokes Law Extension to the Dispersion Number	41
5. Maximum Throughput for PS12 Solvent.....	42

TABLE OF CONTENTS (contd)

	<u>Page</u>
C. TRUEX Processing of Mark 42 Targets.....	43
1. Flowsheet Development.....	44
2. Flowsheet Implementation.....	50
D. Construction of Minicontactors	50
IV. VERIFICATION TESTS WITH PLUTONIUM-BEARING WASTES.....	51
A. Batch 2	51
B. Batch 3	51
1. Flowsheet Development.....	52
2. Solvent Cleanup	54
3. Description of Batch 3	55
4. Batch Tests.....	56
5. Processing of Batch 3.....	57
6. Analysis of Samples Collected during Processing of Batch 3.....	57
C. Batch 4	66
V. ADVANCED EVAPORATOR TECHNOLOGY	68
A. Laboratory-Scale Evaporator	68
1. Data Acquisition System.....	68
2. Other Modifications	72
3. Demonstration Runs.....	72
B. Evaporator/Concentrator Upgrade	73
1. Evaporator Design and Procurement	73
2. Concentrator Design and Purchase	73
3. Equipment Layout.....	75
C. Transportable Evaporator Program.....	75
VI. SUPPORT TO ARGONNE'S WASTE MANAGEMENT OPERATIONS.....	78
A. Laboratory Experiments.....	78
1. Davies-Grey Waste Solutions	78

DISCLAIMER

Portions of this document may be illegible in electronic image products. Images are produced from the best available original document.

TABLE OF CONTENTS (contd)

	<u>Page</u>
2. Simulated Waste Solutions of RCRA Metals	80
3. Simulated Waste Solutions of Sodium Dichromate.....	91
4. Scintillation Cocktail.....	95
 B. Equipment for Alkaline Sulfide Precipitation.....	 96
1. Treatment Hood	96
2. Treatment Vessel.....	96
3. Mixing.....	96
4. Process Control	96
5. High Temperature Shutdown.....	98
6. Transfer Pump.....	98
 C. Development of Filter Skid.....	 98
 D. Regulatory Permits.....	 101
 E. Cesium Removal from Wastewater	 102
1. Resin Studies.....	102
2. Setup of Resin Column	105
 VII. MAGNETICALLY ASSISTED CHEMICAL SEPARATIONS	 108
A. Particle Morphology	108
B. Particle Coating Process.....	110
C. Transuranic and Cesium Separation Capabilities	110
D. Gamma-Irradiation Studies.....	111
 VIII. MOLYBDENUM-99 TARGET PROCESSING.....	 113
A. The Cintichem Process.....	113
B. Use of Uranium Metal Foil or Uranium Silicide Fuels.....	115
 REFERENCES.....	 117

LIST OF FIGURES

<u>No.</u>	<u>Title</u>	<u>Page</u>
1.	Batch Contacts with Clean Organic Phases	17
2.	Batch Contacts with Clean Aqueous Phases.....	17
3.	Solvent Extraction Process.....	18
4.	Export File Corresponding to Fig. 2, Batch Contacts with Clean Aqueous Phases	19
5.	Setup for Multiple Runs with Clean Organic Phase	20
6.	Setup to Create a Similar Export File Corresponding to Fig. 5	21
7.	Export File Corresponding to Fig. 6	22
8.	Export File in Fig. 7 Modified to Simulate the Flowsheet Given in Fig. 6	23
9.	Flowsheet for the Series of Contacts Given in Table 2.....	25
10.	Flowsheet Modified to Create a Similar Export File Corresponding to Fig. 9.....	26
11.	Export File Corresponding to Fig. 10	27
12.	Modified Export File Simulating the Flowsheet Given in Fig. 9.....	28
13.	Stage-to-Stage Profile for All Components in Batch Contact Flowsheet.....	29
14.	Distribution Ratios for Pu(III) and Am(III) between Nitric Acid and TRUEX/NPH as Function of Acid Concentration	34
15.	Distribution Ratios for Bismuth as a Function of Nitric Acid Concentration at 25°C.....	35
16.	Effect of O/A Ratio, Solvent Batch, Dispersed Phase, and Aqueous Phase Composition on Dispersion Number, $N(D_i)$, for PS12.....	37
17.	Effect of O/A Ratio, Solvent Batch, and Aqueous Phase Composition on Amount of A in O for Aqueous-Dispersed Operation Using PS12	38
18.	Effect of Temperature, Dispersed Phase, and Aqueous Phase Composition on N_{D_i} for PS12 at O/A Ratio of 1.0	39

LIST OF FIGURES (contd)

<u>No.</u>	<u>Title</u>	<u>Page</u>
19.	Effect of Temperature and Aqueous Phase Composition on A in O for Aqueous-Dispersed Operation Using PS12 with O/A Ratio of 1.0.....	39
20.	TRUEX-SREX Flowsheet for Cold Tests	40
21.	TRUEX Flowsheet Calculated for Mark 42 Targets	44
22.	Proposed Flowsheet for Processing Batch 3.....	54
23.	Total Alpha Activity in the NonTRU Raffinate (DW).....	59
24.	Concentration of Americium and Plutonium in the NonTRU Raffinate (DW) during the Initial Startup.....	59
25.	Concentration of Americium and Plutonium in the NonTRU Raffinate (DW) during the Second Startup.....	59
26.	Concentration of Americium and Plutonium in the Americium Product (EW).....	60
27.	Americium Split in the Americium Product (EW).....	61
28.	Concentration of Americium and Plutonium in the Plutonium Product (FW).....	61
29.	Summary of Batch 3 Processing.....	65
30.	Schematic of C-3 Laboratory-Scale Evaporator Showing Sensors and Sample Points	69
31.	Flow Diagram of an Artisan Rototherm	74
32.	Piping Schematic for the Low-Level Waste Evaporators and Concentrator	75
33.	Floor Plan Showing Evaporator and Concentrator Locations	76
34.	Schematic of a Transportable Evaporator System.....	76
35.	Calibration of Sulfide Electrode at pH of 13.2.....	83
36.	Stability of Sulfide Calibration Standards as Function of Time.....	84
37.	Calibration of Sulfide Electrode in pH Range of 10 to 13 for Sulfide Solutions at Two Concentrations.....	85

LIST OF FIGURES (contd)

<u>No.</u>	<u>Title</u>	<u>Page</u>
38.	Treatment of <u>4M</u> Nitric Acid Using 10% Calcium Hydroxide Slurry and <u>1.9M</u> Sodium Sulfide Solution.....	87
39.	Treatment of <u>1M</u> Copper Sulfate in <u>4M</u> Hydrochloric Acid Using 10% Calcium Hydroxide Slurry and <u>1.9M</u> Sodium Sulfide Solution.....	88
40.	Treatment of <u>0.1M</u> Solution Containing RCRA Metals (Cd, Pb, Hg, and Ag) in <u>4M</u> Nitric Acid by 10% Calcium Hydroxide Slurry and <u>1.9M</u> Sodium Sulfide Solution.....	90
41.	Equipment for Alkaline Sulfide Precipitation.....	97
42.	Piping and Instrumentation Diagram for Filtration Skid	99
43.	Results from Analysis of Column Effluent Using DOWEX AG 50W-X8 Resin	104
44.	Schematic of Ion-Exchange Vessel.....	106
45.	Transmission Electron Micrographs of Bright Field Image of Polyacrolein/Magnetite Particles, Magnetite-Encapsulated Particles, and Charcoal-Cross-Linked N,N,Methylene Bis-acrylamide with Irregular Polymer Shape and Magnetite Particles	109
46.	Dependence of Partition Coefficients for ²⁴¹ Am and ²³⁸ Pu on Nitric Acid Concentration.....	111
47.	Schematic of Cintichem Target.....	114
48.	Schematic Drawing of the Dissolver Flask.....	116

LIST OF TABLES

<u>No.</u>	<u>Title</u>	<u>Page</u>
1.	Equations Needed to Calculate the Jacobian for the Newton-Raphson Method	15
2.	Summary of Contacts Performed to Test the Solvent Extraction Flowsheet (Fig. 9).....	24
3.	Rate of Reduction of Pu(IV) to Pu(III) with Ascorbic Acid and Hydroxylamine.....	32
4.	Distribution Ratios for Pu(III) and Am(III) as a Function of Nitric Acid Concentration.....	33
5.	Distribution Ratios for Bismuth as a Function of Nitric Acid Concentration at 25°C.....	35
6.	Results of Hydraulic Performance Tests in Single-Stage 2-cm Contactor	40
7.	Maximum Throughput for PS12 and 0.1M HNO ₃ in Minicontactor.....	43
8.	Calculated Concentrations of Various Feed and Effluent Streams.....	45
9.	Results from GTM Trials for Developing the Batch 3 Flowsheets	53
10.	Check of Purity for New TRUEX Solvent.....	54
11.	Composition of Batch 3 Waste Pails according to ANL Waste Requisitions	55
12.	Feed Composition Determined by ICP/AES and Anion Chromatography for Batch 3.....	56
13.	Extraction Distribution Ratios from Batch Contacts with a Feed Sample.....	56
14.	Activity Levels in the NonTRU Raffinate (DW).....	58
15.	Activity Levels in the Americium Product (EW)	60
16.	Activity Levels in the Plutonium Product (FW).....	62
17.	Activity Levels in the First Carbonate Wash Feed Samples (GF).....	62
18.	Activity Levels in the Second Carbonate Wash Feed Samples (HF)	63
19.	Activity Levels in Acid Rinse (IF).....	63

LIST OF TABLES (contd)

<u>No.</u>	<u>Title</u>	<u>Page</u>
20.	Activity Levels in the Organic Product (HP).....	64
21.	Activity Levels in the Alumina Column Product (BC).....	64
22.	Activity Levels in the Organic Feed (DX).....	65
23.	Composition of the Batch 4 Waste Pails according to ANL Waste Requisitions	66
24.	Feed Composition Determined by ICP/AES and Anion Chromatography for Batch 4.....	67
25.	Measurements of pH and Concentrations of Cr, Fe, Mo, V, and U in the Davies-Grey Waste Solution and in the Filtrate after Neutralization and Hydroxide Precipitation of the Waste Solution.....	80
26.	Limits for RCRA Metals in Toxicity Characteristic Leaching Procedure.....	81
27.	Filtrate Concentration and TCLP Limits for Metals.....	90
28.	Calibration Data to Adjust Sulfide Set Points.....	98
29.	Activity of Radiochemical Analysis of SWT and HLWV Samples	102
30.	Concentration of the Cations in Water Samples	102
31.	Measured Distribution Ratios for ¹³⁷ Cs with General-Purpose Ion-Exchange Resins.....	103
32.	Batch Distribution Ratios for Cesium-Specific Resins.....	104
33.	Results of Pressure-Drop Test on Resin Bed	107
34.	Partition Coefficient Dependence on Ethanol Volume, Initial Temperature, and Particle Separation Time	110
35.	Composition of Simulated Tank Supernatant for Cesium Removal.....	111
36.	Irradiations of Magnetic Microparticles	112
37.	Characteristics of Cintichem Fuel Element	113
38.	Material Balance for Dissolution of UO ₂ Reported for Cintichem Process	114

SEPARATION SCIENCE AND TECHNOLOGY
SEMIANNUAL PROGRESS REPORT

April-September 1993

ABSTRACT

This document reports on the work done by the Separations Science and Technology Programs of the Chemical Technology Division, Argonne National Laboratory, in the period April-September 1993. This effort is mainly concerned with developing the TRUEX process for removing and concentrating actinides from acidic waste streams contaminated with transuranic (TRU) elements. The objectives of TRUEX processing are to recover valuable TRU elements and to lower disposal costs for the nonTRU waste product of the process. Other projects are underway with the objective of developing (1) evaporation technology for concentrating radioactive waste and product streams such as those generated by the TRUEX process, (2) treatment schemes for liquid wastes stored or being generated at Argonne, (3) a process based on sorbing modified TRUEX solvent on magnetic beads to be used for separation of contaminants from radioactive and hazardous waste streams, and (4) a process that uses low-enriched uranium targets for production of ^{99}Mo for nuclear medicine uses.

SUMMARY

The Division's work in separation science and technology is mainly concerned with developing a technology base for the TRUEX (TRAnsUranic EXtraction) solvent extraction process. The TRUEX process extracts, separates, and recovers TRU elements from solutions containing a wide range of nitric acid and nitrate salt concentrations. The extractant found most satisfactory for the TRUEX process is octyl(phenyl)-N,N-diisobutylcarbamoylmethylphosphine oxide, which is abbreviated CMPO. This extractant is combined with tributyl phosphate and a diluent to formulate the TRUEX process solvent. The diluent is typically a normal paraffinic hydrocarbon or a nonflammable chlorocarbon such as carbon tetrachloride or tetrachloroethylene. The TRUEX flowsheet includes a multistage extraction/scrub section that recovers and purifies the TRU elements from the waste stream and multistage strip sections that separate TRU elements from each other and the solvent.

The objectives of TRUEX processing are to recover valuable TRU elements and to lower disposal costs for the nonTRU waste product of the process. A major thrust of the development efforts has been the Generic TRUEX Model (GTM), which is used with Macintosh or IBM-compatible computers for designing TRUEX flowsheets and estimating cost and space requirements for installing TRUEX processes for treating specific waste streams.

During this report period, new features were added to the GTM so that it could reroute an effluent from one section of the process to another section than the normal one, account for the effects of high solvent loading, account for the effects of temperature, handle extraction

efficiencies of less than 100% at each stage, and automatically calculate the speciation and distribution ratios of aqueous-phase components for a wide variety of feed compositions.

Also, the GTM has been used to simulate a series of batch contact experiments with the TRUEX process. Simulation of the following batch contacts is discussed: a clean or fresh organic phase in each extraction contact, a clean or fresh aqueous phase in each scrub or strip contact, or a combination of clean and fresh organic and aqueous contacts.

Algorithms for the extraction behavior of important feed components continue to be improved by use of our own laboratory measurements and literature data obtained by interactions with other research institutions. In this report period, we performed laboratory experiments on the extraction of zirconium in high fluoride media, reductive stripping of plutonium, and the distribution of bismuth (an important component in the Hanford nuclear waste storage tanks) between the organic and aqueous phases in the TRUEX process. These data will be incorporated into the algorithms and data base generated for the GTM.

An effort was begun to demonstrate the new TRUEX-SREX process, which is a combination of the TRUEX process and a recently invented SREX (strontium extraction) process. Both these processes were invented in the ANL Chemistry Division. The GTM was used to develop a TRUEX-SREX flowsheet that will handle the expected range of feed compositions for dissolved sludge waste from the Hanford site. A 20-stage centrifugal contactor has been set up to verify experimentally the operation of the TRUEX-SREX flowsheet. In preparation for cold tests, we extensively characterized a candidate TRUEX-SREX solvent using a dispersion number test and hydraulic tests in a single-stage minicontactor (2-cm dia). Based on these tests, we concluded that the minicontactor should always be started with the aqueous phase, and this phase should be kept flowing so that it will remain the continuous phase. The only time that the contactor would not be aqueous continuous is if the aqueous/organic flow ratio is so high that the only stable condition is organic-continuous operation.

We also used the GTM to design a flowsheet for recovering TRU elements from aluminum-clad PuO_2 targets for Oak Ridge National Laboratory. The flowsheet was tested four times at Oak Ridge, one cold run and three hot runs. In all four runs, mechanical operation of the equipment and the process went reasonably well. In particular, all dispersions separated at or near expected process flow rates, and no significant amount of oxalate precipitate was formed. Rough measurements of effluent concentrations indicate that the flowsheet performed as anticipated.

A multi-year project on using the TRUEX process for treating plutonium-containing waste from ANL and the New Brunswick Laboratory was completed. In the four batches processed to date (each containing 12-34 g of plutonium), the alpha activities for the feeds were reduced from 21,400-88,000 nCi/mL to below the target of 10 nCi/mL. The alpha-activity decontamination factors for the four batches ranged from 4,000 to 65,500. The test results have demonstrated the ability of the GTM to design workable flowsheets based on waste feed compositions and the use of the TRUEX process for treating real waste streams.

A laboratory-scale evaporator (12 L/h) fabricated by LICON Inc. has been installed at CMT and is being modified for processing with acidic solutions. It will be used to gather

experimental data that will aid in the eventual design of a plant-scale evaporator and to gain experience in operating the LICON evaporator.

A substantial effort during the past year involved support to ANL's Waste Management Operations. Activities included assisting them in purchasing and installing evaporators and concentrators for treating ANL wastewaters; conducting laboratory experiments for the treatment of mixed wastes (Davies-Grey waste, metal waste solutions, dichromate solutions, and cocktail wastes from liquid scintillators); designing, fabricating, and testing a mixed-waste treatment facility; and investigating use of ion exchange resins for removing cesium from wastewater.

Magnetically assisted chemical separation (MACS) processes are being developed for removing contaminants (^{137}Cs , ^{90}Sr , transuranics) from waste solutions. The MACS process combines the selective and efficient separation afforded by chemical sorption with the high physical separation afforded by magnetic recovery of ferromagnetic beads. Studies during this report period involved evaluating polymeric coatings for magnetic particles and measuring the hydrolytic and radiolytic damage to coated particles during processing.

Finally, efforts have been renewed to determine the feasibility of substituting low-enriched uranium for the high-enriched uranium used in the production of ^{99}Mo for medical applications. As a part of this program, we are studying two LEU target designs. The LEU targets will contain either uranium-metal foil or uranium silicide (U_3Si_2). Either UO_2 or various UAl_x alloys are used in current HEU targets. The silicide fuel is being developed as LEU substitute for UAl_x alloys, and the uranium metal foils are being developed as LEU substitute for UO_2 .

I. INTRODUCTION

(G. F. Vandegrift)

The Division's work in separation science and technology is mainly concerned with developing a technology base for the TRUEX (TRansUranic EXtraction) solvent extraction process. The TRUEX process extracts, separates, and recovers TRU elements from solutions containing a wide range of nitric acid and nitrate salt concentrations. The extractant found most satisfactory for the TRUEX process is octyl(phenyl)-N,N-diisobutylcarbamoylmethylphosphine oxide, which is abbreviated CMPO. This extractant is combined with tributyl phosphate (TBP) and a diluent to formulate the TRUEX process solvent. The diluent is typically a normal paraffinic hydrocarbon (NPH) or a nonflammable chlorocarbon such as carbon tetrachloride (CCl₄) or tetrachloroethylene (TCE). The TRUEX flowsheet includes a multistage extraction/scrub section that recovers and purifies the TRU elements from the waste stream and multistage strip sections that separate TRU elements from each other and the solvent. Our current work is focused on facilitating the implementation of TRUEX processing of TRU-containing waste and high-level defense waste, where such processing can be of financial and operational advantage to the DOE community.

The major effort in TRUEX technology-base development involves developing a generic data base and modeling capability for the TRUEX process, referred to as the Generic TRUEX Model (GTM). The GTM will be directly useful for site-specific flowsheet development directed to (1) establishing a TRUEX process for specific waste streams, (2) assessing the economic and facility requirements for installing the process, and (3) improving, monitoring, and controlling on-line TRUEX processes. The GTM is composed of three sections. The heart of the model is the SASSE (Spreadsheet Algorithm for Stagewise Solvent Extraction) code, which calculates multistaged, countercurrent flowsheets based on distribution ratios calculated in the SASPE (Spreadsheet Algorithm for Speciation and Partitioning Equilibria) section. The third section of the GTM, SPACE (Size of Plant and Cost Estimation), estimates the space and cost requirements for installing a specific TRUEX process in a glovebox, shielded-cell, or canyon facility. The development of centrifugal contactors for feed- and site-specific applications is also an important part of the effort.

Four other projects have recently been initiated in separation science and technology. The objectives of these projects are to develop (1) a membrane-assisted solvent extraction method for treating natural and process waters contaminated by volatile organic compounds, (2) evaporation technology for concentrating radioactive waste and product streams such as those generated by the TRUEX process, (3) a process based on sorbing modified TRUEX solvent on magnetic beads to be used for separation of contaminants from radioactive and hazardous waste streams, and (4) a process that uses low-enriched uranium targets for production of ⁹⁹Mo for nuclear medicine uses.

II. THE GENERIC TRUEX MODEL

(J. M. Copple, R. A. Leonard, M. C. Regalbuto, J. Sedlet, and G. F. Vandegrift)

A. Summary of Recent Improvements

The main function of the GTM is flowsheet calculations for user-specified waste streams to be treated by the TRUEX process. The two main files used in these calculations are SASPE (Spreadsheet Algorithms for Speciation and Partitioning Equilibria), which calculates the extraction behavior of each component in the feed waste, and SASSE (Spreadsheet Algorithm for Stagewise Solvent Extraction), which calculates mass balances. These two sections iterate to a unique solution for the compositions of each stage and effluent in a specific flowsheet. A new version of the Generic TRUEX Model, GTM version 2.7, was released during this year. Its new features are briefly described below.

Stage Efficiency. Stage efficiency has been added to the SASSE worksheet. Stage efficiency is the amount of mass transfer that will take place in a stage divided by the amount that would take place if the stage were an equilibrium stage, i.e., if it has a fractional efficiency of 1.0 (100%).

Temperature Effect. Distribution ratios for various extracted species typically decrease as temperature increases. A temperature correction factor, applicable from 10 to 70°C, has been added for the following elements: La, Ce, Pr, Nd, Pm, Sm, Eu, Gd, Am, Pu(III), and Cm. The distribution ratio for Pu(IV) has no temperature effect built into the GTM. However, because this distribution ratio is not a strong function of temperature, this omission should not have much effect on the calculated GTM values. A temperature correction of other species will be added in the future.

User-Specified Distribution Ratios. By specifying initial distribution ratios for some of the feed components, the user can (1) speed up the GTM calculations and (2) achieve convergence for the distribution ratios of a component that would not otherwise converge because of interactions set up between adjacent stages during the GTM iterations.

Reroute of Section Effluent. In modeling solvent extraction processes, we have defined our flowsheet so that the aqueous phase flows from right to left, and the organic phase flows from left to right. As the GTM was previously set up, the aqueous and organic effluents from section "i" either continued on to the next section (aqueous to section $i - 1$, organic to $i + 1$), were taken as external effluents, or were split between the two options. A further option has been added to the GTM: section effluent can now be rerouted to a section other than its normal section.

Solvent Loading. The effect of solvent loading by metal salts on the extraction of species has not been accounted for in previous versions of the GTM. Since the TRUEX process is a waste treatment process, the effects of solvent loading will be small in most cases. However, in some special cases the solvent loading can be high. The GTM was upgraded so that TRUEX flowsheets can be generated where loading is extremely high (close to 100%). See Sec. II.B for further discussion.

Distribution Ratio Improvements. Based on our investigation of zirconium extraction behavior, we have changed the form of Zr(IV) that we treat in the GTM from Zr^{4+} to ZrO^{2+} . Also, the GTM equations for calculating the distribution ratio for $H_3PO_4^{3-}$, Cd(II), Zr(IV), and F^- were improved. Our own laboratory data were used to improve distribution ratio calculations for PO_4^{3-} and Cd^{2+} . Our own data and data collected at Pacific Northwest Laboratory on TRUEX processing of actual neutralized cladding removal waste were analyzed with respect to the high distribution ratios of Zr(IV) and F^- in concentrated solutions of both. These data were modeled based on the extractability of $ZrO(NO_3)_2$ and $ZrOF_2$. Analysis of these data is not complete, but an upgraded model, which will be further improved in the near future, is included in the GTM version.

Additional Diluent. Based on limited experimental data acquired in the ANL Chemistry Division, the extraction behaviors of Sr, Na, Mg, Al, Ca, Mn, Ni, Cu, and Cs have been modeled for the TRUEX-SREX process (Sec. III.B.5). In addition, the extraction behavior of nitric acid has been modeled when diamyl(amyl)phosphonate (DAAP) is used in place of TBP in the TRUEX-SREX solvent. Because DAAP is a much stronger extractant than TBP, significantly more nitric acid is extracted into the solvent and must be taken into account.

Many of the new developments discussed above are only accessible to the experienced GTM user; they are currently being made more accessible through changes in the user-friendly front end of the GTM.

B. Development of Loading Module

The effect of solvent loading by metal salts on the extraction of species has been accounted for in previous versions of the GTM. Since TRUEX is a waste treatment process, the effects of solvent loading will be small in most cases. Nonetheless, when the concentration of rare earth fission products is high, solvent loading by a combination of these species together with Fe, U, and transuranic (TRU) elements can lead to solvent loading. In these cases, the solvent is not loaded with only one species but by a combination of more than ten species. A mathematical algorithm was developed in order to calculate solvent loading. In the previous versions of the Loading Module, material balances for all components loading the solvent were solved. For the solvent, however, only CMPO was considered. In this new module, we have included TBP. Also, all possible species that can be formed between the loading elements CMPO and TBP have been accounted for. The inclusion of these species has significantly changed the number of terms present in the material balance equations. For every component that loads the solvent, all the possible species that can be formed between CMPO and TBP need to be taken into account. Instead of having the concentration of a given component in the organic and aqueous phases as variables, we now have the aqueous and the organic phase concentrations of all the possible species as variables. A new algorithm has been developed in order to solve the material balance equations.

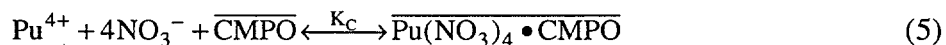
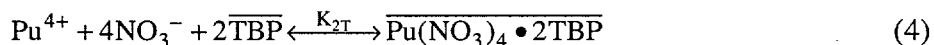
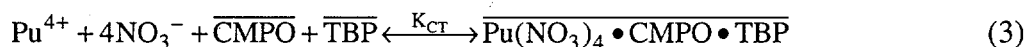
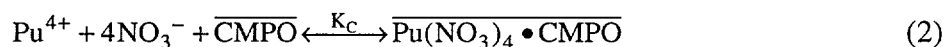
As in the previous Loading Module, a Newton-Raphson method is used to solve for all compositions. But we have manipulated the material balance equations in order to reduce the number of equations and unknowns. This was accomplished by writing all equations in terms of the aqueous phase composition, the composition of CMPO and TBP, and the distribution ratios.

Once the aqueous phase compositions are known as well as the CMPO and TBP compositions, all other species compositions can be calculated.

The algorithm needed for the Loading Module is given in the next subsections. This algorithm has been programmed in the form of an Excel macro and will be tested in the next report period. Revisions to this algorithm will be done as needed.

1. Algorithm for CMPO-TBP Loading

Before we consider solvent loading by multiple components, let us focus on the case in which only one loading component is present, in this case, Pu^{IV} , which can tie up CMPO and TBP by forming several different species:



For this case since Pu^{IV} has a maximum exponential dependence on CMPO or TBP of 2, it can associate with either two CMPOs, two TBPs, one CMPO and one TBP, one CMPO or one TBP. Thus, a maximum of five possible species can be formed. If the exponential dependence n was 1, we could only form two species by associating with either one CMPO or one TBP. If n was 3, we could form nine different species: all the ones that were formed when n is 2 plus those associated with either three CMPOs, three TBPs, two CMPOs and one TBP, and one CMPO and two TBPs. So, depending on the n value we can calculate, the maximum number of species, n_s , present for a given component is

$$n_s = \sum_{j=1}^N (j+1) \quad (6)$$

To calculate how much Pu^{IV} will load the solvent, we need to obtain the concentration of CMPO and TBP in the organic phase. That requires a material balance for Pu^{IV} , CMPO, and TBP. A material balance for Pu^{IV} can be written as follows:

$$V_a [\text{Pu}^{\text{IV}}]_{\text{aq}}^{\circ} + V_o [\text{Pu}^{\text{IV}}]_{\text{org}}^{\circ} = V_a [\text{Pu}^{\text{IV}}]_{\text{aq}} + V_o \left\{ \begin{array}{l} [\text{Pu}(\text{NO}_3)_4 \cdot 2\text{CMPO}] + [\text{Pu}(\text{NO}_3)_4 \cdot \text{CMPO}] \\ + [\text{Pu}(\text{NO}_3)_4 \cdot \text{CMPO} \cdot \text{TBP}] + [\text{Pu}(\text{NO}_3)_4 \cdot 2\text{TBP}] \\ + [\text{Pu}(\text{NO}_3)_4 \cdot \text{TBP}] \end{array} \right\}_{\text{org}} \quad (7)$$

where V_a is the volume (or the flow rate) of the aqueous phase, and V_o is the volume (or the flow rate) of the organic phase; $[Pu^{IV}]_{aq}^o$ and $[Pu^{IV}]_{org}^o$ are the concentrations of Pu^{IV} in the aqueous and organic phases before loading. Equation 7 can be written in terms of the distribution ratio for every species, $D_{pC,MT}$ (where pC is the number of CMPO molecules in the complex, and MT is the number of TBP molecules in the complex), as follows:

$$[Pu^{IV}]_{aq}^o + \left(\frac{O}{A}\right)[Pu^{IV}]_{org}^o = [Pu^{IV}]_{aq} \left[1 + \left(\frac{O}{A}\right) \{D_{2C} + D_C + D_{C,T} + D_{2T} + D_T\} \right] \quad (8)$$

or in terms of the equilibrium constant $K_{pC,MT}$,

$$[Pu^{IV}]_{aq}^o + \left(\frac{O}{A}\right)[Pu^{IV}]_{org}^o = [Pu^{IV}]_{aq} \left[1 + \left(\frac{O}{A}\right) \left\{ \frac{K_{2C}[CMPO]^2 + K_C[CMPO]}{+ K_{C,T}[CMPO][TBP] + K_{2T}[TBP]^2 + K_T[TBP]} \right\} \right] \quad (9)$$

For CMPO and TBP, the material balance equations are

$$[CMPO] = [CMPO^o] - 2[Pu(NO_3)_4 \cdot 2[CMPO]] - [Pu(NO_3)_4 \cdot CMPO] - [Pu(NO_3)_4 \cdot CMPO \cdot TBP] \quad (10)$$

and

$$[TBP] = [TBP^o] - [Pu(NO_3)_4 \cdot CMPO \cdot TBP] - 2[Pu(NO_3)_4 \cdot 2TBP] - [Pu(NO_3)_4 \cdot TBP] \quad (11)$$

Now written in terms of $K_{pC,MT}$:

$$[CMPO] = [CMPO^o] - [Pu^{IV}]_{aq} \{ K_{2C}[CMPO]^2 + K_C[CMPO] + K_{C,T}[CMPO][TBP] \} \quad (12)$$

and

$$[TBP] = [TBP^o] - [Pu^{IV}]_{aq} \{ K_{C,T}[CMPO][TBP] + 2K_{2T}[TBP]^2 + K_T[TBP] \} \quad (13)$$

Solving Eqs. 9, 12, and 13, we obtain the concentrations of $[Pu^{IV}]_{aq}$, CMPO, and TBP, for a given (O/A) flow ratio and initial values of CMPO, TBP, $[Pu^{IV}]_{aq}$, $[Pu^{IV}]_{org}$, and for $K_{pC,MT}$. The values of $K_{pC,MT}$ are calculated by SASPE within the GTM, but, to do so, the compositions of CMPO, TBP, $[Pu^{IV}]_{org}$, and $[Pu^{IV}]_{aq}$ need to be known. As a result, the need for an iterative solution between SASPE (to calculate equilibrium constants) and the Loading Module (to calculate composition) arises, as in previous versions of the Loading Module. In the past, only one value of K needed to be known per component. In the new module, we need a K value for every species for every component. At present, SASPE is currently being upgraded to reflect this.

To calculate the effects of solvent loading by a number of components, a material balance equation must be derived for every component, as well as CMPO and TBP. This is the subject of the next subsection.

2. Material Balance Equations

The material balance equation for component i can be written:

$$V_a X_{a,i}^0 + V_o X_{o,i}^0 = V_o X_{o,i,T} + V_o X_{o,i,C} + V_o X_{o,i,2T} + V_o X_{o,i,C,T} + V_o X_{o,i,2C} + V_o X_{o,i,3T} + V_o X_{o,i,C,2T} + V_o X_{o,i,2C,T} + V_o X_{o,i,3C} + \dots \quad (14)$$

where $X_{a,i}$ is the concentration of component i in the aqueous phase, and $X_{o,i,pC,mT}$ is the organic concentration for a given species. From the D value definition, we obtain

$$\frac{X_{o,i,T}}{X_{a,i}} = D_{i,T} = K_{i,T} [\text{TBP}] \quad (15)$$

$$\frac{X_{o,i,C}}{X_{a,i}} = D_{i,C} = K_{i,C} [\text{CMPO}] \quad (16)$$

$$\frac{X_{o,i,2T}}{X_{a,i}} = D_{i,2T} = K_{i,2T} [\text{TBP}]^2 \quad (17)$$

$$\frac{X_{o,i,2C}}{X_{a,i}} = D_{i,2C} = K_{i,2C} [\text{CMPO}]^2 \quad (18)$$

$$\frac{X_{o,i,3C}}{X_{a,i}} = D_{i,3C} = K_{i,3C} [\text{CMPO}]^3 \quad (19)$$

$$\frac{X_{o,i,3T}}{X_{a,i}} = D_{i,3T} = K_{i,3T} [\text{TBP}]^3 \quad (20)$$

$$\frac{X_{o,i,C,2T}}{X_{a,i}} = D_{i,C,2T} = K_{i,C,2T} [\text{CMPO}][\text{TBP}]^2 \quad (21)$$

$$\frac{X_{o,i,2C,T}}{X_{a,i}} = D_{i,2C,T} = K_{i,2C,T} [\text{CMPO}]^2 [\text{TBP}] \quad (22)$$

$$\frac{X_{o,i,3C}}{X_{a,i}} = D_{i,3C} = K_{i,3C} [\text{CMPO}]^3 \quad (23)$$

By multiplying both sides of Eqs. 15-23 by $X_{a,i}$, we have $X_{o,i,pC,mT}$ in terms of $X_{a,i}$ and a constant term $[\text{CMPO}]$ to a power and $[\text{TBP}]$ to a power. Substituting $X_{o,i,pC,mT}$ in terms of the aqueous concentration into Eq. 14, we obtain

$$X_{a,i}^o + \left(\frac{O}{A}\right) X_{o,i}^o = X_{a,i} + \left(\frac{O}{A}\right) X_{a,i} \left[\begin{array}{l} K_{i,T}[\text{TBP}] + K_{i,C}[\text{CMPO}] + K_{i,2T}[\text{TBP}]^2 + K_{i,C,T}[\text{CMPO}][\text{TBP}] \\ + K_{i,2C}[\text{CMPO}]^2 + K_{i,3T}[\text{TBP}]^3 + K_{i,C,2T}[\text{CMPO}][\text{TBP}]^2 \\ + K_{i,2C,T}[\text{CMPO}]^2[\text{TBP}] + K_{i,3C}[\text{CMPO}]^3 + \dots \end{array} \right] \quad (24)$$

or

$$X_{a,i} \left[1 + \left(\frac{O}{A}\right) \sum_{m=1}^n \sum_{p=0}^m K_{i,pC,(m-p),T} [\text{CMPO}]^p [\text{TBP}]^{(m-p)} \right] - X_{a,i}^o - \left(\frac{O}{A}\right) X_{o,i}^o = 0 \quad (25)$$

So for a given component i , Eq. 25 generates the material balance equation based on n_i , the exponential dependence for a given component i . Equation 25 needs to be written for every component i that is loaded into the solvent.

A material balance equation for CMPO can be written as:

$$\begin{aligned} [\text{CMPO}] = [\text{CMPO}^o] &- X_{o,i,C} - X_{o,i,C,T} - 2X_{o,i,2C} - X_{o,i,C,2T} - 2X_{o,i,2C,T} - 3X_{o,i,3C} - \dots \\ &- X_{o,2,C} - X_{o,2,C,T} - 2X_{o,2,2C} - X_{o,2,C,2T} - 2X_{o,2,2C,T} - 3X_{o,2,3C} - \dots \\ &\vdots \\ &\vdots \\ &- X_{o,N,C} - X_{o,N,C,T} - 2X_{o,N,2C} - X_{o,N,C,2T} - 2X_{o,N,2C,T} - 3X_{o,N,3C} - \dots \end{aligned} \quad (26)$$

where all X's are concentrations in the organic phase for every component for every species; N is the total number of components loaded in the solvent. Written in terms of the aqueous phase

$$\begin{aligned}
[\text{CMPO}] = & [\text{CMPO}^0] - X_{a,1}K_{1,C}[\text{CMPO}] - X_a K_{1,C,T}[\text{CMPO}][\text{TBP}] & (27) \\
& - 2X_{a,1}K_{1,2C}[\text{CMPO}]^2 - X_{a,1}K_{1,C,2T}[\text{CMPO}][\text{TBP}]^2 \\
& - 2X_{a,1}K_{1,2C,T}[\text{CMPO}]^2[\text{TBP}] - 3X_{a,1}K_{1,3C}[\text{CMPO}]^3 - \dots \\
& \vdots \\
& \vdots \\
& - X_{a,N}K_{N,C}[\text{CMPO}] - X_{a,N}K_{N,C,T}[\text{CMPO}][\text{TBP}] - 2X_{a,N}K_{N,2C}[\text{CMPO}]^2 \\
& - X_{a,N}K_{N,C,2T}[\text{CMPO}][\text{TBP}]^2 - 2X_{a,N}K_{N,2C,T}[\text{CMPO}]^2[\text{TBP}] - 3X_{a,N}
\end{aligned}$$

or

$$[\text{CMPO}] - [\text{CMPO}^0] + \sum_{i=1}^N X_{a,i} \sum_{m=1}^{n_i} \sum_{p=1}^m p \cdot K_{i,pC,(m-p),T}[\text{CMPO}][\text{TBP}]^{(m-p)} = 0 \quad (28)$$

Equation 27 generates the material balance equation for CMPO based on n_i , the exponential dependence for component i , and N , the total number of components that load the solvent.

A material balance equation for TBP can be written as:

$$\begin{aligned}
[\text{TBP}] = & [\text{TBP}^0] - X_{o,1,T} - 2X_{o,1,2T} - X_{o,1,C,T} - 3X_{o,1,3T} - 2X_{o,1,C,2T} - X_{o,1,2C,T} - \dots & (29) \\
& - X_{o,2,T} - 2X_{o,2,2T} - X_{o,2,C,T} - 3X_{o,2,3T} - 2X_{o,2,C,2T} - X_{o,2,2C,T} - \dots \\
& \vdots \\
& \vdots \\
& - X_{o,N,T} - 2X_{o,N,2T} - X_{o,N,C,T} - 3X_{o,N,3T} - 2X_{o,N,C,2T} - X_{o,N,2C,T} - \dots
\end{aligned}$$

Written in terms of the aqueous phase:

$$\begin{aligned}
[\text{TBP}] = & [\text{TBP}^0] - X_{a,1} \left[K_{1,T}[\text{TBP}] + 2K_{1,2T}[\text{TBP}]^2 + K_{1,C,T}[\text{CMPO}][\text{TBP}] + 3K_{1,3T}[\text{TBP}]^3 \right] & (30) \\
& + 2K_{1,C,2T}[\text{CMPO}][\text{TBP}]^2 + K_{1,2C,T}[\text{CMPO}]^2[\text{TBP}] \\
& \vdots \\
& \vdots \\
& - X_{a,N} \left[K_{N,T}[\text{TBP}] + 2K_{N,2T}[\text{TBP}]^2 + K_{N,C,T}[\text{CMPO}][\text{TBP}] + 3K_{N,3T}[\text{TBP}]^3 \right] \\
& + 2K_{N,C,2T}[\text{CMPO}][\text{TBP}]^2 + K_{N,2C,T}[\text{CMPO}]^2[\text{TBP}] + \dots
\end{aligned}$$

or

$$[\text{TBP}] - [\text{TBP}^0] + \sum_{i=1}^N X_{a,i} \sum_{m=1}^{n_i} m-1 \sum_{p=0}^{m-1} (m-p) \cdot K_{i,pC,(m-p),T}[\text{CMPO}][\text{TBP}]^{(m-p)} = 0 \quad (31)$$

Equation 31 generates the material balance equation for TBP based on n_i , the exponential dependence for component i and N , and the total number of components loaded in the solvent.

Equations 25, 28, and 31 will generate a total of $N+2$ equations with $N+2$ unknowns. This system of $N+2$ nonlinear equations can be solved by the Newton-Raphson method described in the next section.

3. Solution Method

A system of nonlinear equations can be solved by using the Newton-Raphson method.¹ Nonlinear systems present the problem of having multiple solutions. This problem will be solved in the same fashion as before. If a "nonphysical solution" is obtained (i.e., negative concentrations and/or concentrations greater than the initial concentration), the initial guess is changed, moving us in a different solution path. This problem was easily solved in the past, and we believe that will be the case in the new CMPO-TBP Loading Module.

The following algorithm describes the procedure used, as well as the interaction of the Loading Module with the other existing models inside the GTM:

- (1) The initial concentrations for all components in the aqueous and organic phase ($[X_{i,a}]^0$ and $[X_{i,o}]^0$) are obtained from SASSE.
- (2) Using SASPE, the tracer distribution ratio for all species of any given component $X_{i,o,pC,mT}$ is obtained:

$$K_{i,pC,mT} = \frac{D_{i,pC,mT}}{[CMPO^0]^p [TBP^0]^m} \quad (32)$$

where $[CMPO^0]$ and $[TBP^0]$ are the initial concentrations of CMPO and TBP.

- (3) The concentration for every component and the extractants is calculated by using Eqs. 25, 28, and 31, where the set given by these equations represents the mass balance for every species, $i = 1, \dots, N$, and the material balance for the solvent CMPO ($i = N + 1$) and TBP ($i = N + 2$). Two vectors of concentrations can then be created, as follows; vector \underline{I} , which contains the initial concentrations from SASSE, and vector \underline{X} , which contains the concentrations of all components that satisfy the material balance equations:

$$\underline{I} = [X_{a,1}^0], [X_{a,2}^0], \dots, [X_{a,N}^0], [CMPO^0], [TBP^0] \quad (33)$$

$$\underline{X} = [X_{a,1}], [X_{a,2}], \dots, [X_{a,N}], [CMPO], [TBP] \quad (34)$$

Equations 25, 28, and 31 can be rewritten as:

$$F_i = X_{a,i} \left[1 + \left(\frac{O}{A} \right) \sum_{m=1}^{n_i} \sum_{p=0}^m K_{1,pC,(m-p),T} [\text{CMPO}]^p [\text{TBP}]^{(m-p)} \right] - X_{a,i}^o - \left(\frac{O}{A} \right) X_{o,i}^o = 0 \quad (35)$$

for $i = 1, \dots, N$,

$$F_{N+1} = [\text{CMPO}] - [\text{CMPO}^o] + \sum_{i=1}^N X_{a,i} \sum_{m=1}^{n_i} \sum_{p=1}^m p \cdot K_{i,pC,(m-p),T} [\text{CMPO}] [\text{TBP}]^{(m-p)} = 0 \quad (36)$$

and

$$F_{N+2} = [\text{TBP}] - [\text{TBP}^o] + \sum_{i=1}^N X_{a,i} \sum_{m=1}^{n_i} \sum_{p=1}^m p \cdot K_{i,pC,(m-p),T} [\text{CMPO}] [\text{TBP}]^{(m-p)} = 0 \quad (37)$$

Equations 33 through 37 can be solved by using a Newton-Raphson technique for nonlinear equations and using as an initial approximation the vector of $\underline{\mathbf{I}}$. Thus,

$$\begin{bmatrix} X_1 \\ X_2 \\ \vdots \\ X_N \\ X_{N+1} \\ X_{N+2} \end{bmatrix}^{k+1} = \begin{bmatrix} X_1 \\ X_2 \\ \vdots \\ X_N \\ X_{N+1} \\ X_{N+2} \end{bmatrix}^k - \Phi_k^{-1} \begin{bmatrix} F_1 & (X_1, X_2, \dots, X_N, X_{N+1}, X_{N+2}) \\ F_2 & (X_1, X_2, \dots, X_N, X_{N+1}, X_{N+2}) \\ \vdots & \vdots \\ F_N & (X_1, X_2, \dots, X_N, X_{N+1}, X_{N+2}) \\ F_{N+1} & (X_1, X_2, \dots, X_N, X_{N+1}, X_{N+2}) \\ F_{N+2} & (X_1, X_2, \dots, X_N, X_{N+1}, X_{N+2}) \end{bmatrix} \quad (38)$$

where Φ_k^{-1} represents the inverse of the Jacobian in the k^{th} iteration. The Jacobian is defined as follows:

$$\Phi_k = \begin{bmatrix} \frac{\delta F_1}{\delta X_1}, \frac{\delta F_1}{\delta X_2}, \dots, \frac{\delta F_1}{\delta X_N}, \frac{\delta F_1}{\delta X_{N+1}}, \frac{\delta F_1}{\delta X_{N+2}} \\ \frac{\delta F_2}{\delta X_1}, \frac{\delta F_2}{\delta X_2}, \dots, \frac{\delta F_2}{\delta X_N}, \frac{\delta F_2}{\delta X_{N+1}}, \frac{\delta F_2}{\delta X_{N+2}} \\ \vdots \\ \frac{\delta F_N}{\delta X_1}, \frac{\delta F_N}{\delta X_2}, \dots, \frac{\delta F_N}{\delta X_N}, \frac{\delta F_N}{\delta X_{N+1}}, \frac{\delta F_N}{\delta X_{N+2}} \\ \frac{\delta F_{N+1}}{\delta X_1}, \frac{\delta F_{N+1}}{\delta X_2}, \dots, \frac{\delta F_{N+1}}{\delta X_N}, \frac{\delta F_{N+1}}{\delta X_{N+1}}, \frac{\delta F_{N+1}}{\delta X_{N+2}} \\ \frac{\delta F_{N+2}}{\delta X_1}, \frac{\delta F_{N+2}}{\delta X_2}, \dots, \frac{\delta F_{N+2}}{\delta X_N}, \frac{\delta F_{N+2}}{\delta X_{N+1}}, \frac{\delta F_{N+2}}{\delta X_{N+2}} \end{bmatrix} \quad (39)$$

The equations necessary to generate all the partials in the Jacobian are given in Table 1. Once the system has converged, i.e.,

$$\left[\frac{X_i^{K+1} - X_i^K}{X_i^{K+1}} \right] \leq 0.0001 \quad \text{for } i = 1, \dots, N + 2 \quad (40)$$

values for the aqueous concentrations as well as CMPO and TBP are obtained.

The organic concentration for every species for every component can be obtained from Eq. 32 and the definition of the distribution ratio:

$$X_{o,i,pC,mT} = X_{a,i} K_{i,pC,mT} [\text{CMPO}]^p [\text{TBP}]^m \quad (41)$$

(4) Distribution ratios for every component can now be recalculated as

$$D_i = \sum_{m=1}^{n_i} \sum_{p=0}^m D_{i,pC,(m=p)T} \quad (42)$$

or

$$D_i = \frac{\sum_{m=1}^{n_i} \sum_{p=0}^m D_{o,i,pC,(m=p)T}}{X_{a,i}} \quad (43)$$

and passed to SASSE.

Table 1. Equations Needed to Calculate the Jacobian for the Newton-Raphson Method

$$\frac{\delta F_1}{\delta X_1} = \left[1 + \left(\frac{O}{A} \right) \sum_{m=1}^{n,i} \sum_{p=0}^m K_{pC(m-p)T} [\text{CMPO}]^p [\text{TBP}]^{m-p} \right] \quad \text{for } i = 1, \dots, N$$

$$\frac{\delta F_1}{\delta X_{j,i \neq j}} = 0 \quad \text{for } i = 1, \dots, N \text{ and } j = 1, \dots, N$$

$$\frac{\delta F_1}{\delta X_{N+1}} = X_{a,i} \left(\frac{O}{A} \right) \sum_{m=1}^{n,i} \sum_{p=1}^m p \cdot K_{pC(m-p)T} [\text{CMPO}]^{p-1} [\text{TBP}]^{m-p} \quad \text{for } i = 1, \dots, N$$

$$\frac{\delta F_1}{\delta X_{N+2}} = X_{a,i} \left(\frac{O}{A} \right) \sum_{m=1}^{n,i} \sum_{p=0}^{m-1} (m-p) \cdot K_{pC(m-p)T} [\text{CMPO}]^p [\text{TBP}]^{m-p-1} \quad \text{for } i = 1, \dots, N$$

$$\frac{\delta F_{N+1}}{\delta X_1} = \sum_{m=1}^{n,i} \sum_{p=1}^m p \cdot K_{pC(m-p)T} [\text{CMPO}]^p [\text{TBP}]^{(m-p)} \quad \text{for } i = 1, \dots, N$$

$$\frac{\delta F_{N+1}}{\delta X_{N+1}} = 1 + \sum_{i=1}^N X_{a,i} \sum_{m=1}^{n_i} \sum_{p=1}^m p^2 \cdot K_{i,pC(m-p)T} [\text{CMPO}]^{(p-1)} [\text{TBP}]^{(m-p)}$$

$$\frac{\delta F_{N+1}}{\delta X_{N+2}} = \sum_{i=1}^N X_{a,i} \sum_{m=2}^{n_i} \sum_{p=1}^{m-1} p \cdot (m-p) \cdot K_{pC(m-p)T} [\text{CMPO}]^p [\text{TBP}]^{m-p-1}$$

$$\frac{\delta F_{N+2}}{\delta X_1} = \sum_{m=1}^{n_i} \sum_{p=0}^{m-1} (m-p) K_{pC(m-p)T} [\text{CMPO}]^p [\text{TBP}]^{m-p} \quad \text{for } i = 1, \dots, N$$

$$\frac{\delta F_{N+2}}{\delta X_{N+1}} = \sum_{i=1}^N X_{a,i} \sum_{m=2}^{n_i} \sum_{p=1}^{m-1} p \cdot (m-p) \cdot K_{pC(m-p)T} [\text{CMPO}]^{p-1} [\text{TBP}]^{m-p}$$

$$\frac{\delta F_{N+2}}{\delta X_{N+2}} = 1 + \sum_{i=1}^N X_{a,i} \sum_{m=1}^{n_i} \sum_{p=0}^{m-1} (m-p)^2 K_{pC(m-p)T} [\text{CMPO}]^p [\text{TBP}]^{m-p-1}$$

- (5) SASSE will then recalculate concentrations for all components and pass recalculated values to SASPE and the Loading Module.
- (6) SASPE recalculates and passes new D values to the Loading Module, which in turn will calculate a new set of D values.
- (7) Iteration steps 1 through 6 will continue until the D values from the Loading Module are constant.

In previous versions, to decrease the computational time needed for convergence in the Newton-Raphson method (step 3), all species that have the same exponential dependence on the extractant and similar D values were grouped as one "pseudo-component" that possesses the same characteristics as all these species and, therefore, behaved in a similar fashion. This enabled us to represent a large number of components as one, write one mass balance and distribution ratio equation instead of several, and solve the Newton-Raphson with fewer equations and variables than before. Since our material balance equations are now written in terms of the aqueous phase concentrations and the concentrations of CMPO and TBP, our system of equations has $N+2$ equations and $N+2$ unknowns. In the past, material balance equations were written in terms of the organic and aqueous phases and CMPO, making a system of $2N+1$ equations with $2N+1$ unknowns. Even though we have added TBP and all the species, the new algorithm has $N-1$ equations fewer than before, making the need for a pseudo-component unnecessary. If during testing of the algorithm within the GTM, we realize that the Loading Module is too slow, we will return to the pseudo-component concept as before.

4. Excel Implementation

The algorithm presented above was implemented in an Excel macro named CMPO_TBP>Loading_Module. The upper portion of the macro contains all the necessary input data: initial concentrations, D values, number of components, etc., as well as the converge values for the concentrations. The rest of the macro contains the code necessary to implement the algorithm. This macro is currently being tested. We also await the necessary information to upgrade SASPE to calculate the D values needed for all components that are loaded in the solvent. These D values will be upgraded in order to reflect the presence of all possible species. The data needed for the SASPE upgrade are currently being researched. We are using literature data and some data collected in CMT several years ago to model the behavior of Pu, U, Bi, and rare earth elements in their extraction by TBP alone. These models will be mechanistically correct and will use the thermodynamic activities of water, nitrate ion, and hydrogen ion in their formulations. The models will be added to SASPE and will increase the model's accuracy when high solvent loading decreases the concentration of CMPO available to extract these species; under these conditions, extraction by TBP, which has been until this point ignored in the GTM, is an important factor in predicting the extraction behavior of these species in the TRUEX process.

C. Use of GTM to Calculate Effects of Batch Contacts

The GTM can be used to simulate a series of batch contact experiments. It has been our experience that there is some confusion on how to set up batch contacts. Some differences exist between batch contacts and GTM flowsheet calculations.

First, batch contacts are usually done in series. As an example, consider the cases given in Figs. 1 and 2. In the case of clean organic-phase contacts (Fig. 1), three batch extractions are performed. First, the aqueous phase is contacted with a clean organic phase (contact 1); after equilibrium is reached, the two phases are separated. The equilibrated aqueous phase from contact 1 is then contacted with fresh solvent (contact 2). After the two phases reach equilibrium, the aqueous phase is separated and contacted a third time with fresh organic (contact 3), equilibrated, and separated again. In this case, the volume ratio of organic to aqueous is 2/1. The batch contacts described in Fig. 1 are used to simulate an extraction section. The contact sequence given in Fig. 2 simulates a scrub and/or strip section. (Note: Numbers in parentheses in these two figures, as well as subsequent flowsheets, indicate relative flow rates.)

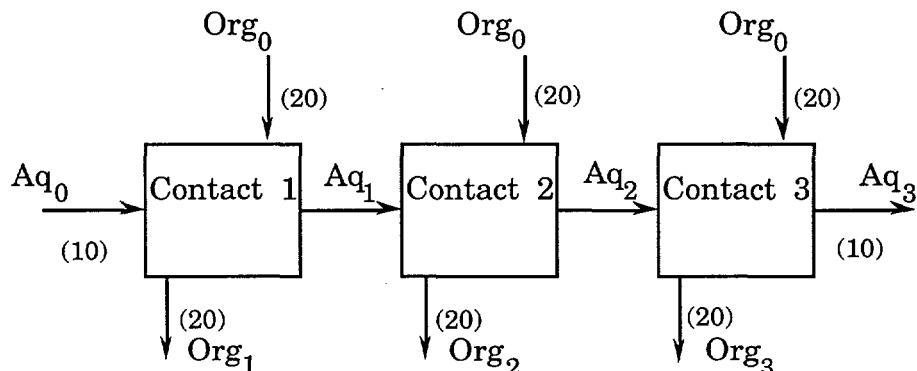


Fig. 1. Batch Contacts with Clean Organic Phases. (In this and following figures, numbers in parentheses are relative flow rates.)

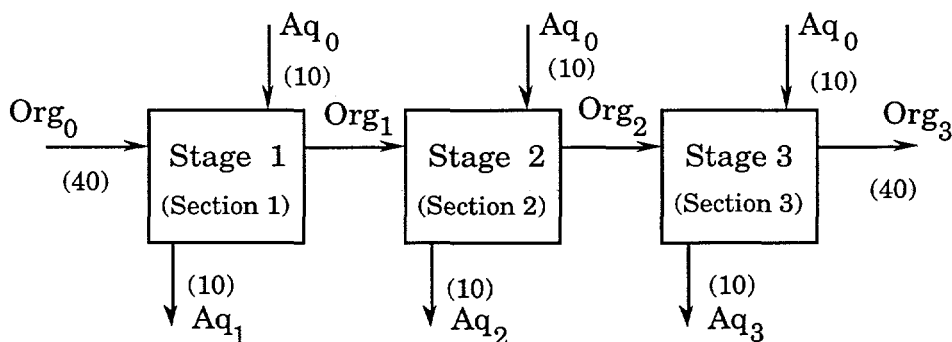


Fig. 2. Batch Contacts with Clean Aqueous Phases

Second, the GTM is, in general, a model for continuous countercurrent solvent extraction. As an example, consider the three-stage extraction section given in Fig. 3. The organic phase

enters stage one (Org_0), and the aqueous phase enters stage three (Aq_0). Note that in stage one, the clean organic phase (Org_0) contacts the aqueous effluent from stage two (Aq_2). In stage two, the organic phase exiting stage one (Org_1) contacts the aqueous phase exiting stage three (Aq_3). In stage three, the organic exiting stage two (Org_2) contacts the clean aqueous phase (Aq_0). The organic-to-aqueous (O/A) flow rate is 2/1 in this example. Solvent extraction processes are more efficient when run countercurrently.

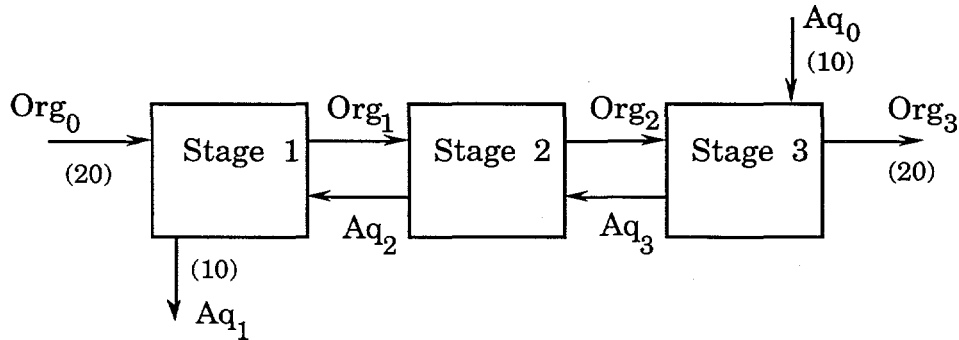


Fig. 3. Solvent Extraction Process

Using the GTM to simulate batch contacts will depend on how the sequence of contacts is performed. Such contacts are usually done by using a clean or fresh organic phase in each extraction contact, a clean or fresh aqueous phase in each scrub or strip contact, or a combination of clean or fresh organic and aqueous contacts (extraction, scrub, strip, and washes). All of these options will be discussed.

1. Clean Aqueous-Phase Contacts

By the nature of the GTM, a sequence of clean aqueous-phase contacts, like the one given in Fig. 2, is very simple to set up since a section is defined in the front end of the GTM by defining an aqueous feed. If the front end is used, three sections with one stage each should be specified. The composition and flow rate for the organic phase should be entered for Section 1. The aqueous-phase composition and flow rate for each aqueous-phase contact should be entered for each section. The fraction of aqueous effluent should be 1 for all sections, since all the aqueous phase is removed in each contact (section). The fraction of organic effluent should be 0 except for the last section, where it should be 1 since the organic only exits the contact sequence from the last section. The GTM front end is the easiest way to create an export file.* Once that export file is created, the user can modify it and run multiple flowsheet calculations. Figure 4 is a portion of the export file that was created when running the GTM's front end for the flowsheet given in Fig. 2.

*An export file contains all the data necessary to run the Generic TRUEX Model. An export file can be generated by running the GTM and halting it, after launching the SASPE-SASSE iteration, when the message displayed in the Excel status bar reads "Starting SASSE Generation Section."

run_SPACE	FALSE		
run_SASSE	TRUE		
file_suffix	Example_Aq		
folder_name	reports		
sections	3		
useable_sections	3		
absolute_feed_rate	0		
year	0		
Recycle	No		
diluent	NPH		
HOTLOC	0		
solvent_extraction_un	OC		
CMFO	0.2		
TBP	1.4		
FOI Input	0.005	0.005	5.00E-03
FAI Input	0.005	0.005	5.00E-03
sec_cl	D	E	F
aq_feed_cl	F	F	F
org_feed_cl	X	0	0
aq_eff_cl	W	W	W
org_eff_cl	0	0	P
section_name	Extraction	Scrub1	Scrub2
stages	1	1	1
QFAI	10	10	10
residence_time	20	20	20
section_type	1	2	2
FEOI Input	1E-09	1E-09	1
FEAI Input	1	1	1
QSOI			
QSAI			
org_sample_name			
aq_sample_name			
stage_efficiency	1	1	1
QFOI	40		
number_of_scrubs	2		
pulse_column_section	0		
proc_temp	25		
ref_temp	25		
number_of_strip1s	0		
number_of_strip2s	0		
KHNO3			
KHF			
KH2C2O4			
number_of_ions	3		
number_of_cations	2		
concn_sec1	1	0	0
concn_sec2	1	0	0
concn_sec3	1	0	0
concn_sec4			
concn_sec5			
concn_sec6			
concn_sec7			
concn_sec8			
concn_sec9			
concn_sec10			
concn_sec11			
org_concn	1.3	0.00001	0.006
ion_names	H	Zr	F

Fig. 4. Export File Corresponding to Fig. 2, Batch Contacts with Clean Aqueous Phases

2. Clean Organic-Phase Contacts

When organic-phase contacts are done in the manner described in Fig. 1, the composition of the aqueous phase equilibrated in an earlier contact must be known before the effect of its contact with a clean organic phase can be calculated. The contacts described in Fig. 1 can be modeled by running the GTM (Option 7) three times: once with the compositions of the clean aqueous (Aq_0) and the clean organic (Org_0) as the feeds to a one-stage extraction process; another with the equilibrated aqueous composition from contact 1 and the clean organic (Org_0) as the feed to a one-stage extraction process; and a third with the equilibrated aqueous composition from contact 2 and the clean organic (Org_0) as the feed to a one-stage extraction process. However, this method is tedious and slow.

We have developed a way to run the GTM with multiple organic feeds. To model clean organic-phase contacts, as described in Fig. 1, the GTM must calculate that flowsheet in the form of Fig. 5. Note that in Fig. 5 the aqueous phase enters the flowsheet at the right side, while in Fig. 1, which describes the sequential batch contacts, it enters at the left. As shown in Fig. 5, Contact 1 in Fig. 1 is equivalent to Section 3; Contact 2 is equivalent to Section 2; and Contact 3 is equivalent to Section 1. This is an important point for comparative purposes when verifying the GTM versus batch contact measurements.

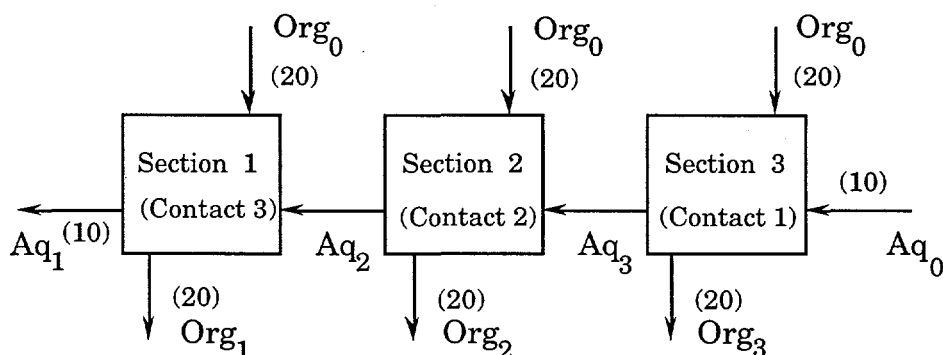


Fig. 5. Setup for Multiple Runs with Clean Organic Phase

At present, the testing of multiple organic feeds is possible only when using the GTM without the front end. However, the easiest way to generate an export file is to create a similar one by using the front end and modifying that file. For the case given in Fig. 1, we will have to generate an export file with three sections containing one stage each (Fig. 6). The GTM currently defines a section by an aqueous feed. For this case flow rates for all aqueous feeds are set to 10. The composition for the organic phase should be entered for Section 1. The aqueous feed composition (Aq_0) should be entered for Section 1. For Sections 2 and 3 an aqueous phase composition of $1M H^+$ can be entered for simplicity. Note that these feeds will eventually be eliminated when simulating clean organic contacts (Fig. 1). The fraction of aqueous effluent should be 0 for all sections except the first, which should be 1, since the aqueous is removed at Section 1. The fraction of the organic effluent should be set to 1 for all sections (these will minimize changes to the export files). Given in Fig. 7 is the portion of the export file generated for this case. Shown in Fig. 8 is the modified export file. A total of 18 lines were modified.

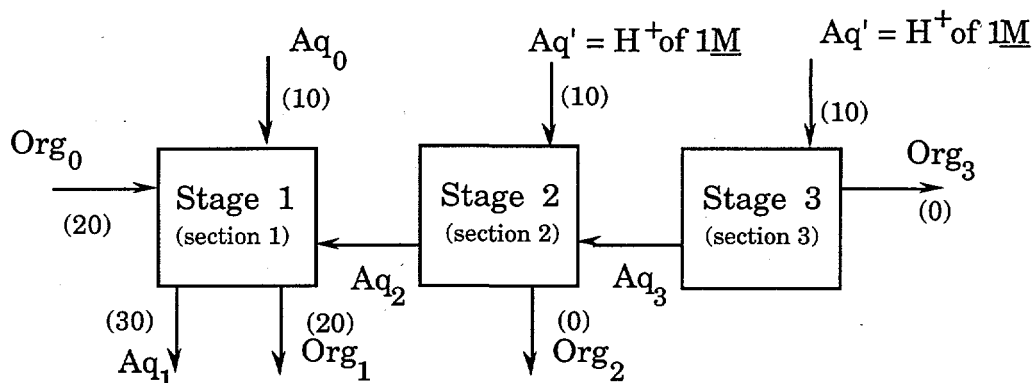


Fig. 6. Setup to Create a Similar Export File Corresponding to Fig. 5

Three of these changes (Org_feed_cl , $section_name$, and $section_type$) are optional and not necessary for computational purposes. They are included so that when generating reports the correct section name and stream identity appear. The other-phase carryover for both organic (FOI_input) phases has been set to zero to simulate batch contacts. The remaining five changes are all necessary for computational purposes.

Creating and modifying export files to simulate batch contacts may seem a cumbersome process at first. However, once a "master" file is generated to simulate a given sequence of batch contacts, the changes necessary to run large sets of data are minimal.

3. Combination Contacts

Combination contacts usually result when a series of batch contacts is performed to simulate a countercurrent solvent extraction flowsheet. Let us illustrate how these series of contacts can be simulated by the GTM for the batch contacts given in Table 2. These sequences of contacts were performed by G. J. Lumetta and J. L. Swanson.² The series of contacts given in Table 2 can be simulated by running the GTM with the flowsheet shown in Fig. 9. Note that in Fig. 9 the aqueous-phase feed composition for Sections 10 to 12 (or contacts J to L) is changed because the complexant wash feed is preset to $0.25M$ HEDPA/ $0.05M$ HNO_3 in the GTM. Also, the aqueous-phase feed composition for Sections 8 and 9 (or contacts H and I) is changed from water to $0.01M$ HNO_3 . This is necessary since water cannot currently be specified for a feed in the GTM.

run_SPACE	FALSE		
run_SASSE	TRUE		
file_suffix	Example_Org		
folder_name	reports		
sections	3		
useable_sections	3		
absolute_feed_rate	0		
year	0		
Recycle	No		
diluent	NPH		
HOTLOC	0		
solvent_extraction_un	CC		
CMFO	0.2		
TBP	1.4		
FOI_input	0.005	0.005	5.00E-03
FAI_input	0.005	0.005	5.00E-03
sec_cl	D	E	F
aq_feed_cl	F	F	F
org_feed_cl	X	0	0
aq_eff_cl	W	0	0
org_eff_cl	P	P	P
section_name	Extraction	Scrub1	Scrub2
stages	1	1	1
QFAI	10	10	10
residence_time	20	20	20
section_type	1	2	2
FEOI_input	1	1	1
FEAI_input	1	0	0
QSOI			
QSAI			
org_sample_name			
aq_sample_name			
stage_efficiency	1	1	1
QFOI	20		
number_of_scrubs	2		
pulse_column_section	0		
proc_temp	25		
ref_temp	25		
number_of_strlp1s	0		
number_of_strlp2s	0		
KHNO3			
KHF			
KH2C2O4			
number_of_ions	3		
number_of_cations	2		
concn_sec1	5.04	0.01	0.04
concn_sec2	1	0	0
concn_sec3	1	0	0
concn_sec4			
concn_sec5			
concn_sec6			
concn_sec7			
concn_sec8			
concn_sec9			
concn_sec10			
concn_sec11			
org_concn	1E-15	1E-15	1E-15
ion_names	H	Zr	F

Fig. 7. Export File Corresponding to Fig. 6

run_SPACE	FALSE		
run_SASSE	TRUE		
file_suffix	Example_Org_M		
folder_name	reports		
sections	3		
useable_sections	3		
absolute_feed_rate	0		
year	0		
Recycle	No		
diluent	NPH		
HOTLOC	0		
solvent_extraction_uni	CC		
CMFO	0.2		
TBP	1.4		
FOI_input	0	0	0
FAI_input	0	0	0
sec_cl	D	E	F
aq_feed_cl	F	F	F
org_feed_cl	X	X	X
aq_eff_cl	W		0
org_eff_cl	P	P	P
section_name	Extraction1	Extraction2	Extraction3
stages	1	1	1
QFAI	0	0	10
residence_time	20	20	20
section_type	1	1	1
FEOI_input	1	1	1
FEAI_input	1	0	0
QSOI			
QSAI			
org_sample_name			
aq_sample_name			
stage_efficiency	1	1	1
QFOI	20	20	20
number_of_scrubs	2		
pulse_column_section	0		
proc_temp	25		
ref_temp	25		
number_of_strip1s	0		
number_of_strip2s	0		
KHNO3			
KHF			
KH2C2O4			
number_of_ions	3		
number_of_cations	2		
concn_sec1			
concn_sec2			
concn_sec3	5.04	0.01	0.04
concn_sec4			
concn_sec5			
concn_sec6			
concn_sec7			
concn_sec8			
concn_sec9			
concn_sec10			
concn_sec11			
org_concn	1E-15	1E-15	1E-15
ion_names	H	Zr	F

Fig. 8. Export File in Fig. 7 Modified to Simulate the Flowsheet Given in Fig. 6

Table 2. Summary of Contacts Performed to Test the Solvent Extraction Flowsheet (Fig. 9)

Contact	Step	Aqueous Phase	Organic Phase	O/A	Organic Vol., mL
A	Extr 1	Feed ^a	TRUEX Solvent	0.33	8
B	Extr 2	From A	TRUEX Solvent	0.33	1
C	Extr 3	From B	TRUEX Solvent	0.33	0.67
D	Scrub 1	1.5M HNO ₃ + 0.05M H ₂ C ₂ O ₄	From A	1	7
E	Scrub 2	1.5M HNO ₃ + 0.05M H ₂ C ₂ O ₄	From D	1	6
F	Scrub 3	2.3M HNO ₃	From E	1.5	5
G	Scrub 4	2.3M HNO ₃	From F	1.5	4
H	Scrub 5	Water	From G	3	3.5
I	Scrub 6	Water	From H	3	3
J	Strip 1	0.21M HEDPA ^b	From I	3	2.5
K	Strip 2	0.21M HEDPA ^b	From J	3	2
L	Strip 3	0.21M HEDPA ^b	From K	3	1.5
M	Wash	0.21M Na ₂ CO ₃	From L	1	1

^aThe feed composition is 0.1M Zr, 1.14M Na, 0.049M K, 0.045M Al, 0.035M Si, 0.004M U, 0.0004M La, 0.37M F, 0.01M H₂C₂O₄, 1.7M H⁺, 1.9 x 10⁻⁸M Am, and 6.2 x 10⁻⁶M Pu.

^b1-hydroxyethane-1,1-diphosphonic acid.

As discussed in the case of clean organic-phase contacts, the testing of multiple organic feeds is presently only possible when using the GTM without the front end. To obtain an export file corresponding to Fig. 9, we created a similar one by using the front end and modifying it. The result is given in Fig. 10. The last two sections (12 and 13) have been cut in Fig. 10 since the GTM can only currently handle 11 sections when the front end is used. These two sections can be added when modifying the export file. Figure 11 shows the export file generated for Fig. 10. Figure 12 shows the modified export file corresponding to Fig. 9. We are also able to generate a summary of all the flow rates coming in and out, the composition of all feeds and effluents, and a stage-to-stage profile for each component in the process. The stage profile is shown in Fig. 13.

Other sequences of batch contacts can be simulated by the GTM by following a similar strategy as given here. In future versions of the GTM, we will include the possibility of having multiple organic feeds and more than 11 sections in the front end, making the creation of the export file simpler.

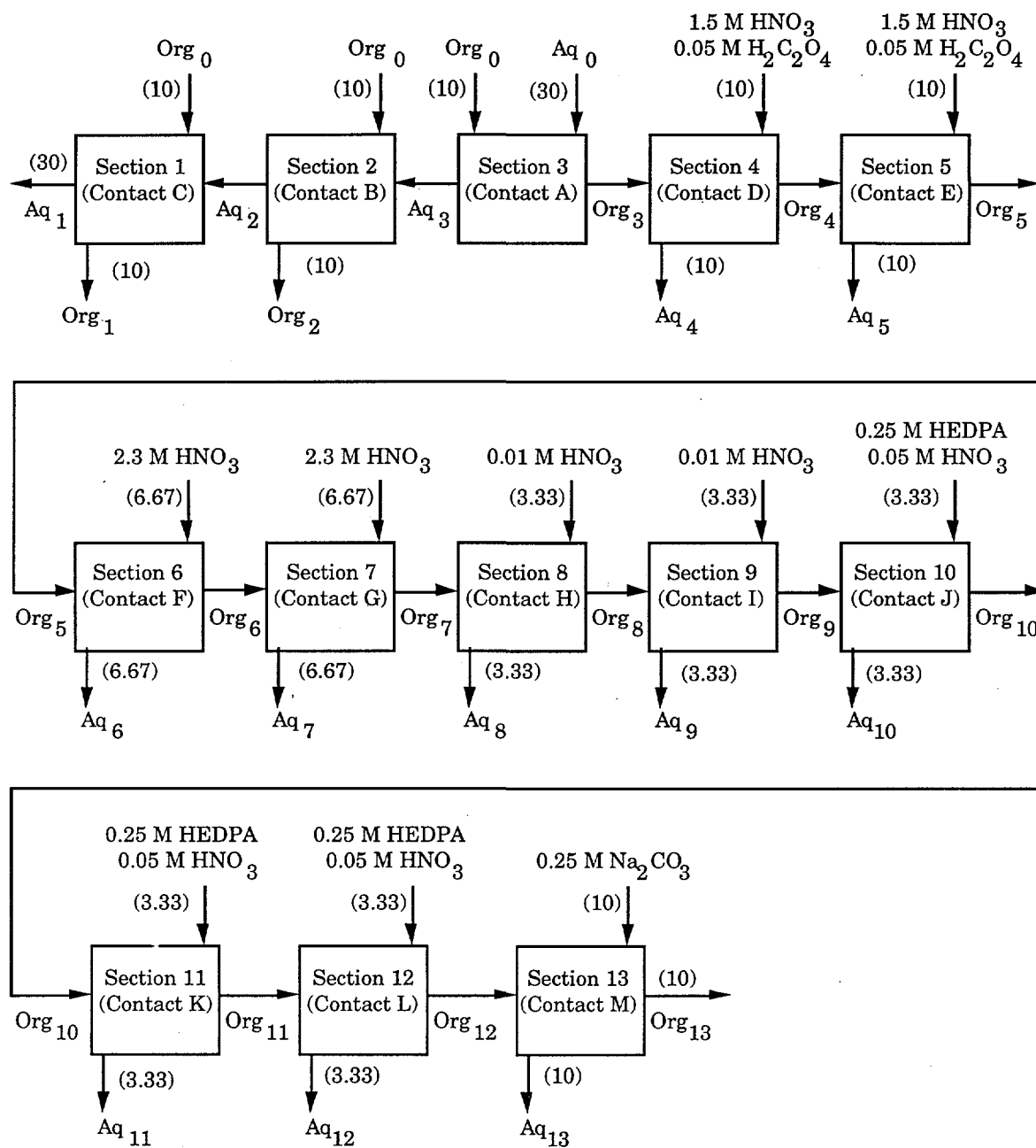


Fig. 9. Flowsheet for the Series of Contacts Given in Table 2. Org₀ is the TRUEX solvent, and Aq₀ is given in Table 2. Relative flow rates are given in parentheses.

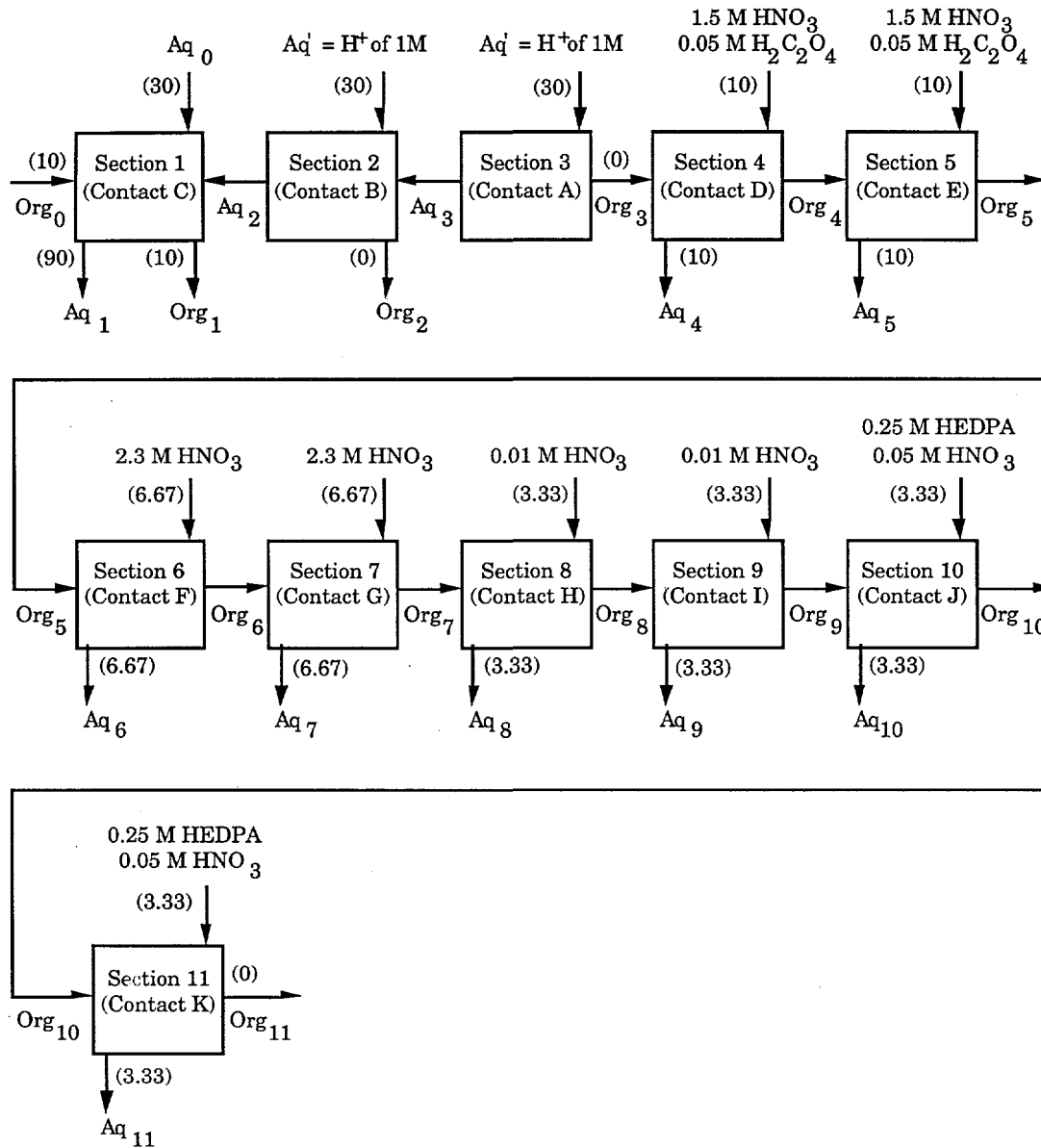


Fig. 10. Flowsheet Modified to Create a Similar Export File Corresponding to Fig. 9

Component Name	Phase	Section No. Stage No.	Stage-to-Stage Profile for each Component				
			1	2	3	4	5
			1	2	3	4	5
H	Aqueous	x, M	1.018E+00	1.205E+00	1.416E+00	1.661E+00	1.604E+00
	Organic	y, M	5.626E-01	6.315E-01	7.031E-01	6.418E-01	6.376E-01
	D(effective)		5.529E-01	5.240E-01	4.967E-01	3.863E-01	3.975E-01
Al	Aqueous	x, M	4.496E-02	4.497E-02	4.499E-02	4.494E-05	4.490E-08
	Organic	y, M	4.496E-05	4.497E-05	4.499E-05	4.494E-08	4.490E-11
	D(effective)		1.000E-03	1.000E-03	1.000E-03	1.000E-03	1.000E-03
Na	Aqueous	x, M	1.188E+00	1.188E+00	1.189E+00	1.187E-03	1.186E-06
	Organic	y, M	1.188E-03	1.188E-03	1.189E-03	1.187E-06	1.186E-09
	D(effective)		1.000E-03	1.000E-03	1.000E-03	1.000E-03	1.000E-03
La	Aqueous	x, M	3.422E-07	4.243E-06	5.039E-05	8.147E-05	7.635E-05
	Organic	y, M	1.170E-05	1.384E-04	1.049E-03	9.674E-04	8.910E-04
	D(effective)		3.420E+01	3.263E+01	2.081E+01	1.187E+01	1.167E+01
ZrO	Aqueous	x, M	7.813E-02	8.367E-02	9.073E-02	2.463E-02	3.077E-03
	Organic	y, M	1.660E-02	2.117E-02	2.782E-02	3.192E-03	1.142E-04
	D(effective)		2.125E-01	2.530E-01	3.067E-01	1.296E-01	3.712E-02
UO2	Aqueous	x, M	1.564E-10	4.724E-08	1.511E-05	3.849E-05	5.645E-05
	Organic	y, M	1.412E-07	4.518E-05	1.195E-02	1.192E-02	1.186E-02
	D(effective)		9.033E+02	9.564E+02	7.914E+02	3.096E+02	2.101E+02
Am	Aqueous	x, M	3.953E-12	7.908E-11	1.512E-09	2.524E-09	2.442E-09
	Organic	y, M	2.254E-10	4.300E-09	5.246E-08	4.994E-08	4.750E-08
	D(effective)		5.701E+01	5.438E+01	3.469E+01	1.979E+01	1.945E+01
Pu_4	Aqueous	x, M	5.908E-11	2.426E-09	1.237E-07	4.431E-07	6.779E-07
	Organic	y, M	7.102E-09	3.639E-07	1.823E-05	1.779E-05	1.711E-05
	D(effective)		1.202E+02	1.500E+02	1.473E+02	4.014E+01	2.524E+01
F	Aqueous	x, M	3.222E-01	3.345E-01	3.500E-01	4.794E-02	6.840E-03
	Organic	y, M	3.711E-02	4.648E-02	5.990E-02	1.197E-02	5.127E-03
	D(effective)		1.152E-01	1.389E-01	1.711E-01	2.496E-01	7.496E-01
C2O4	Aqueous	x, M	8.989E-03	9.370E-03	9.712E-03	4.158E-02	3.876E-02
	Organic	y, M	1.145E-03	1.026E-03	8.629E-04	9.282E-03	2.052E-02
	D(effective)		1.274E-01	1.095E-01	8.884E-02	2.232E-01	5.294E-01

Fig. 13. Stage-to-Stage Profile for All Components in Batch Contact Flowsheet

6	7	8	9	10	11	12	13
6	7	8	9	10	11	12	13
2.087E+00	2.235E+00	1.131E+00	6.463E-01	5.000E-02	5.000E-02	5.000E-02	1.000E-12
7.797E-01	8.230E-01	4.498E-01	2.380E-01	6.000E-03	6.000E-03	6.000E-03	1.000E-12
3.736E-01	3.682E-01	3.979E-01	3.682E-01	1.200E-01	1.200E-01	1.200E-01	1.000E+00
6.721E-11	1.006E-13	3.012E-16	9.019E-19	2.700E-21	8.085E-24	2.421E-26	2.418E-29
6.721E-14	1.006E-16	3.012E-19	9.019E-22	2.700E-24	8.085E-27	2.421E-29	2.418E-32
1.000E-03							
1.776E-09	2.658E-12	7.959E-15	2.383E-17	7.135E-20	2.136E-22	6.396E-25	6.389E-28
1.776E-12	2.658E-15	7.959E-18	2.383E-20	7.135E-23	2.136E-25	6.396E-28	6.389E-31
1.000E-03							
6.584E-05	6.235E-05	7.472E-05	1.069E-04	2.231E-03	6.678E-06	2.000E-08	1.998E-11
8.471E-04	8.055E-04	7.806E-04	7.450E-04	2.231E-06	6.678E-09	2.000E-11	1.998E-14
1.287E+01	1.292E+01	1.045E+01	6.969E+00	1.000E-03	1.000E-03	1.000E-03	1.000E-03
1.560E-04	1.204E-05	2.988E-06	1.719E-06	1.678E-06	5.024E-09	1.504E-11	1.501E-14
1.016E-05	2.128E-06	1.133E-06	5.605E-07	1.678E-09	5.024E-12	1.504E-14	3.452E-17
6.512E-02	1.767E-01	3.791E-01	3.261E-01	1.000E-03	1.000E-03	1.000E-03	2.300E-03
2.599E-05	1.809E-05	3.158E-05	4.654E-05	3.532E-02	1.268E-04	4.554E-07	5.460E-10
1.184E-02	1.183E-02	1.182E-02	1.180E-02	4.239E-05	1.522E-07	5.465E-10	4.805E-13
4.557E+02	6.539E+02	3.742E+02	2.536E+02	1.200E-03	1.200E-03	1.200E-03	8.800E-04
2.148E-09	2.075E-09	2.518E-09	3.670E-09	1.280E-07	2.689E-11	5.652E-15	3.956E-19
4.606E-08	4.468E-08	4.384E-08	4.262E-08	8.957E-12	1.883E-15	3.957E-19	2.769E-23
2.144E+01	2.153E+01	1.741E+01	1.161E+01	7.000E-05	7.000E-05	7.000E-05	7.000E-05
1.331E-07	5.053E-08	2.102E-07	6.849E-07	4.535E-05	4.313E-06	4.102E-07	1.434E-08
1.702E-05	1.699E-05	1.692E-05	1.669E-05	1.587E-06	1.509E-07	1.436E-08	1.721E-11
1.279E+02	3.361E+02	8.047E+01	2.436E+01	3.500E-02	3.500E-02	3.500E-02	1.200E-03
3.304E-03	1.878E-03	1.369E-03	9.972E-04	7.463E-04	5.363E-04	3.853E-04	3.275E-04
2.924E-03	1.671E-03	1.215E-03	8.829E-04	6.344E-04	4.558E-04	3.275E-04	3.275E-08
8.849E-01	8.895E-01	8.878E-01	8.854E-01	8.500E-01	8.500E-01	8.500E-01	1.000E-04
2.031E-02	7.312E-03	1.621E-03	7.570E-04	1.056E-03	7.711E-04	5.628E-04	5.065E-04
6.972E-03	2.094E-03	1.555E-03	1.303E-03	9.508E-04	6.940E-04	5.066E-04	5.065E-08
3.432E-01	2.864E-01	9.591E-01	1.721E+00	9.000E-01	9.000E-01	9.000E-01	1.000E-04

Fig. 13. (contd)

D. Modeling Studies of Zr and F Behavior

Data on TRUEX processing of a Neutralized Cladding Removal Waste (NCRW) were extracted from a report by Swanson³ and compared with GTM predictions. The NCRW sludge is currently being stored in underground tanks at the Hanford site (Richland, Washington). This sludge contains large amounts of zirconium and sodium compounds, primarily hydroxides and fluorides. It also contains U, Pu, and Am, and a mixture of fission products typical of those present in irradiated reactor fuel. In this study, the bulk of the sludge was first dissolved in nitric acid, then Am and Pu were extracted from zirconium and other inert components by the TRUEX solvent at appropriate extraction and scrubbing conditions.

To establish a correlation that accurately calculates distribution ratios for zirconium and fluoride, more information needed to be known about which zirconium species were present. To that end, we prepared a series of Zr/F/NO₃ solutions where zirconium was at the macro-concentration level, and contacted these solutions with the TRUEX solvent. Both organic and aqueous phases were analyzed for zirconium concentration by neutron activation analysis. These results were used to upgrade the model in the GTM that calculates distribution ratios for zirconium and fluoride. This was accomplished by evaluating two different sets of formation constants for Zr/F species: values reported by Kotrly and Sucha⁴ and values reported by Murphy⁵ for the Idaho Chemical Process Plant (ICPP). Two versions of the GTM were created. We then used the GTM to calculate zirconium and fluoride speciation in our experimental contacts. Our goal was to see if any of the different Zr/F species could be used to calculate the distribution ratio for zirconium. This could only be accomplished by obtaining the major species present in the aqueous phase and assuming the extractability of this dominant species.

Using the literature values for Zr/F complexes, we calculated that ZrF₂⁺ and ZrF₃⁺ were dominant species in the contact solutions. The ZrF₃⁺ was usually the dominant species, followed very closely by ZrF₂⁺. Since ZrF₃⁺ is not a neutral species, we decided to use ZrF₂⁺ instead, assuming it extracted as ZrOF₂. For the values reported by Ref. 5, we calculated that ZrF₂⁺ was the dominant species and, as in the case of the literature values, we assumed that ZrOF₂ was the extractable species. A model to calculate distribution ratios for zirconium was then proposed. The model assumes that the distribution ratio for zirconium was proportional to the concentration of ZrF₂⁺ in the aqueous phase. We then calculated the equilibrium constant by fitting our experimental data to the new model for both GTM versions.

After obtaining the equilibrium constant, we recalculated the distribution ratios for zirconium and compared them, one more time, to the experimental values. The version of the GTM that used the ICPP formation constants⁵ generated distribution ratios that were closer to the experimental values.

The new model using ICPP formation constants and assuming the extractability of ZrOF₂ was then validated with Swanson's data on TRUEX processing of real waste.³ The distribution ratios calculated for both zirconium and fluoride were in agreement with those reported by Swanson.³ Clearly, neither set of complexation constants (Refs. 4 or 5) is absolutely correct for the system. More detailed studies on Zr/F complexation and extraction of zirconium are still needed. As a result of our data collection, we have significantly improved our model to calculate

distribution ratios for both zirconium and fluoride. Additional Zr/F/NO₃ data will be looked at in order to improve our model further. The new data will be collected for low F/Zr ratios, where we have observed a strong dependence on nitrate activity.

E. Database Enhancement

The mechanistic- and thermodynamic-based equations in the GTM predict the solution and extraction behavior of TRUEX feed components over a wide range of possible waste stream and processing conditions. Efforts are continuing on adding extraction data for components of interest at DOE waste sites.

1. Reductive Stripping of Plutonium

A promising and potentially useful method for removing plutonium from the solvent phase in the TRUEX process is to reduce Pu(IV) to Pu(III). Plutonium(IV) has a large distribution ratio between the organic and aqueous phases, while Pu(III) has a much lower distribution ratio, expected to be similar to Am(III). Two important variables in this stripping procedure are (1) the rate of reduction of Pu(IV) to Pu(III) in aqueous solution, since the reducing agents used are not soluble in the solvent phase, and (2) the distribution ratio of Pu(III) as a function of acid concentration.

a. Rate of Reduction

Solutions containing 8.6×10^{-4} mg of Pu(IV) in 0.02M HNO₃ were made 0.1M in ascorbic acid and 0.005M in hydroxylamine nitrate (the reducing agents). These solutions were allowed to stand for varying amounts of time (4 to 18 min) and then extracted with TRUEX/NPH solvent. The distribution ratio is a measure of the rate of reduction. The results are shown in Table 3. The distribution ratio in the control sample, 18.7, is that expected for Pu(IV). The distribution ratios in the reduced solutions were low, 0.26 to 0.3. At 0.02M HNO₃ the distribution ratio for ²⁴¹Am is about 0.05. If the ratio for Pu(III) is similar, then about 2% of the plutonium remained in the IV state. These results call for a study of the reduction conditions necessary to obtain more complete reduction.

Table 3. Rate of Reduction of Pu(IV) to Pu(III)
with Ascorbic Acid and Hydroxylamine

	Dist. Ratio	Material Balance, %
Control ^a Reduction	18.7	96.5
4 min	0.30	99.5
8 min	0.30	99.6
18 min	0.26	99.1

^aNo reducing agent.

b. Distribution Ratio of Pu(III)

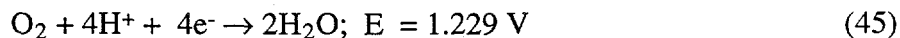
Reductive stripping of Pu(IV) can be an effective means to recover plutonium from the TRUEX solvent. This is true because Pu(III) distribution ratios are orders of magnitude lower than those for Pu(IV) at the same nitric acid concentration. Thus, Pu(III) distribution ratios were measured as a function of nitric acid concentration between 0.01 and 2.0M. Although the distribution ratio for Pu(III) should be very similar to that for Am(III) (the latter ratio had been measured and studied earlier), a direct measurement for Pu(III) to confirm this hypothesis was needed. Distribution ratios for Pu(III) were measured at four acid concentrations (0.01, 0.05, 0.5, and 2M) by contacting the aqueous phases four successive times with pre-equilibrated TRUEX/NPH. Ascorbic acid (with hydrazine hydrate present as a nitrite "getter") was used as the reducing agent. To ensure that the reduction was complete, four successive extractions were performed since each extraction preferentially removes Pu(IV), which has a distribution ratio greater than that for Pu(III). Thus, at the fourth extraction no Pu(IV) should remain. Small amounts of Pu(IV) would give erroneously high ratios. The initial plutonium concentration in the aqueous phase was about $1.6 \times 10^{-8}M$. The ascorbic acid and hydrazine concentrations were 0.14M and 0.11M, respectively. Contact time (vortexing) was 1 min at 25°C.

The distribution ratios obtained are given in Table 4 and plotted in Fig. 14, together with the ratios obtained earlier for Am(III). Comparison of the distribution ratios for Pu(III) and Am(III) shows reasonable agreement. The successive extractions for the Pu(III) gave regularly decreasing values. At 0.01 and 0.05M HNO₃, the plutonium ratio for the fourth extraction agrees with the americium ratio, while agreement is only fair for the other three extractions. At the two higher acid concentrations (0.5 and 2.0M), the agreement is also reasonable for the first two extractions (considering the counting errors), but by the third and fourth extraction, the results were very unreliable. To obtain good values, higher concentrations of plutonium are needed. The question marks in the table indicate that amount of plutonium remaining could not be measured accurately.

Table 4. Distribution Ratios for Pu(III) and Am(III) as a Function of Nitric Acid Concentration

[HNO ₃], M	Pu(III) Dist. Ratios				Am(III) Dist. Ratios
	Extr. #1	Extr. #2	Extr. #3	Extr. #4	
0.01	0.065	0.045	0.023	0.011	0.013
0.05	0.56	0.66	0.376	0.19	0.21
0.5	15.0	12.8	19.2	4.5(?)	11.4
2.0	40.0	44.5	81(?)	---	30.4

Another factor that should be considered in measuring distribution ratios by the mixing procedure used here is the large amount of air incorporated into the liquid phases during vortexing. The standard electrode potentials for the redox reaction are:



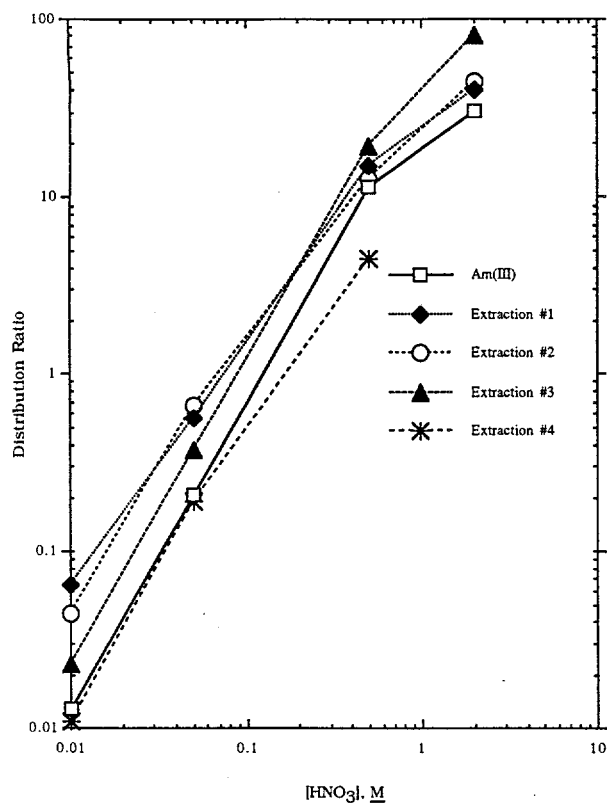


Fig. 14.

Distribution Ratios for Pu(III) and Am(III) between Nitric Acid and TRUEX/NPH as Function of Acid Concentration. See Table 4.

It is possible that some plutonium will be oxidized during vortexing, especially at the higher acid concentrations. Distribution ratios measured in 2M HNO₃ were higher than expected, and this may be due to Pu(III) oxidation. Oxidation of ascorbic acid by air may also occur, but since the aqueous phases remained colorless after vortexing, and only became discolored after standing overnight, this should not be a significant factor.

2. Behavior of Bismuth

The distribution of bismuth between the phases in the TRUEX process is important for the early Hanford waste contained in single-shell tanks because the initial method for separating plutonium from neutron-irradiated uranium used bismuth phosphate to coprecipitate plutonium and sodium bismuthate to oxidize Pu(IV) to Pu(VI). Thus, Hanford wastes contain large amounts of bismuth, on the order of grams per liter.

Present work on this project consists of using measurable amounts of bismuth (in the milligram range) to determine the distribution ratios for its extraction into the TRUEX solvent. A spectrophotometric method is being used to analyze the concentrations of bismuth in both the aqueous and organic phases after an extraction. This method measures the intensity of the yellow iodobismuth complex.⁶ For organic phase analysis, isopropyl is added to solubilize the organic phase in the aqueous potassium solution that develops the color.

The distribution ratio of bismuth was measured as a function of nitric-acid concentration (0.05 to 8.0M). The bismuth concentration in the aqueous was 1.5×10^{-3} M (0.3 mg/mL). The results are given in Table 5 and plotted in Fig. 15. As shown, the ratio

increases with increasing nitric acid concentrations until a maximum is reached at 1.0M HNO_3 . The ratio then decreases due to competition for CMPO by nitric acid, which is present in high concentrations relative to the bismuth and is also extracted. This decreases substantially the CMPO available to extract the bismuth. Americium shows a similar effect, and both bismuth and americium are 3+ ions in solution.

Table 5. Distribution Ratios for Bismuth as a Function of Nitric Acid Concentration at 25°C

$[\text{HNO}_3], \text{ M}$	Dist. Ratio
0.05	2.6
0.10	10.2
0.20	31.0
0.50	35.2
1.0	39.4
2.0	35.9
5.0	9.7
8.0	3.0

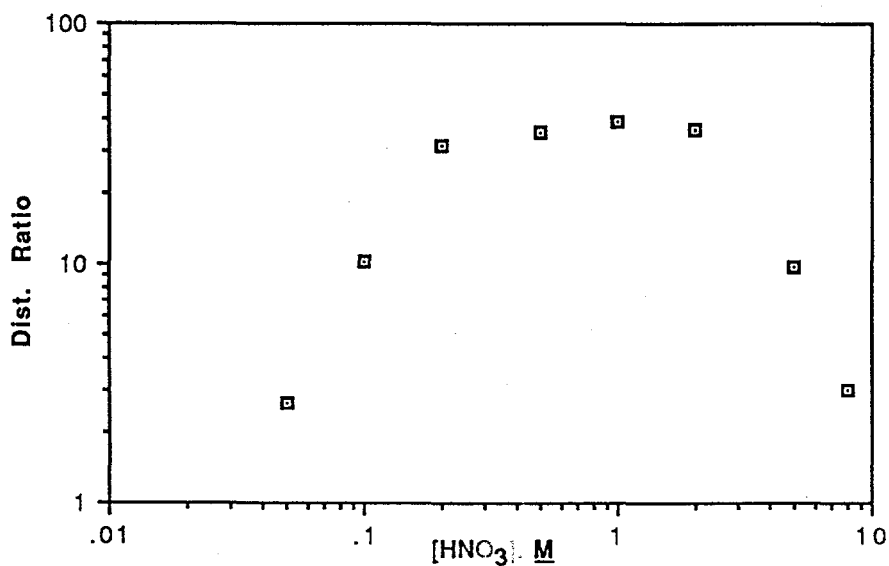


Fig. 15. Distribution Ratios for Bismuth as a Function of Nitric Acid Concentration at 25°C

III. CENTRIFUGAL CONTACTOR DEVELOPMENT

(R. A. Leonard, D. B. Chamberlain, C. J. Conner, D. G. Wygmans, and G. F. Vandegrift)

The Argonne centrifugal contactor is modified as necessary to work with specific solvent extraction processes. For each new process, solution densities and organic-to-aqueous (O/A) flow ratios are reviewed, and if necessary, the rotor weirs are modified. In support of our contactor development efforts, vibrational measurements are made with proximity probes and real-time analyzers. The results are related to rotor design by the use of a vibrational model for rotating systems. In FY 1993, we are using the centrifugal contactors to conduct a cold test of the TRUEX-SREX flowsheet. In addition, we are providing technical support for the processing of Mark 42 targets at Oak Ridge National Laboratory and of dissolved sludge from Hanford tanks.

A. Combined TRUEX-SREX Processing

A new solvent extraction process has been developed at Argonne that will selectively extract and partition U, Am, Pu, Sr, and Tc from Hanford dissolved sludge wastes (DSW). This process is a combination of the TRUEX process and the recently developed SREX (strontium extraction) process. This program is being carried out in cooperation with E. P. Horwitz, M. Deitz, and H. Diamond of the ANL Chemistry Division.

The cold tests (nonradioactive) of the TRUEX-SREX flowsheet will use a 20-stage centrifugal contactor system (2-cm minicontactors). The combined TRUEX-SREX solvent contains 0.2M CMPO, 0.2M crown ether (the specific crown ether is 4,4'(5')-di-t-butylcyclohexano-18-crown-6, usually referred to as CE), and 1.2M diamyl amyolphosphonate (usually written as DA[AP] or DAAP) in Isopar L. This combined solvent is designated here as PS12. As a part of the cold tests, aqueous samples will be taken from the bottom of selected minicontactor stages, and tetrahydrofuran-2,3,4,5-tetracarboxylic acid (THFTCA) will be used as the stripping agent. After the cold tests of the combined TRUEX-SREX flowsheet are completed and any process problems resolved, we will move on to a hot (radioactive) test of the process flowsheet.

During this report period, additional PS12 solvent was prepared, tested, and compared with earlier results. Because the dispersion number results were borderline acceptable, we tested the solvent in a 2-cm centrifugal contactor to assess its hydraulic performance. Based on these results, we are preparing for a cold test of the combined TRUEX-SREX flowsheet.

B. Solvent Properties

We carried out density, viscosity, dispersion number (N_{Di}), and one-stage hydraulic measurements for a new batch of PS12 solvent. The one-stage hydraulic tests indicate that the maximum throughput possible with the PS12 solvent is higher than predicted by the corresponding N_{Di} results. In an attempt to understand the difference between the N_{Di} and one-stage tests, our dispersion band model was extended by the use of Stokes law. Finally, the maximum throughput was measured for PS12 and compared with the value predicted by the N_{Di} measurements.

1. Density and Viscosity

The density and viscosity for the PS12 solvent used here are essentially the same as the values for the earlier batch of this solvent. These properties are 866 g/L and 5.2 mPa•s, respectively, compared with 865 g/L and 5.4 mPa•s measured earlier (ANL-95/4, p. 16). These differences are within experimental error, which is ± 1 g/L for the density and ± 0.2 mPa•s for the viscosity.

2. Dispersion Number

The dimensionless dispersion number (N_{Di}) for the PS12 solvent under aqueous-dispersed operation was measured in 100-mL graduated cylinders on a batch basis. The results, shown in Fig. 16, indicate that N_{Di} for the new PS12 solvent is lower by a factor of two when compared with earlier results for the PS12 solvent (ANL-95/4, pp. 16-17). The results shown in Fig. 16 are for two different aqueous phases, 0.1M HNO₃ and 0.25M Na₂CO₃. We did not examine any organic-dispersed cases with the earlier batch of PS12. However, for the new PS12 solvent, we had several organic-dispersed tests. These organic-dispersed cases, which are also included in Fig. 16, give N_{Di} values higher than any of those for the aqueous-dispersed tests. They suggest that, whenever possible, we should try to establish and maintain aqueous-dispersed (organic-continuous) conditions in the stages of the centrifugal contactor.

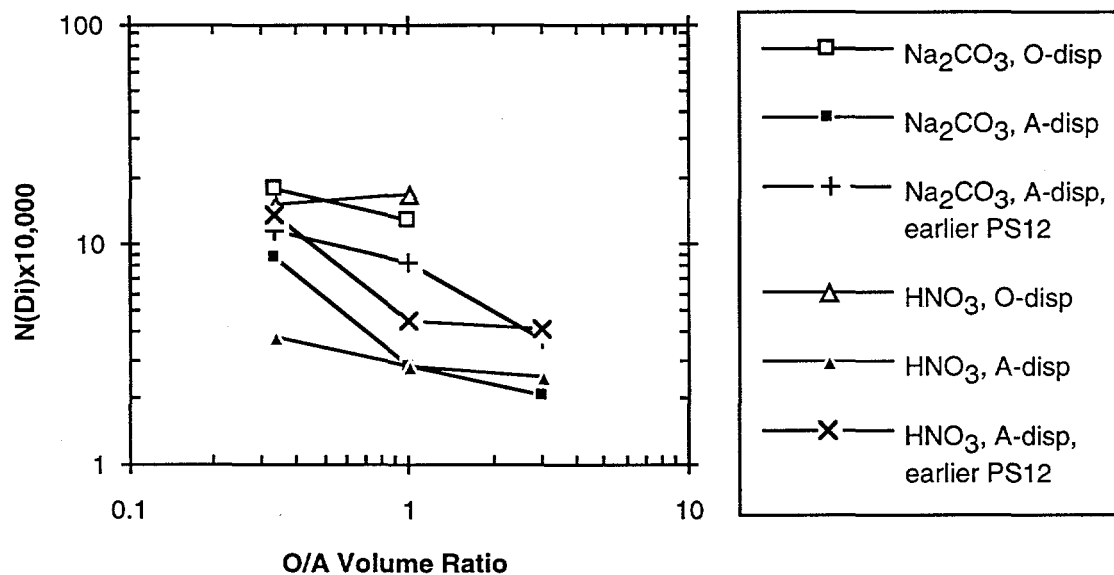


Fig. 16. Effect of O/A Ratio, Solvent Batch, Dispersed Phase, and Aqueous Phase Composition on Dispersion Number, $N(Di)$, for PS12

In addition to having lower N_{Di} values, the aqueous-dispersed conditions gave significant (>1%) other-phase carryover of aqueous phase in the organic effluent (A in O). Typical results, shown in Fig. 16, indicate no particular trend with respect to the choice of aqueous phase or the solvent batch. We did achieve slightly increased A in O at higher O/A volume ratios. The

organic-dispersed tests are not included in Fig. 17 because of their very low A in O values, typically <0.1%.

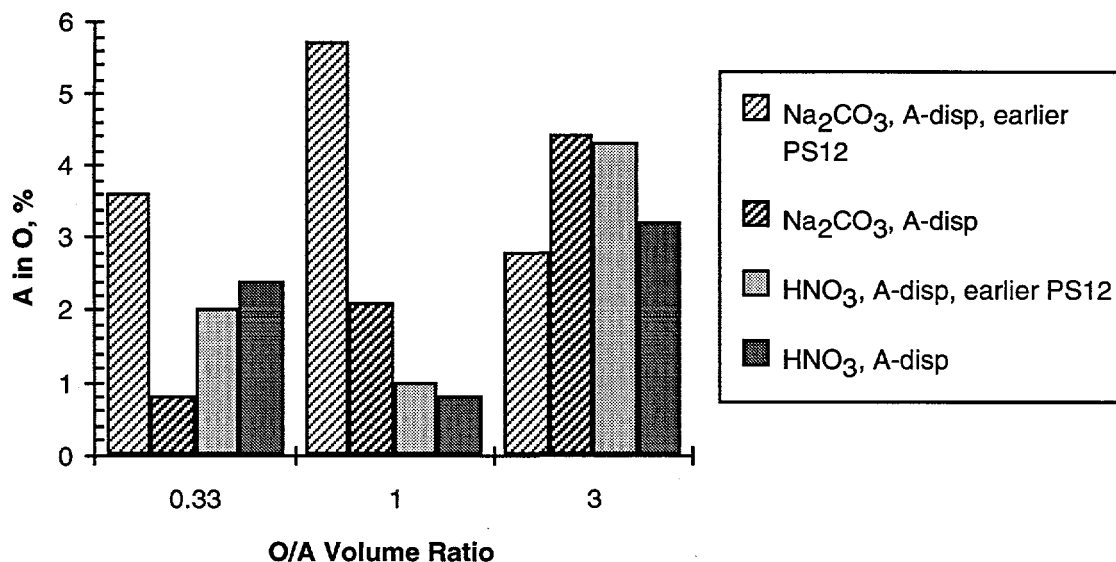


Fig. 17. Effect of O/A Ratio, Solvent Batch, and Aqueous Phase Composition on Amount of A in O for Aqueous-Dispersed Operation Using PS12

One possibility raised by the differences in N_{D_i} for these two batches of PS12 is that temperature had an effect. To check this, we measured N_{D_i} at 20, 25, and 30°C using the new batch of PS12 solvent, an O/A volume ratio of 1.0, and two different aqueous phases, 0.1M HNO₃ and 0.25M Na₂CO₃. The results, given in Fig. 18, show very little effect of temperature on N_{D_i} over this temperature range. However, the amount of A in O decreases with increasing temperature, as shown in Fig. 19. The organic-dispersed tests are not included here as they had very low A in O values, typically <0.1%. Also, we observed no aqueous-dispersed conditions for the 0.25M Na₂CO₃ tests at 30°C. Since the earlier batch of PS12 is no longer available, the effect of temperature on N_{D_i} and A in O could not be measured for comparison purposes.

In discussing the differences between the earlier and new batches of PS12 with P. Horwitz (Chemistry Division), he suggested that the crown ether may be the cause. It is a new product, exhibiting significant variations from batch to batch.

The lower values for N_{D_i} in aqueous-dispersed operation are very significant because we earlier observed that, for 30% TBP in normal dodecane (nDD), centrifugal contactors typically operate in an aqueous-dispersed manner for O/A flow ratios greater than about 0.5. The low results for the batch N_{D_i} values reported here show that, when the minicontactors are used, the maximum acceptable flow rate may be much lower than desirable. The current plans call for the organic flow rate to be 12 mL/min, based on a N_{D_i} of 8×10^{-4} . However, the batch N_{D_i} results suggest that the organic-feed flow should be only 3 mL/min, based on a N_{D_i} of 2×10^{-4} . At the lower flow rate, the sampling flow rates of 0.33 mL/min for eight of the 20 stages could become

very significant, and the contactor would take four times longer to reach steady state. Based on these results, we initiated single-stage 2-cm contactor tests to determine just how much lower, if any, the flow rate must be. These tests are reported next.

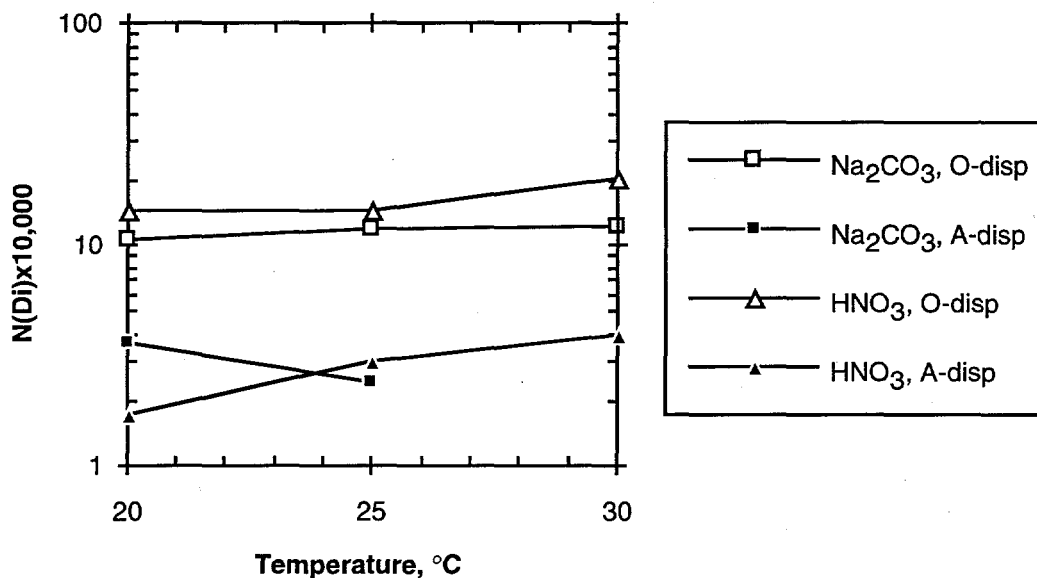


Fig. 18. Effect of Temperature, Dispersed Phase, and Aqueous Phase Composition on N_{Di} for PS12 at O/A Ratio of 1.0

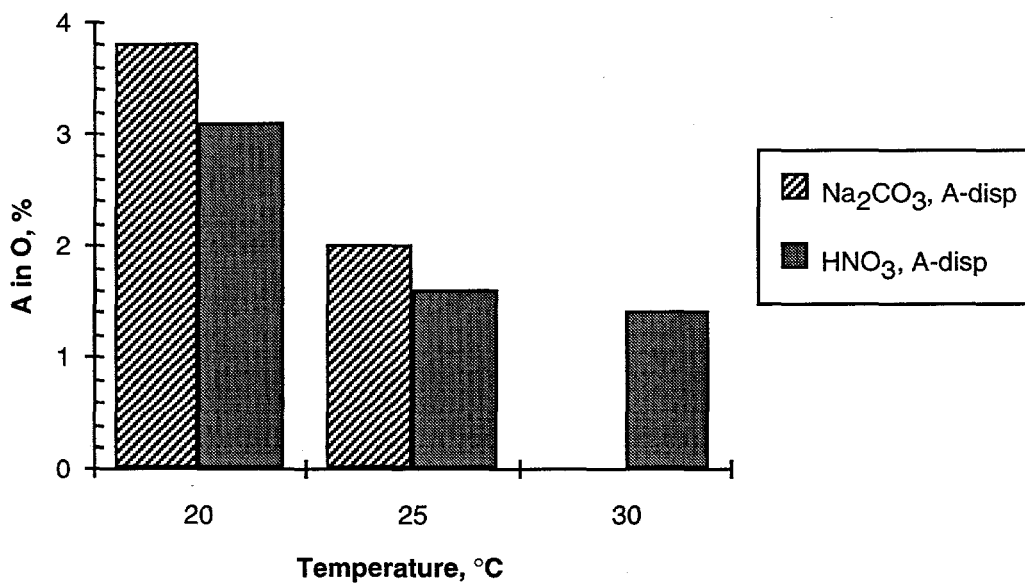


Fig. 19. Effect of Temperature and Aqueous Phase Composition on A in O for Aqueous-Dispersed Operation Using PS12 with O/A Ratio of 1.0

3. Hydraulic Tests

To evaluate the hydraulic performance of the 2-cm contactor for the TRUEX-SREX tests shown in Fig. 20, we performed single-stage contactor tests over the range of desired flow rates. In these tests, the aqueous phase was either 0.1M HNO_3 or $0.25\text{M Na}_2\text{CO}_3$, and the organic phase was the PS12 solvent. The results, given in Table 6, show that, for an organic flow rate of 12 mL/min , contactor operation will be good for aqueous (0.1M HNO_3) flow rates from 3 to 24 mL/min . In fact, at an O/A flow ratio of 1.0, operation at a total throughput of 48 mL/min was no problem. Additionally, for an organic flow rate of 12 mL/min , contactor operation will be good for aqueous ($0.25\text{M Na}_2\text{CO}_3$) flow rates of 6 mL/min .

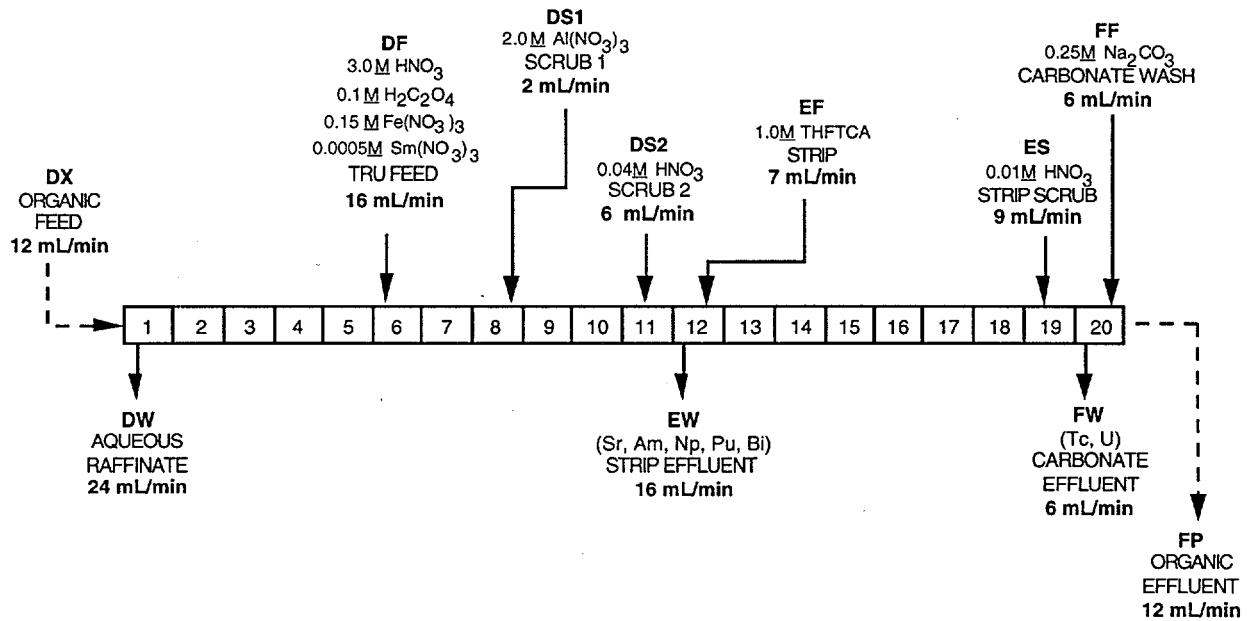


Fig. 20. TRUEX-SREX Flowsheet for Cold Tests

Table 6. Results of Hydraulic Performance Tests in Single-Stage 2-cm Contactor

Aqueous Phase	O/A Flow Ratio	Initial Continuous Phase	Flow Rate, mL/min	Other-Phase Carryover, %		Effluent Appearance	
				O in A	A in O	A	O
0.1M HNO_3	0.50	A	36.1	<0.1	0.04	sl. hazy	v. clr
0.1M HNO_3	0.49	O	36.1	<0.1	0.02	v. clr	v. sl. hazy
0.1M HNO_3	0.94	A	24.3	<0.1	<0.1	v. clr	v. clr
0.1M HNO_3	0.94	O	24.3	<0.1	<0.1	v. clr	v. clr
0.1M HNO_3	1.00	A	48.0	<0.1	0.03	sl. hazy	hazy
0.1M HNO_3	0.97	O	48.3	<0.1	0.06	sl. hazy	cloudy
0.1M HNO_3	1.84	A	18.2	<0.1	0.04	v. clr	v. v. sl. hazy
0.1M HNO_3	1.84	O	18.2	<0.1	0.04	v. clr	v. clr
0.1M HNO_3	3.63	A	15.1	<0.1	<0.1	v. clr	v. clr
0.1M HNO_3	3.18	A	15.8	<0.1	0.02	v. clr	v. clr
0.1M HNO_3	5.15	O	14.1	<0.1	<0.1	v. clr	v. clr
$0.25\text{M Na}_2\text{CO}_3$	1.94	A	18.5	<0.1	<0.1	v. clr	v. cldy
$0.25\text{M Na}_2\text{CO}_3$	1.91	O	18.4	<0.1	<0.1	v. clr	v. cldy

At each throughput and flow ratio, the test was done twice. In the one test, the initial phase in the mixing zone was the organic phase; in the other test, the aqueous phase. As a result, we get both organic- and aqueous-continuous operation, respectively, in the mixing zone if both types of operation are possible for that particular throughput and flow ratio. As Table 6 shows, the initial continuous phase had only a minimal effect on the results. These results indicate that the flow rates chosen for the TRUEX-SREX flowsheet can be used without any problem. Given the dispersion numbers above, we had expected that the operational flow rates would be as much as four times lower than the desired flow rates. A further surprise was the small amount of other-phase carryover. The dispersion numbers indicated that A in O should be 1 to 4%. Instead, all values for A in O were <0.1%.

This work shows that the dispersion number must be cautiously used to predict the hydraulic performance of centrifugal contactors.

4. Stokes Law Extension to the Dispersion Number

Initially, we thought the amount of A in O for the 0.25M Na₂CO₃ tests listed in Table 6 would be quite high because the organic effluent was so cloudy. Even after 28 h, the 48 mL of organic effluent (initially aqueous-continuous startup) in a 50-mL graduated cylinder showed only 1.0 mL of crystal clear organic phase at the top; the other 47 mL was still very cloudy. In addition, the 48 mL of organic effluent (initially organic-continuous startup) in a 100-mL graduated cylinder showed only 3.0 mL of crystal clear organic phase at the top; the other 45 mL was still very cloudy. However, when we extracted 30 mL of the organic phase from each cylinder and spun it in a laboratory centrifuge, the amount of aqueous phase was too small to be measured, less than 0.02 mL. Based on the dispersion number results, we had expected 2 to 6% A in O.

These results suggested a revised model for the coalescence of the dispersion band in the separating zone. This revised model consists of two parts: the present dispersion band model to which N_D applies, and a new non-dispersion-band model where other-phase droplets do not coalesce until they reach the bulk phase. In the second part of this model, the droplets act as solid spheres moving in the accelerational force field to the other-phase region. The dimensionless Reynolds number for the droplet as a spherical particle, N_{Re} , is given by

$$N_{Re} = \frac{D_p u \rho}{\mu} \quad (46)$$

where D_p is the particle diameter, u is the particle velocity relative to the continuous fluid, ρ is the fluid density, and μ is the fluid viscosity. If $N_{Re} < 0.1$, then Stokes law gives u (now the terminal velocity) as

$$u = \frac{a D_p^2 (\rho_p - \rho)}{18\mu} \quad (47)$$

where a is the accelerational force field, and ρ_p is the density of the particle (dispersed-phase droplet).⁷ The dispersion number implies that the droplet velocity (hence, the residence time in the

separating zone) is proportional to the square root of the acceleration. Stokes law implies that droplet velocity (hence, the residence time in the separating zone) is proportional to the first power of the acceleration. As a result, centrifugal contactors operating at 100 to 400 g's will be more effective than the gravity settling used in the standard N_{Di} test for cases which are controlled by non-dispersion-band operation. Thus, the unexpected results reported in Sec. III.B.2 occur because of the better performance that is possible in centrifugal contactors when separation is controlled by the movement of non-coalescing droplets in the continuous phase. The Stokes law model indicates that, for the results with 0.25M Na_2CO_3 in PS12, where the crystal clear region was only 5-mm thick after a day of gravity settling, the droplets of A in O must be on the order of 2 μm or less.

Applying Stokes law to the PS12 solvent, we calculated that a 2-cm contactor can extract droplets of 10 μm or greater (droplet velocity of 1.3 cm/min or greater). By contrast, the standard gravity-settling test used to measure N_{Di} can remove droplets 100 μm or greater (droplet velocity of 1 cm/min or greater).

5. Maximum Throughput for PS12 Solvent

To provide a better basis for comparing one-stage hydraulic performance tests with the gravity-settling N_{Di} results, we measured the maximum throughput of the PS12 solvent at an O/A flow ratio of 1.0. Because the contactor operates at high g forces, droplet movement in the viscous PS12 solvent will be faster (the Stokes law factor). As a result, the maximum throughput for the two phases ($q_{T,\text{max}}$) could be higher than that predicted by gravity-settling N_{Di} values. Note that $q_{T,\text{max}}$ is the point where, as the total flow increases, >1% other-phase carryover occurs in one of the effluent streams.

The single-stage 2-cm contactor (minicontactor) tests were made with an aqueous phase of 0.1M HNO_3 and an organic phase of PS12. The results, given in Table 7, show the effect of the initial continuous phase, the total throughput, and solvent aging. To make one phase the initial continuous phase, we fill the rotor with the more-dense phase (0.1M HNO_3). Then we stop this flow and allow the annular mixing zone to pump out as much liquid as it can. Finally we start the flow of the phase that is to be the initial continuous phase. After it is flowing out its effluent port for a period, the mixing zone should contain only this initial continuous phase when the flow of the other phase is started.

The $q_{T,\text{max}}$ depends on which phase was initially the continuous phase, as clearly seen in Table 7. When the aqueous phase was the initial continuous phase in the 2-cm contactor, $q_{T,\text{max}}$ was 84 ± 6 mL/min; when the organic phase, 41 ± 5 mL/min. For the organic-continuous tests, we saw greater than 1% other-phase carryover in both effluents at $q_{T,\text{max}}$. For this condition, N_{Di} for the separation of the two phases in the contactor rotor was calculated to be 2.1×10^{-4} . For the aqueous-continuous tests, we found greater than 1% other-phase carryover only for A in O at $q_{T,\text{max}}$. Thus, N_{Di} was greater than 4×10^{-4} for aqueous-continuous operation. These N_{Di} numbers for continuous-flow operation (2.1×10^{-4} and $>4 \times 10^{-4}$) show reasonable agreement with the equivalent batch N_{Di} numbers for the PS12 solvent (2.8×10^{-4} and 17×10^{-4} , respectively). Thus, the Stokes law factor does not seem to be as important as was expected.

Table 7. Maximum Throughput for PS12 and 0.1M HNO₃ in Minicontactor

Test No.	Date	Initial Cont. Phase	Total Throughput, mL/min	O/A Flow Ratio	Percent		Notes ^a
					O in A	A in O	
1	7/15/93	A	48.0	1.00	< 0.1	0.03	
2	9/24/93	A	78.2	0.94	< 0.1	0.2	
3	9/22/93	A	78.5	0.91	< 0.1	0.2	
4	9/22/93	A	79.2	0.97	< 0.1	0.5	q _{Max} =84±6 mL/min
5	9/24/93	A	89.3	0.92	< 0.1	2.5	> 1% A in O
6	9/22/93	A	91.0	0.95	< 0.1	0.9	> 1% A in O
7	9/22/93	A	101.0	0.93	< 0.1	1.4	> 1% A in O
8	9/24/93	O	36.5	0.91	< 0.1	0.2	q _{Max} =41±5 mL/min
9	9/24/93	O	45.9	0.86	5.3	11	> 1% both ø's
10	7/15/93	O	48.3	0.97	< 0.1	0.06	
11	9/24/93	O	57.0	0.84	7.4	19	> 1% both ø's
12	9/24/93	O	79.5	0.92	15	28	> 1% both ø's
13	9/24/93	O	90.0	0.88	17	31	> 1% both ø's

^a ø = other-phase carryover.

The PS12 solvent did seem to perform worse with age. This was deduced in two ways. First, it was observed qualitatively by the yellow tint of the solution. At first the solvent had a very light straw yellow color. By the end of the tests, its color was a deep yellow. Second, solvent changes were seen quantitatively by repeat tests for both aqueous-continuous conditions (tests 5 and 6, separated by two days) and organic-continuous conditions (tests 9 and 10, separated by two months). In each case, the first test was satisfactory (less than 1% other-phase carryover in both effluents), while the second test was not.

This work shows that the initial continuous phase is important. On the basis of these tests, we should always start the minicontactor with the aqueous phase and keep this phase flowing so that it will remain the continuous phase. The only time that the contactor would not be aqueous continuous is if the O/A flow ratio is so high that the only stable condition is organic-continuous operation.

C. TRUEX Processing of Mark 42 Targets

We supported the ORNL Radiochemical Engineering Development Center (REDC), formerly the Solvent Extraction Test Facility (SETF), in the TRUEX processing of Mark 42 targets. (These targets are aluminum-clad and contain PuO₂ in an aluminum matrix. They had been irradiated to a very high burnup.) Using the GTM, we designed a TRUEX flowsheet so that Pu, Am, and Cm could be recovered from these targets by using the three existing banks of 16-stage mini-mixer-settlers in a hot cell at REDC. We then worked with REDC people in formulating test plans. We also discussed initial test results with them. In FY 1994, we will work with REDC to better understand the analytical results as they become available. The data will be used to verify and improve the ability of the GTM to model flowsheets with very high solvent loading.

1. Flowsheet Development

The TRUEX flowsheet developed for processing Mark 42 targets is given in Fig. 21. The component concentrations in the various feed streams are given in Table 8 along with the component concentrations in the various effluent streams calculated using the GTM. While GTM calculations are normally done at 25°C, a temperature correction factor was added so that the D values for the Am, Cm, and rare earth components were evaluated at 45°C. No temperature correction factor was added to the D value calculated for plutonium, as it is not significantly affected by changing temperature.

The flowsheet was reviewed by ORNL personnel to ensure that it was compatible with the desired effluent concentrations and the special equipment requirements for TRUEX processing of Mark 42 targets at ORNL. Specific process design goals were to (1) reduce the concentration of transuranic elements in the aqueous (DW) raffinate to less than 100 nCi/mL, (2) allow less than 0.1% of the plutonium in the DF feed to leave in the Am (EW) effluent, (3) allow less than 0.1% of the Am, Cm, and rare earths in the DF feed to leave in the plutonium (FW) effluent, and (4) effectively strip plutonium from the solvent before it is recycled. Several aspects of the flowsheet are discussed: (1) feed composition, (2) ORNL equipment, (3) extraction section, (4) scrub sections, (5) first strip sections, (6) second strip section, and (7) solvent cleanup.

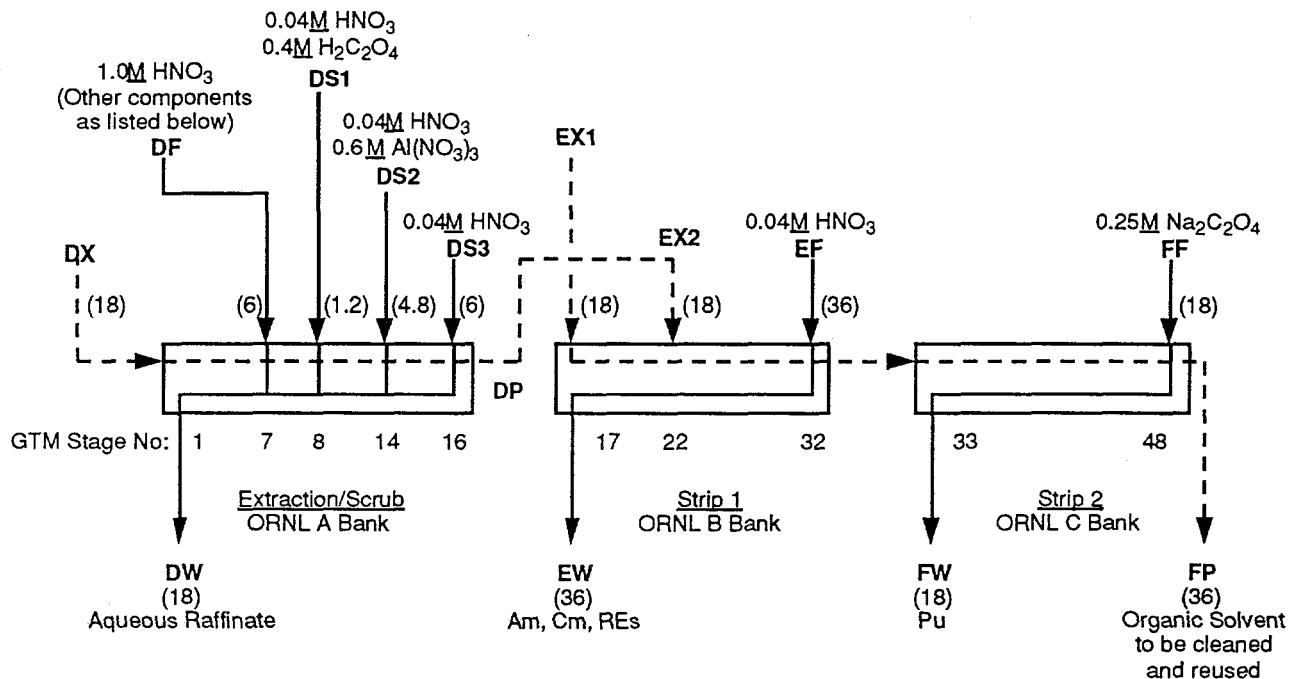


Fig. 21. TRUEX Flowsheet Calculated for Mark 42 Targets

a. Feed Composition

The expected composition of the DF feed to the TRUEX process is given in Table 8. It corresponds to one segment of a Mark 42 target, which consists of eight segments. This segment was dissolved in 15 L of 1M HNO₃. The initial caustic dissolution eliminates most of the Al matrix of the target, as well as most of the ³H, ¹²⁹I, ⁸⁵Kr, Si, Tc, and Cs. It should also eliminate some of the Sr and Zn. The DF composition includes the major components left after the caustic dissolution, except for the molybdenum. Molybdenum was omitted as it is not in the GTM. This omission should not be a problem as molybdenum is kept in the aqueous phase by the oxalate. To reduce GTM computation time as well as the size of the final report files, the rare earths are lumped together and included as the neodymium concentration, which is a typical lanthanide, the one with the highest concentration in the Mark 42 target.

Table 8. Calculated Concentrations of Various Feed and Effluent Streams

Stream Identity	Section Number	Section Name	Stage Number	Phase	Flow Direction	Flow Rates, mL/min	Component Concentration, M			
							H	Al	Cu	Mg
DX	1	Extraction	1	O	in	18	1E-15	1E-15	1E-15	1E-15
EX1	5	Strip_1_Scrub	17	O	in	18	0	0	0	0
EX2	6	Strip_1	22	O	in	18.0	0.1264	8.7E-08	4E-24	7E-23
DF	1	Extraction	7	A	in	6	1	0.015	0.004	0.064
DS1	2	Scrub_1	8	A	in	1.2	0.84	0	0	0
DS2	3	Scrub_2	14	A	in	4.8	0.04	0.6	0	0
DS3	4	Scrub_3	16	A	in	6	0.04	0	0	0
EF	6	Strip_1	32	A	in	36	0.04	0	0	0
DW	1	Extraction	1	A	out	17.9	0.286	0.1658	1.3E-03	0.021
EW	5	Strip_1_Scrub	17	A	out	36.1	0.1017	2.6E-07	1E-23	2E-22
FP	6	Strip_1	32	O	out	36.0	2.3E-03	2E-32	8E-49	1E-47

Stream Identity	Component Concentration, M								
	Nd	Zr	Cd	Pd	RuNO	Am	Pu(IV)	Cm	C2O4
DX	1E-15	1E-15	1E-15	1E-15	1E-15	1E-15	1E-15	1E-15	1E-15
EX1	0	0	0	0	0	0	0	0	0
EX2	0.0160	6.8E-10	5.5E-13	2E-23	4.4E-05	9.98E-04	3.7E-03	9.98E-04	6.2E-11
DF	0.048	0.019	0.003	0.024	0.021	0.003	0.011	0.003	0
DS1	0	0	0	0	0	0	0	0	0.4
DS2	0	0	0	0	0	0	0	0	0
DS3	0	0	0	0	0	0	0	0	0
EF	0	0	0	0	0	0	0	0	0
DW	1.3E-12	6.4E-03	1.01E-03	8.0E-03	7.0E-03	4.4E-14	6.8E-17	2.8E-13	0.0268
EW	8.0E-03	3.4E-10	3.9E-13	7E-23	5.5E-14	5.0E-04	2.0E-13	5.0E-04	3.1E-11
FP	5.2E-13	7.7E-15	3E-38	5E-48	2.2E-05	1.0E-13	1.83E-03	3.8E-15	2E-31

b. Equipment

The ORNL equipment for which this TRUEX flowsheet was designed consisted of three banks, each with a 16-stage mixer-settler. Organic and aqueous effluents can only be taken at the ends of a bank of mixer-settlers. However, a feed stream can be added to any

stage in a bank. The mixer-settlers in the shielded cell operate at 40 to 45°C. Only two pumps with special ORNL-design connections, called TRU connections, are available in the cell. These pumps were probably used for the DF and DX feeds. A third in-cell pump was required because the EX1 feed is also a hot (radioactive) feed. The pumps for the cold (non-radioactive) aqueous feeds are located outside the shielded cell. The banks of mixer-settlers are stacked one above the other so that the solvent can flow from the ORNL A bank to the B bank and then to the C bank (sections D, E, and F, respectively, of the flowsheet) by gravity.

Our information on the mixer-settlers is that they need to be operated between an O/A flow ratio of 1 and 10. For this range of O/A flow ratios, the operation is probably organic continuous, even though the unit is started up by introducing the aqueous phases first. The flowsheet was designed so that it stays within this range of flow ratios, except for the organic scrub section of the strip section, stages 17-21.

Results from two 1990 neodymium tests in the cold 16-stage mixer-settler at ORNL⁸ could not be used to estimate stage extraction efficiency. The data were difficult to use because there was some uncertainty in the feed flow rate. More important, however, the neodymium concentrations were so high that uncertainties in GTM modeling at high solvent loading needed to be resolved with the same data that would give extraction efficiency. However, extraction efficiency appears to be 80% or higher. For the GTM results given in Table 8, it was assumed that extraction efficiency was 100% at each stage.

A more important concern is the manner in which the DF feed is introduced into stage 7 in Fig. 21. If this feed is not mixed immediately so that most of the Am, Cm, and rare earths are extracted into the solvent, they will form an oxalate precipitate. The cold neodymium test which we proposed and which ORNL carried out (see below) was important, as it demonstrated that the DF feed was being properly injected.

The DF feed is held in a 20-L tank. Since it is operated at up to 75% of capacity, the DF feed for a test can be no greater than 15 L. It was thought that this tank would limit test duration. However, the key to test duration proved to be the organic solvent which provides both the DX and EX1 feeds. The solvent effluent (FP) was not recycled during a test. Since the total solvent inventory was less than 40 L, it limited the duration of each test to less than 18 h at a feed rate (both organic feeds) of 36 mL/min (2.16 L/h). Subtracting startup and shutdown times for the mixer settlers, actual run times were 10 to 14 h.

An evaluation of the 1990 neodymium tests in the cold mixer-settler at ORNL indicates that total throughputs on the order of 40-45 mL/min (2.4-2.7 L/h) are reasonable for this unit. The total throughput can be up to 83 mL/min (5 L/h) in the O/A flow ratio range from 1 to 10.⁸ On the basis of this information, we set the DF feed rate at 6 mL/min (0.36 L/h), as shown in Fig. 21. Thus, the highest process flow rate (both phases) is 72 mL/min (4.3 L/h), which occurs in the americium (also curium and rare earth) strip section of the first strip.

c. Extraction Section

For the aqueous raffinate to be a non-TRU waste, the alpha activity in the DW effluent must be less than 100 nCi/mL. To compensate for an extraction efficiency that might

be as low as 80%, the design criterion was set at 0.1 nCi/mL. For the DF feed chosen, this means that the decontamination factors (DF) must be 6×10^6 for plutonium, 3×10^6 for americium, and 6×10^8 for curium. The values on Table 8 indicate that these design criteria are met.

After the first hot test, the DW concentrations will very likely be controlled by the activity remaining in the solvent. If this is the case, the subsequent DW concentrations will indicate the effectiveness of solvent cleanup between runs. Based on our recent demonstrations of the TRUEX process at ANL, achieving 0.1 nCi/mL in the DW effluent will be very difficult. Problems occur due to undissolved plutonium colloid in the DF feed and to TRU elements entering the extraction section with the recycled solvent. However, a DW effluent of 10 to 100 nCi/mL is a realistic goal.

d. Scrub Sections

As shown in Fig. 21, there are three scrub sections. The first scrub section introduces the oxalic acid as a complexant, which keeps Zr, Ru, Rh, and Mo out of the solvent. The second scrub section introduces the aluminum, which keeps the oxalic acid out of the strip section, where the low acid concentrations would allow rare earth oxalates to precipitate. In addition, GTM calculations show that if oxalic acid were present at concentrations greater than $2 \times 10^{-7}M$ in the first strip, the plutonium would not separate from the Am, Cm, and rare earths. The desired separation is that (1) less than 0.1% of the plutonium ends up with the Am, Cm, and rare earths in the EW effluent and (2) less than 0.1% of the Am, Cm, and rare earths ends up in the FW effluent with the plutonium.

The third scrub section keeps the aluminum out of the strip section and, along with the second scrub, helps to control the nitric acid concentration in stage 22, where the rerouted organic DP effluent from the scrub section becomes the EX2 feed to the first strip section. On the basis of the GTM calculations of Am and Pu distribution ratios for various component concentrations, the optimum HNO_3 concentration in the equilibrated aqueous phase at stage 22 was determined to be $0.09 \pm 0.01M$. The stage-to-stage GTM calculations of the TRUEX flowsheet indicate that the concentration of HNO_3 will be slightly high here, $0.11M$, but this concentration is close enough to the optimum that it should still work well.

e. Oxalate Precipitation in the Extraction/Scrub Sections

If enough oxalate is added to the extraction section of the TRUEX flowsheet, the only components that will be extracted are the Pu, Am, Cm, and the rare earths. However, the addition of oxalic acid to the DF feed would immediately cause these elements to precipitate as oxalates. To avoid this, the required oxalate is added as oxalic acid in a separate DS1 feed to the first scrub stage.

To understand oxalate precipitation better, we used the SASPE in the GTM to determine the concentration of the various species in a given aqueous solution. A procedure, now included in the GTM, was developed so that one can do this easily. From literature data giving the overall component concentrations at which an oxalate precipitate appears, the species concentrations were calculated by SASPE. The solubility product was then calculated for $Pu(C_2O_4)_2$ as $[Pu][C_2O_4]^2$ and for $Am_2(C_2O_4)_3$ as $[Am]^2[C_2O_4]^3$. The solubility product for

$\text{Pu}(\text{C}_2\text{O}_4)_2$ was determined to be 9.5×10^{-22} , based on an arithmetic average of 28 data points.⁹ The median for these plutonium data is 5.6×10^{-22} ; the geometric mean, 3.8×10^{-22} . The solubility product for $\text{Am}_2(\text{C}_2\text{O}_4)_3$ was determined to be 1.2×10^{-25} , based on an arithmetic average of 24 data points.¹⁰ The median for these americium data is 6.6×10^{-26} ; the geometric mean, 3.7×10^{-26} . In applying the solubility product for $\text{Am}_2(\text{C}_2\text{O}_4)_3$ to the TRUEX flowsheet, we combined the concentrations of Am, Cm, and all the rare earths to give a single effective americium concentration.

Applying the americium solubility product ($K_{\text{sp,Am}}$) to the TRUEX Mark 42 flowsheet in Fig. 21, stage 8 is the stage closest to $K_{\text{sp,Am}}$; stage 7 is the next closest. However, even for stage 8, $K_{\text{sp,Am}}$ is a factor of 10 lower than the geometric mean.

Applying the plutonium solubility product ($K_{\text{sp,Pu}}$) to the TRUEX Mark 42 flowsheet, stage 8 is again the stage closest to $K_{\text{sp,Pu}}$; stage 7 is the next closest. The value for $K_{\text{sp,Pu}}$ in stage 8 is 4.9×10^{-22} , slightly above the geometric mean but less than the median. The value for $K_{\text{sp,Pu}}$ in stage 7 is 3.0×10^{-22} , slightly below the geometric mean. Thus, there was a real concern that a $\text{Pu}(\text{C}_2\text{O}_4)_2$ precipitate would occur at stage 8. The workers at ORNL were alerted to this possibility, but it did not occur. In the ORNL setup, precipitate formation is very easy to detect because the front wall of the settling zones is made of glass.

If, for example, two target segments are included in the 15 L of DF feed, then the higher concentrations of Am, Cm, and the rare earths in the DF feed stage would form a precipitate there. Because we were so close to the precipitation limit, we asked Dennis Benker and Kevin Felker at ORNL to test the extraction/scrub section experimentally, with neodymium as a stand-in for all the Am, Cm, and other rare earths in their cold 16-stage mixer-settler before the hot tests. As noted above, they did this test and found no problems.

f. First Strip Sections

As shown in Fig. 21, there are two first strip sections. The first section is a strip scrub section that uses fresh solvent, the EX1 feed, to scrub out plutonium from the EW effluent. The second section is the normal strip section where Am, Cm, and the rare earths are stripped from the solvent by dilute nitric acid. Because of the nitric acid in the EX2 feed, the Am, Cm, and rare earths are slightly pinched in the strip 1 scrub section. To model the reroute of the organic effluent from stage 16 to stage 22, we first had to modify the GTM. This ability to reroute stage effluents to a stage other than the normal next stage has been made available to all GTM users in version 2.7 (see Sec. II.A).

g. Second Strip Sections

We recommended $0.25\text{M Na}_2\text{C}_2\text{O}_4$ for use in the second strip section, where plutonium is stripped from the solvent. This is a very efficient operation and really needs only a small fraction of the stages provided. An alternative scrubbing agent would be $(\text{NH}_4)_2\text{C}_2\text{O}_4$. Based on ANL experience, this oxalate can be used safely. However, it was not recommended since ammonium nitrate, which would be formed, can cause problems under certain conditions. A safety review is required to be sure that these conditions will not occur. Ammonium oxalate does have the advantage of decomposing to gases when heated and leaving the plutonium

behind. If $\text{Na}_2\text{C}_2\text{O}_4$ is used, one can use an ion exchange column to separate sodium from plutonium. Alternatively, one can calcine the residual left after evaporation of the EW effluent, then remove the soluble Na_2O from the insoluble PuO_2 by dissolution of the Na_2O .

The plutonium solubility product for stage 33 of the TRUEX Mark 42 flowsheet, the plutonium strip stage with the highest $K_{\text{sp,Pu}}$, was calculated to be 6.5×10^{-26} . This is well below $K_{\text{sp,Pu}}$, so that we expected no $\text{Pu}(\text{C}_2\text{O}_4)_2$ to precipitate in this strip section, and in subsequent tests at ORNL, none was observed. This strip section works without plutonium oxalate precipitation because the acid concentration is low. This makes the oxalate ion concentration high, and so, ties up the $\text{Pu}(\text{IV})$ ion as a soluble tris-oxalato complex.

Because of familiarity with hydroxyl amine nitrate (HAN), ORNL used this as a plutonium stripping agent for the second hot test. Our objections to HAN were: (1) the reduction of $\text{Pu}(\text{IV})$ to $\text{Pu}(\text{III})$ is slow and the process may not be complete, and (2) nitrate salt is introduced. This salt increases the D value for $\text{Pu}(\text{III})$ and makes it harder to strip. Because of our objections, ORNL used a lower than normal HAN concentration.

h. Solvent Cleanup

Based on our experience at ANL, we recommended that the FP solvent be cleaned by washing two or three times with 0.25M Na_2CO_3 , followed by an acid rinse with 0.1M HNO_3 . Because the amount of radiolytic damage to the solvent can be large when curium is extracted, we recommended that the solvent quality be checked. If the solvent is degraded, it should also be passed through a column packed with activated neutral alumina particles.¹¹ Because of the difficulty in carrying out the Na_2CO_3 wash step in the shielded cell, only one Na_2CO_3 wash was used between ORNL tests.

To determine solvent quality for a TRUEX solvent with 0.2M CMPO and 1.4M TBP in NPH, the D value for americium should be measured at 0.01 , 0.05 , and 2.0M HNO_3 for the fresh solvent, the unwashed solvent, and the washed solvent. The alpha activity should also be measured to determine whether the final solvent has acceptable activity levels. The alpha activity should be less than allowed in DW. The D_{Am} value at 0.01M HNO_3 should be 0.02 ± 0.01 . This test is a sensitive measure of acid impurities and the degradation products that can limit the stripping of Am, Cm, and the rare earths. However, D_{Am} at 0.01M HNO_3 can be high and the solvent still give good process operation as long as D_{Am} at 0.05M HNO_3 is within specifications, that is, 0.23 ± 0.02 . This test at 0.05M HNO_3 is very important, as it is done at an acid level actually being used to strip Am, Cm, and the rare earths from the solvent in the process. If it is high, further solvent cleanup is required. The D_{Am} value at 2.0M HNO_3 should be 28 ± 3 . This D_{Am} gives a measure of CMPO loss as D_{Am} is roughly proportional to the concentration of CMPO to the third power. If CMPO is low, probably from solvent degradation, CMPO should be added to the solvent to increase D_{Am} for 2.0M HNO_3 to that of the fresh solvent.

Another factor affecting solvent quality is the loss of diluent. This is determined by measuring the increase in density between the fresh solvent and the used solvent (FP effluent). If required, diluent is added to the solvent to return it to its original density. Based on measurements at ANL, the density of fresh TRUEX solvent (0.2M CMPO and 1.4M TBP in NPH) should be 852 g/L at 25°C .

2. Flowsheet Implementation

The TRUEX Mark 42 flowsheet was tested four times at ORNL, one cold (non-radioactive) run and three hot (radioactive) runs. The cold run used a 16-stage mixer-settler carrying out the extraction/scrub operation in stages 1 through 16 of Fig. 21. The cold DF feed contained 0.065M Nd in 1.0M HNO₃. This neodymium concentration is essentially equal to the total rare earth plus actinide concentration expected in the hot DF feed.

The first and second hot runs used a "tracer" DF feed, which contained 2.5% of the normal DF feed diluted with 1.0M HNO₃. The first hot run followed the flowsheet shown in Fig. 21. The second hot run deviated from the flowsheet in two ways. First, the concentration of H₂C₂O₄ in the DS1 feed was lowered to 0.17M rather than 0.4M to assess what affect this might have on the plutonium separation from Am, Cm, and the rare earths in the first strip section. Second, the FF feed for the second strip section did not contain any sodium oxalate. Instead, its composition was 0.05M HAN and 0.01M HNO₃.

The third hot test used the normal DF feed as shown in Fig. 21. The plutonium strip (FF) flow rate was reduced from 18 mL/min (1.08 L/h) to 4.5 mL/min (0.27 L/h). The operation of the plutonium strip section had been close to its maximum flow rate in the first hot test, as deduced from the occasional appearance of emulsion (dispersion) in the plutonium (FW) effluent, so the FF flow rate was lowered to improve section operability. During the third hot test, the first strip section started to flood. To correct this, the EF feed rate was lowered from 36 mL/min (2.16 L/h) to 20.8 mL/min (1.25 L/h). The need for this change was surprising; the first strip section had not been a problem in the first two hot runs. This test was the last of the four tests done at ORNL.

In all four tests, mechanical operation of the equipment and the process went reasonably well. In particular, all dispersions separated at or near expected process flow rates, and no significant amount of oxalate precipitate was formed. Rough measurements of effluent concentrations based on their activity indicate that the TRUEX Mark 42 flowsheet was performing about as expected. When detailed analytical data are available, we will determine how well the GTM works at high solvent loadings. In particular, recent model developments that should improve the GTM at high solvent loadings (Sec. II.A) can be evaluated.

D. Construction of Minicontactors

Pacific Northwest Laboratory (PNL) is installing two pilot-scale centrifugal-contactor systems on the Hanford site in Richland, Washington. These systems will be used to evaluate solvent extraction flowsheets, especially the TRUEX process, for the cleanup of tank waste. In support of this work, we are building a multistage 2-cm (mini) contactor for PNL. Three sets of drawings, sent to PNL in September 1993, show the changes that will be made to the basic mini-contactor design to meet PNL needs. These changes include a common manifold for the exiting air for each bank of four stages, an electrical plug-in connection at the junction box for each rotor motor, and staggered lengths for the inlet and outlet tubes at each contactor stage so that one can access the Swagelok-type fitting more easily.

IV. VERIFICATION TESTS WITH PLUTONIUM-BEARING WASTES

(D. B. Chamberlain, C. J. Conner, J. C. Hutter, R. A. Leonard, D. G. Wygmans,
and G. F. Vandegrift)

Laboratory verification tests of the TRUEX process are being carried out to (1) develop a better understanding of the chemistry of the TRUEX process, (2) test and verify process modifications, and (3) verify the computer model being developed for predicting species extraction behavior and calculating flowsheets for treatment of specific wastes. Current verification tests are being completed using plutonium-residue solutions generated by the New Brunswick Laboratory (NBL). These solutions, generated from the analysis of plutonium samples, have been accumulating over the past several years at NBL and ANL. They contain varying concentrations of nitric, sulfuric, phosphoric, and hydrochloric acids, plus U, Pu, Np, and Am.

The TRUEX solvent extraction process, used to generate the nonTRU waste stream and recover the plutonium from the NBL waste, is being completed in a 20-stage 4-cm centrifugal contactor installed in a glovebox. The organic solvent is TRUEX-nDD. The nonTRU raffinate produced from the TRUEX process will be further processed to make it acceptable for handling by ANL's Waste Management by neutralizing the solution with NaOH so that the final pH is between 6 and 9. The plutonium oxalate stream will be further processed by evaporating the solution to dryness, then calcining the resulting solids in an oven at 600°C to produce PuO₂. The plutonium oxide will then be returned to Waste Management for disposal as a TRU waste.

Four batches of NBL waste have been processed over a period of two years. Two batches remain but will not be processed because of insufficient funds. The equipment used to process the NBL wastes has been completely removed from the glovebox used for these tests because no additional processing will be done, and the glovebox is needed for testing TRUEX-SREX flowsheets. Equipment removed from the glovebox was placed in 55-gal drums. These drums were disposed of as solid radioactive waste. Disposition of the Pu and U recovered from Batch 2 is discussed below. Details on the processing of Batch 3 and 4 are also reported.

A. Batch 2

The Pu and U recovered from the processing of Batch 2 were disposed of as solid radioactive waste. Originally, the oxide product was to be assigned a batch number, converted to metal, and shipped to the Idaho National Engineering Laboratory. However, the logistics in returning the recovered plutonium has proven to be costly, difficult, and time-consuming. Therefore, we were forced to dispose of the oxide as solid waste. Even though this material had to be disposed of as waste, there was a significant reduction in TRU waste volume.

B. Batch 3

With the removal of Batch 2 material, preparations were made for the receipt of Batch 3. Prerun preparations included a flowsheet analysis (with the GTM) to reduce the amount of americium recovered in the plutonium product, fresh solvent preparation and old solvent cleanup, and general glovebox cleanup. When the seven waste pails containing Batch 3 arrived, the contents of the pails, plus several bottles containing waste from sampling of Batch 2 and the acidified carbon-

ates from the previous run, were added to the feed tank. Once all of the solutions were combined, a sample was taken for various constituents. Processing was started and completed in one day.

1. Flowsheet Development

For Batch 2, the americium split between the americium product and the plutonium product was poor; approximately 50% of the americium ended up in the plutonium product. To increase the amount of americium recovered in the americium product, several changes to the originally planned flowsheet were investigated:

- Increasing the americium strip (EF) flow rate
- Decreasing the aqueous feed (DF) flow rate
- Increasing the organic solvent (DX) flow rate
- Increasing the scrub (DS) flow rate
- Changing the stage location and flow rate for the americium strip (EW)
- Increasing the number of stages in the americium strip section

These changes were evaluated using GTM Version 2.5a. Results from these runs are listed in Table 9.

All of the changes made to the flowsheet had little impact on the americium and plutonium recoveries. However, even these small changes can give a feel for what factors are important in obtaining good product streams. Based upon these GTM trials, we made the following observations:

- Increasing the organic solvent flow rate (DX) hurts americium recovery by increasing the amount of the americium in the plutonium product. This is probably due to the increased nitric acid that is extracted and brought into the americium strip section.
- Increasing the americium strip flow rate (EF) improves americium recovery but hurts plutonium recovery; more of the plutonium is stripped with the americium.
- Decreasing the aqueous waste feed rate (DF) from 120 to 100 mL/min decreases americium recoveries.
- Increasing the scrub flow rate (DS) has little impact on Am or Pu recoveries.
- Relocating EW from stage 11 to stage 12 significantly decreases americium recovery.
- Adding an eighth americium strip stage improves americium recoveries, while only slightly increasing the amount of plutonium in the americium product.

Table 9. Results from GTM Trials for Developing the Batch 3 Flowsheets

Changes to Flowsheets ^b	Flow Rates, mL/min				Am Strip Stages	Am Product Stream, %		Organic Product Stream, ^a %	
	DX	DF	DS	EF		[Am]	[Pu]	[Am]	[Pu]
1 Initial flowsheet ^c	50	120	30	50	7	99.91	0.17	0.09	99.83
2 Increased EF to 60 and EW to 3.6	50	120	30	60	7	99.84	0.38	0.16	99.62
3 Increased EF to 70 and EW to 4.2	50	120	30	70	7	99.93	0.54	0.07	99.46
4 Increased EF to 80 and EW to 4.8	50	120	30	80	7	99.96	0.66	0.04	99.34
5 Moved EW from stage 11 to stage 12	50	120	30	50	7	97.27	0.34	2.73	99.66
6 Added strip stage, increased EF to 60, and EW to 3.6	50	120	30	60	8	99.98	0.38	0.02	99.62
7 Added strip stage, increased DX to 60	60	120	30	50	8	97.14	0.04	2.86	99.96
8 Added strip stage, increased DS to 70, decreased DF to 100	50	100	70	50	7	98.82	0.14	1.18	99.86
9^d Added strip stage, increased DS to 60, held EW at 3	50	120	30	60	8	99.98	0.32	0.02	99.68
10 Added strip stage, increased EF to 70	50	120	30	70	8	99.99	0.37	0.01	99.63
11 Added strip stage, increased EF to 80	50	120	30	80	8	--e--	--e--	--e--	--e--
12 Decreased DF to 100	50	100	30	50	7	99.05	0.17	0.95	99.83
13 Added strip stage, decreased DF to 100	50	100	30	50	8	99.89	0.17	0.11	99.83
14 Added strip stage, decreased DF to 100, increased DS to 70	50	100	70	50	8	99.86	0.14	0.14	99.86

^a Because ammonium oxalate, the plutonium strip solution, has not been incorporated into the model, the Pu and Am concentrations in the organic product leaving the americium strip section were used to evaluate flowsheets.

^b Flow rates in mL/min.

^c This flowsheet was used as a comparison with other flowsheets. In this flowsheet, the EW effluent was removed from stage 11 at a rate of 3 mL/min.

^d This run selected as "best" flowsheet.

^e This flowsheet not modeled with the GTM.

Based upon these runs, the flowsheet modeled as Run 9 was selected for processing Batch 3 (Fig. 22). For this flowsheet, one stage was taken from the plutonium strip section

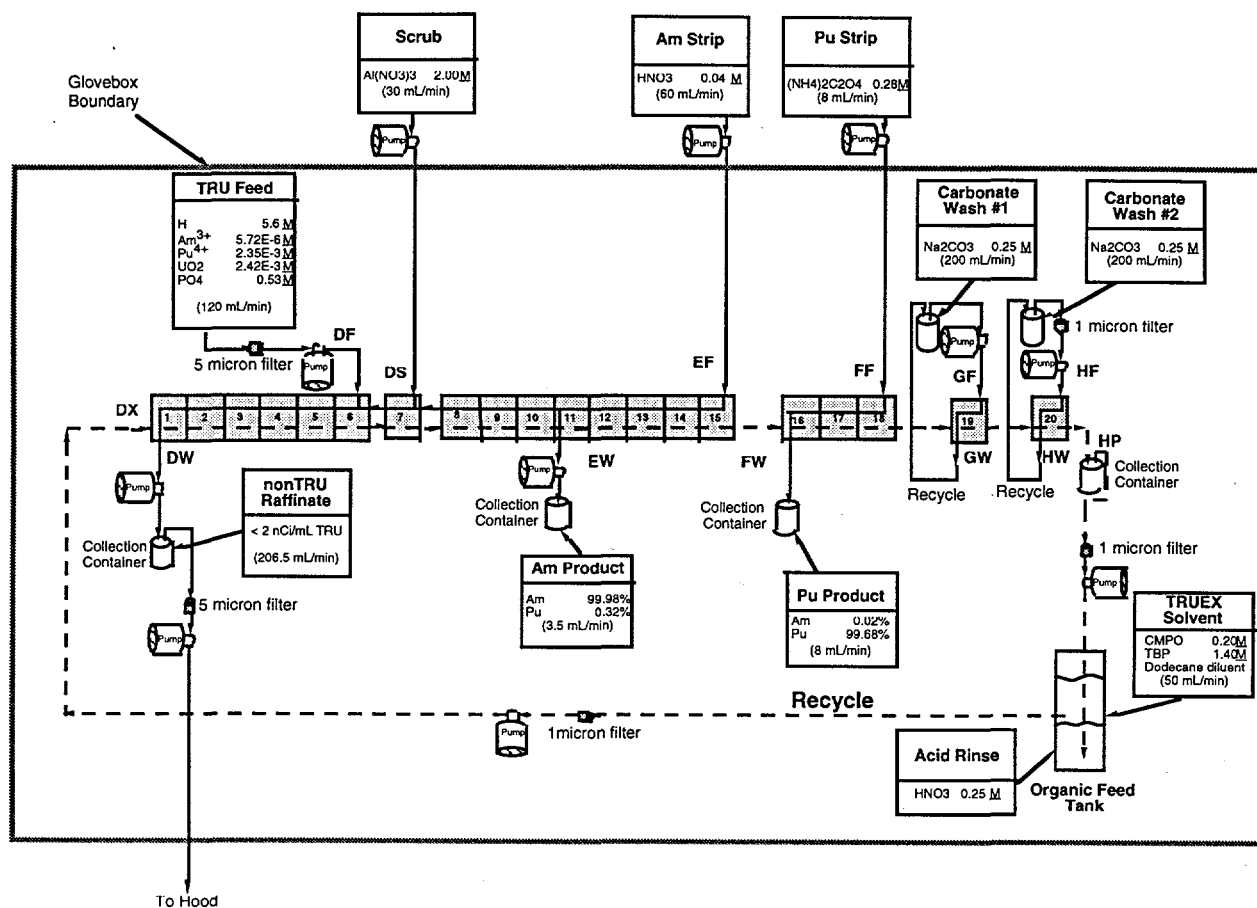


Fig. 22. Proposed Flowsheet for Processing Batch 3

and added to the americium strip section. This should not significantly impact plutonium recoveries since the distribution ratio for plutonium with 0.28M $(\text{NH}_4)_2\text{C}_2\text{O}_4$ is approximately 0.001. In addition, the scrub solution was increased from 50 to 60 mL/min.

2. Solvent Cleanup

Additional solvent was required to process Batch 3. Therefore, new solvent was prepared in two 1 liter batches and was checked for purity by determining the americium distribution ratios at 0.01 and 2M HNO_3 . These ratios for the new solvent compared favorably with the expected ones, as shown in Table 10.

Table 10. Check of Purity (determined by americium distribution ratio) for New TRUEX Solvent

Solvent Batch	Experimental		Expected ^a	
	0.01M HNO_3	2M HNO_3	0.01M HNO_3	2M HNO_3
Batch 1	0.0112	28.1	0.012	29.7
Batch 2	0.0102	25.6	0.012	29.7

^aFrom C. Conner, CMT Division.

A sample of the solvent used to process Batch 2 was taken the night before the run was scheduled to be completed. An aliquot of this organic was liquid scintillation counted, and the activity levels were far too high (128 dpm/ μ L) to be used without additional cleaning. Additional solvent cleaning is accomplished using an activated alumina column. Therefore, the morning of the run, 1 L of new solvent was used to load the alumina column that had been thoroughly cleaned. This kept the alumina column from being contaminated by the dirty organic during the loading process. The organic reservoir was also drained and thoroughly cleaned. The dirty solvent was contacted once with 0.25M Na_2CO_3 and run through the alumina column, where it was pumped back to the organic reservoir through fresh 0.1M HNO_3 to reacidify the solvent. The solvent was assumed to be clean and was used for processing Batch 3.

3. Description of Batch 3

The seven waste pails containing the waste to be processed as Batch 3 arrived on June 1, 1993. These pails contained an estimated 28.18 g of plutonium and 28.79 g of uranium. The composition of each waste pail as reported on the waste form is shown in Table 11.

Table 11. Composition of Batch 3 Waste Pails according to ANL Waste Requisitions

Waste Pail No.	No. of Bottles	Amount, g		
		Pu	U-235	U-238
287114	21	2.042	0.000	0.000
287345	21	1.682	0.001	0.209
388406	26	10.747	0.190	26.673
287263	18	1.678	0.000	0.000
288411	23	1.979	0.003	0.461
287302	18	2.987	0.545	0.447
287070	18	7.073	0.062	0.201
Total	145	28.18	0.801	27.99

The bottles from the waste pails were added to the feed tank on June 1-2, 1993. Two bottles were set aside that said "U Waste Only"; a small sample was taken from each bottle for liquid scintillation and gamma counting. Because gamma counting indicated the presence of Am-241 in the bottles, they needed to be processed and were added to the feed tank. Also, the sodium carbonate waste solutions from processing of Batch 2 Waste were acidified and then added to the feed tank, as were aqueous liquid waste bottles from the hoods. After all additions were made to the feed tank, the total volume was 58 L.

After mixing the feed tank, a sample was taken and analyzed by inductively coupled plasma/atomic emission spectroscopy (ICP/AES) for U and Pu, and by anion chromatography for F^- , Cl^- , NO_3^- , HPO_4^{2-} , and SO_4^{2-} . The results of the analysis are shown in Table 12. There was a substantial difference in the quantities of Pu and U reported for the waste forms (Table 11) and those determined by ICP/AES (Table 12). The difference is difficult to explain but could be because the ICP/AES determination of Pu and U is not accurate enough. Prior to taking any action, an analysis will be done on the oxide product to determine how much material was recovered. However, additional feed analysis might be necessary.

Table 12. Feed Composition Determined by ICP/AES and Anion Chromatography for Batch 3

Component	Concentration	
	$\mu\text{g/mL}$	M
U	115 ^a	4.8×10^{-4}
Pu	640 ^b	2.7×10^{-3}
F ⁻	32	1.7×10^{-3}
Cl ⁻	600	1.7×10^{-2}
NO ₃ ⁻	110,000	1.77
HPO ₄ ²⁻	18,000	0.19
SO ₄ ²⁻	1,340	1.4×10^{-2}

^aFor a feed volume of 58 L, the feed contains 6.67 g of uranium.

^bFor a feed volume of 58 L, the feed contains 37.12 g of plutonium.

4. Batch Tests

The other portion of the feed sample was used in a six-stage batch extraction test. The first extraction was done inside the glovebox. In a test tube, 2.43 mL of TRUEX-nDD, 5.81 mL of feed, 1.45 mL of 2M Al(NO₃)₃, and 2.74 mL of 0.04M HNO₃ were combined to simulate the ratio of the feeds in the extraction section. The tube was shaken and the phases separated. All of the aqueous and a small part of the organic were removed from the glovebox. The organic and aqueous phases were centrifuged to remove any entrained liquid and sampled. The aqueous phase was contacted five additional times with fresh organic at an O/A ratio of 0.24; both phases were sampled after each contact. The alpha distribution ratio for each extraction is shown in Table 13.

Table 13. Extraction Distribution Ratios from Batch Contacts with a Feed Sample

Extraction No.	Alpha Dis. Ratio
1	89.8
2	48.7
3	41.4
4	21.5
5	6.04
6	0.99

By the sixth extraction, the total alpha activity had been reduced to 1680 dpm/mL, which is <1 nCi/mL. The low distribution ratio in the last extraction stage suggests that the remaining alpha activity is due to some unextractable species. Based on the results of this batch test, Fig. 21 seemed adequate to process Batch 3. Therefore, processing started on June 10, 1993, and was completed in 9.5 h.

5. Processing of Batch 3

Processing proceeded smoothly, with only two major problems encountered during the run. The first problem was the loss of the americium strip feed at 325 min. The liquid level in the feed tank dropped below the level of the pump suction pickup. Additional feed was added to the tank to raise the level. However, loss of the strip feed for an unknown period of time seriously affected the overall flowsheet by allowing americium into the plutonium strip section and beyond. The second problem was the deterioration of the DF feed pump flow rate at 415 min. The DW flow rate was measured several times and was found to be decreasing. The feed filter was changed but did not significantly affect the DW flow rate. Therefore, the process was stopped, a new DF pump head was installed, and the process restarted. The DW returned to the appropriate flow rate. However, a cold feed was not used during the restart.

6. Analysis of Samples Collected during Processing of Batch 3

Samples collected during the processing of Batch 3 were both liquid scintillation and gamma counted to determine the Pu and Am concentrations in the various streams. Americium concentrations were determined by 59.5 keV gamma-ray. Plutonium concentrations were determined by scintillation counting and corrected for americium alpha activity. (The americium activity is calculated from the gamma count and subtracted from the scintillation activity to give plutonium concentration.) The plutonium concentration could not be corrected for uranium, as no uranium gamma-rays were seen in any of the samples. However, uranium is present in the feed, which will add to the overall scintillation counts. Thus, the reported plutonium concentrations are actually slightly higher than the actual concentration. For consistency in counting geometry, gamma samples were diluted as necessary to produce a 1 mL sample, and 10 mL of Ultima Gold was used as the scintillation fluid for all samples. The results reported are only preliminary; some samples have duplicates that were not in good agreement, and additional aliquots need to be taken and counted. Those samples not in good agreement are noted. A zero time was arbitrarily set as the time when the cold feed was switched to hot feed. Thus, samples taken prior to this point have negative sampling times.

For the sample analyses, the DW raffinate exited stage 1, where it was pumped to a 4-L surge tank located in the glovebox. Then, the raffinate was pumped from the surge tank into carboys located inside a Kiwani hood. The DW raffinate samples were collected from a line that exited into the carboy about every 15-20 min. In addition to total alpha activity, the concentrations of Am and Pu are reported in Table 14.

Figure 23 shows the total alpha activity in the DW raffinate. A small activity spike is seen after the switch was made from cold feed to hot feed at 0 min. A much larger spike is seen when the hot feed was restarted, after the feed pump failure at 445 min. When this pump was restarted no cold feed was used. This large activity spike in the raffinate emphasizes the need for use of a cold feed during startup. Figures 24 and 25 show the Am and Pu concentrations during the two startup spikes. Prior to the restart of the hot feed (DF), pump activity levels were at about 1 nCi/mL, well below the TRU limit of 100 nCi/g, but greater than the 0.1 nCi/g limit set by ANL's Waste Management. However, in the past, the precipitation that occurred during neutralization removed any residual activity down to <0.1 nCi/mL. To verify that raffinate contains some unextractable species, a batch contact using new TRUEX solvent and raffinate from sample DW 29

Table 14. Activity Levels in the NonTRU Raffinate (DW)

DW Sample No.	Time, min	Plutonium Concentration, g/L	Americium Concentration, g/L	Total Alpha, dpm/mL
1 ^a	-10	4.8E-05	5.4E-08	8.6E+03
2 ^a	-5	1.94E-05	1.71E-08	3.41E+03
3	1	2.56E-05	2.44E-08	4.53E+03
4	2	2.32E-05	1.21E-08	4.04E+03
5	3	3.99E-05	2.04E-08	6.93E+03
6	4	4.84E-05	2.84E-08	8.43E+03
7	5	5.64E-05	3.44E-08	9.83E+03
8	8	5.74E-05	3.24E-08	9.98E+03
9	9	5.55E-05	3.55E-08	9.69E+03
10 ^a	10	5.65E-05	3.45E-08	9.85E+03
12	11	4.68E-05	2.85E-08	8.15E+03
13 ^a	13	5.24E-05	3.00E-08	9.11E+03
14	18	3.31E-05	2.10E-08	5.77E+03
15	20	3.22E-05	2.22E-08	5.63E+03
16	22	3.05E-05	2.14E-08	5.33E+03
17	24	2.87E-05	2.23E-08	5.04E+03
18	67	1.68E-05	1.96E-08	3.01E+03
19	95	9.00E-06	1.71E-08	1.66E+03
20 ^a	105	8.02E-06	1.92E-08	1.51E+03
21 ^a	130	1.23E-05	1.92E-08	2.23E+03
22 ^a	160	1.13E-05	2.00E-08	2.07E+03
23 ^a	200	2.14E-05	1.90E-08	3.77E+03
24 ^a	242	1.58E-05	2.16E-08	2.85E+03
25	277	9.74E-06	2.37E-08	1.83E+03
26	315 ^b	9.71E-06	1.24E-08	1.74E+03
27	345	6.96E-06	2.55E-08	1.38E+03
28	376 ^b	8.24E-06	1.95E-08	1.55E+03
29 ^a	407	1.87E-05	1.38E-08	3.28E+03
30 ^a	445	9.37E-06	1.06E-08	1.67E+03
31 ^a	470	2.72E-04	1.75E-08	4.62E+04
32 ^a	472	1.07E-04	2.12E-08	1.83E+04
33 ^a	474	4.97E-05	2.58E-08	8.63E+03
34 ^a	476	3.51E-05	2.69E-08	6.15E+03
35 ^a	479	2.55E-05	3.04E-08	4.56E+03
36 ^a	501	1.05E-05	3.76E-08	2.07E+03
37	517	8.14E-06	3.54E-08	1.65E+03
38	547	7.70E-06	3.40E-08	1.57E+03
39 ^c	565	2.39E-05	2.28E-08	4.23E+03

^aDuplicate liquid scintillation counts not in good agreement.

^bTime is estimated.

^cDuplicate liquid scintillation sample not counted.

was performed. For O/A=2, a distribution ratio of 0.65 was obtained. This distribution ratio is too low for further TRU EX processing to be useful. Therefore, the raffinate was neutralized to pH 6-9 by using 10M NaOH and sent to Waste Management for disposal.

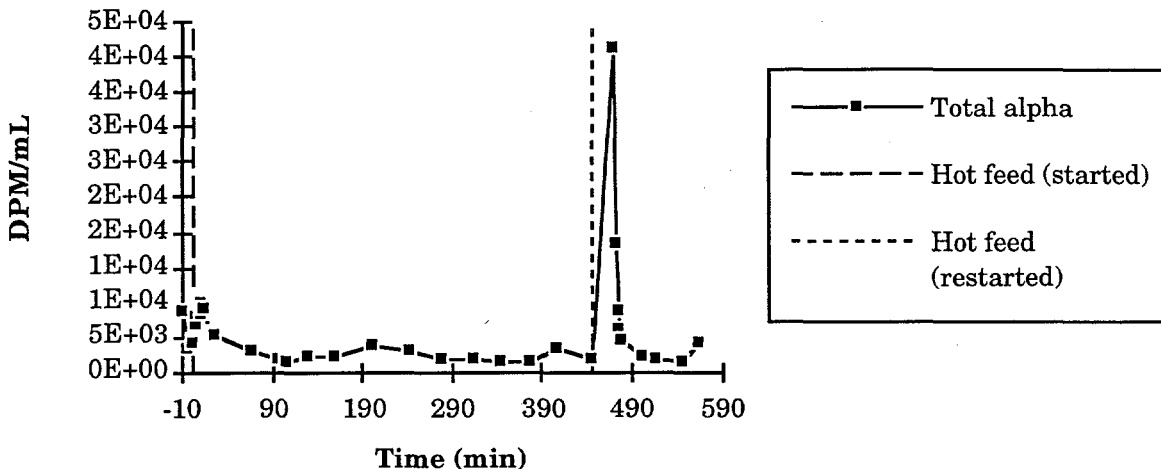


Fig. 23. Total Alpha Activity in the NonTRU Raffinate (DW)

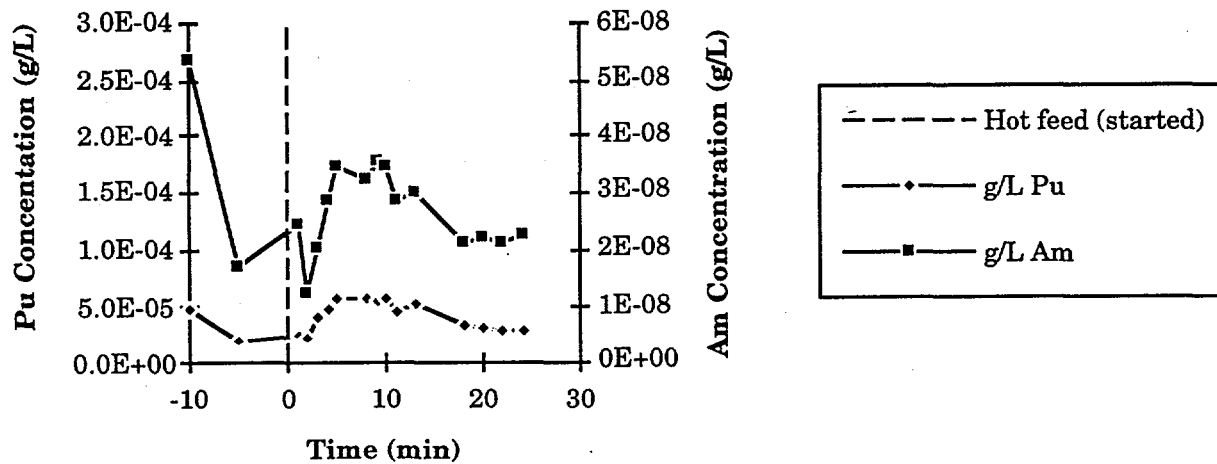


Fig. 24. Concentration of Americium and Plutonium in the NonTRU Raffinate (DW) during the Initial Startup

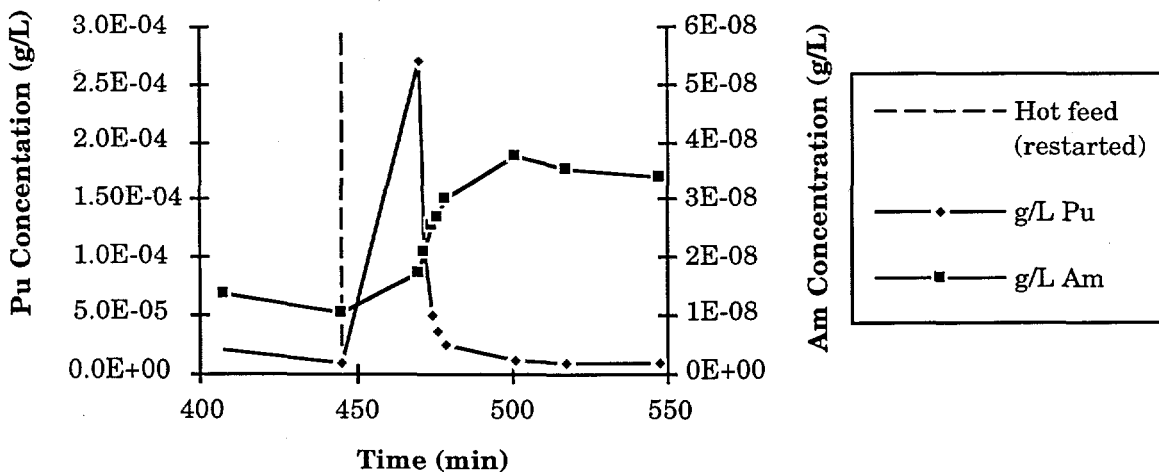


Fig. 25. Concentration of Americium and Plutonium in the NonTRU Raffinate (DW) during the Second Startup

The americium product stream (EW) is taken as a portion of the aqueous phase flowing from stage 11 to stage 10. Table 15 reports the Am and Pu concentrations in the americium product samples. Plutonium concentrations in this stream strongly depend on americium concentration. Therefore, plutonium concentrations are not very accurate. This table shows that the plutonium concentrations in this section are greater than the americium concentrations; this is not unexpected, as the plutonium concentration in the organic phase that enters this section is 270 times greater than the americium concentration.

Table 15. Activity Levels in the Americium Product (EW)

EW Sample No.	Time, min	Plutonium Concentration g/L	Americium Concentration, g/L	Total Alpha, dpm/ μ L
1 ^a	40	9.98E-02	9.01E-03	85,600
2	100	1.36E-01	1.40E-02	130,200
3	160	1.43E-01	2.03E-02	178,800
4	220	4.68E-01	1.64E-02	204,000
5	280	2.41E-01	2.75E-02	250,000
6	340	<0 ^b	4.13E-02	312,000
7	400	7.69E-01	1.57E-02	250,000
8	480	6.41E-01	1.86E-02	250,000
9	520	7.99E-01	2.31E-02	312,000

^aSample taken from collection tank not from contactor effluent. The following samples are collected from effluent leaving contactors.

^bConcentrations of <0 are obviously impossible; they occur due to the error in calculating plutonium concentration for this stream.

Figure 26 shows the Am and Pu concentrations in the americium product. As can be seen, the loss of the strip feed to this section had a significant effect on the concentration of americium in the EW raffinate. With the loss of this feed, nitric acid is not effectively scrubbed from the organic phase. Therefore, the americium D value remains high, and americium is not stripped from the organic phase but is carried over into the plutonium strip section. Figure 27

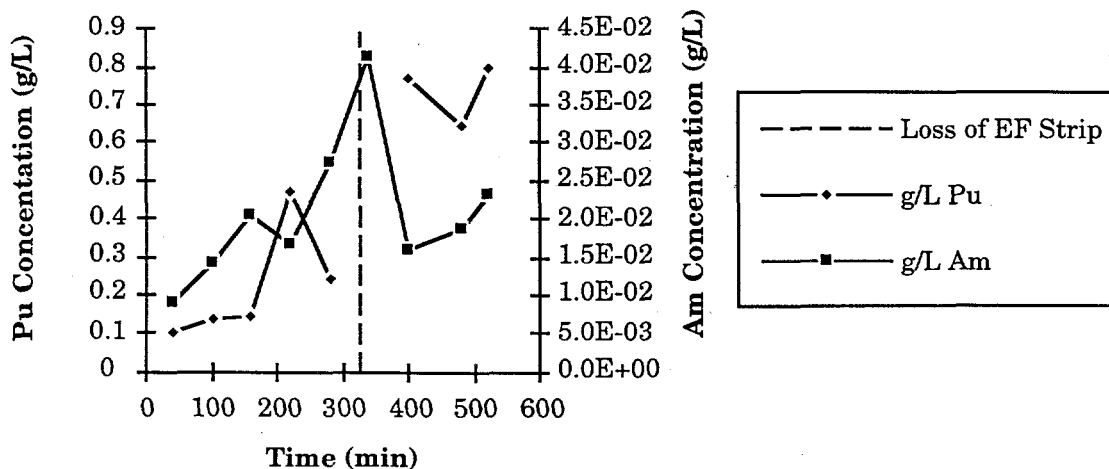


Fig. 26. Concentration of Americium and Plutonium in the Americium Product (EW)

shows the fraction of Am and Pu recovered in the americium product, as compared to the total amount recovered in both the Am and Pu products. As can be seen, the loss of the americium strip feed significantly affected the split of americium between these two raffinates. The fractional recovery in the americium product went from nearly 100% down to about 50%.

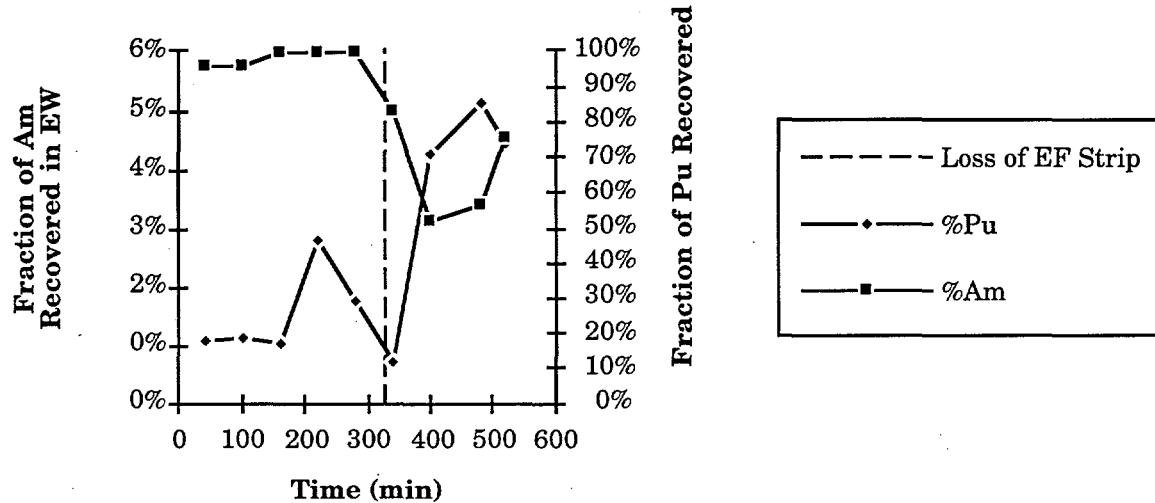


Fig. 27. Americium Split in the Americium Product (EW)

In the FW raffinate (plutonium product stream), the Pu and U are recovered by using an ammonium oxalate strip that exits stage 16. Figure 28 shows the Am and Pu concentration in the plutonium product. As was discussed earlier, when the americium strip was lost, a large increase in the concentration of americium was noted. Table 16 reports the Am and Pu concentration in the plutonium product samples, as well as the total alpha activity. The concentration of americium in this stream is 10-100 times lower than in the americium strip section.

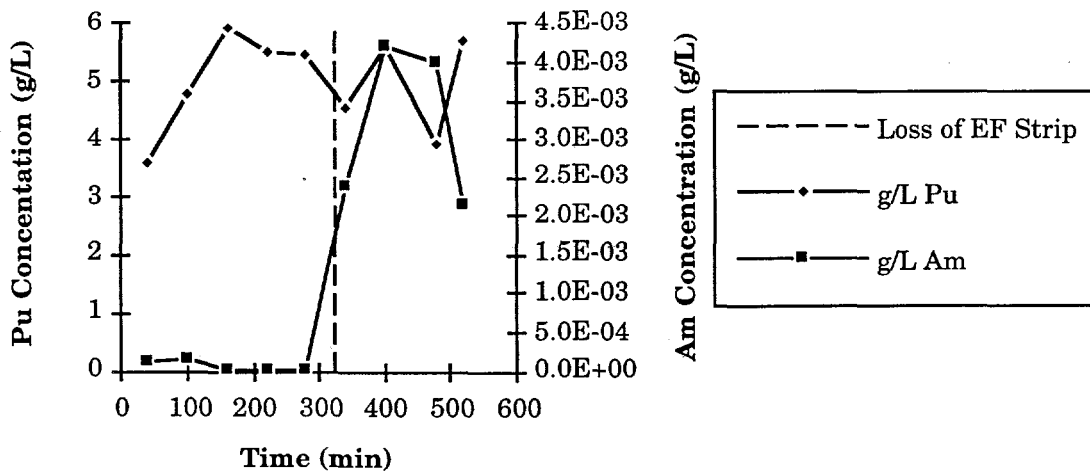


Fig. 28. Concentration of Americium and Plutonium in the Plutonium Product (FW)

Table 16. Activity Levels in the Plutonium Product (FW)

FW Sample No.	Time, min	Plutonium Concentration, g/L	Americium Concentration, g/L	Total Alpha, dpm/ μ L
1 ^{a,b}	40	3.61E+00	1.17E-04	614,000
2	100	4.80E+00	1.74E-04	816,000
3 ^a	160	5.93E+00	3.48E-05	1,010,000
4	220	5.51E+00	1.50E-05	936,000
5	280	5.49E+00	1.36E-05	932,000
6	340	4.56E+00	2.37E-03	792,000
7	400	5.62E+00	4.19E-03	986,000
8	480	3.94E+00	4.01E-03	698,000
9	520	5.71E+00	2.16E-03	986,000

^aDuplicate gamma-ray samples not in good agreement.

^bSample taken from collection tank, not from contactor effluent; following samples collected from effluent leaving contactors.

In the GF feed (first carbonate wash), the raffinate from this stream is recycled to the feed tank, which holds ~1.5 L of solution. Samples for this stream were collected from the feed tank. Table 17 reports the Am and Pu concentrations and total alpha activity in the first carbonate feed samples. This stream was replaced with the second carbonate feed at 265 min. At the same time, the second carbonate feed was replaced with fresh carbonate. This was done to alleviate the problem of excessive activity in the first carbonate wash. During processing, activity levels steadily built in the first carbonate wash feed. To slow the buildup, the plutonium strip feed was increased, at 52 min, to better strip Am and Pu from the solvent. Prior to running the next batch of waste, the carbonate raffinates will be acidified and added to the feed tank.

Table 17. Activity Levels in First Carbonate Wash Feed Samples (GF)

GF Sample No. ^a	Time, min	Plutonium Concentration, g/L	Americium Concentration, g/L	Total Alpha, dpm/ μ L
0	-20	1.1E-05	2.5E-08	2.0
1	40	1.12E-03	6.35E-07	195
2	100	2.97E-03	7.53E-07	509
3	160	4.53E-03	1.04E-06	776
4	220	6.38E-04 ^b	c	108 ^b
5	280	2.57E-03	7.47E-07	442
6	340	2.96E-03	2.18E-05	668
7	400	2.83E-04	3.32E-06	73.3
8	480	4.37E-03	1.94E-05	889
9	520	5.39E-03	1.92E-05	1,060

^a Samples collected from 1.5-L feed tank, not effluent from contactors.

^b The GW4 sample did not contain enough sample to count duplicates.

^c The GW4 sample did not contain enough sample to prepare aliquots for gamma counting.

The HF feed (second carbonate wash) is also recycled to a 1.5 L feed tank. Samples for this stream were collected from the feed tank. Table 18 reports the Am and Pu con-

centration and total alpha activity in the second carbonate feed samples. As stated earlier, this stream was replaced with fresh carbonate at 265 min.

Table 18. Activity Levels in Second Carbonate Wash Feed Samples (HF)

HF Sample No. ^a	Time, min	Plutonium Concentration, g/L	Americium Concentration, g/L	Total Alpha, dpm/ μ L
0 ^b	-20	1.1E-05	5.3E-08	2.27
1	40	1.37E-04	4.41E-07	26.6
2	100	2.26E-04	5.05E-07	42.3
3	160	2.99E-04	5.29E-07	54.7
4	220	7.21E-04	9.06E-07	122
5 ^c	280	2.98E-04	1.57E-07	51.8
6	340	2.60E-04	5.58E-06	86.6
7	400	3.51E-03	2.00E-05	749
8	480	3.29E-04	3.41E-06	81.9
9	520	3.80E-04	2.70E-06	85.0

^a Samples collected from 1.5-L feed tank, not effluent from contactors.

^b Duplicate gamma-ray counts not in good agreement.

^c Duplicate liquid scintillation counts not in good agreement.

The IF samples were taken from the 0.1M HNO₃ rinse that the organic phase bubbles through when it enters the solvent reservoir. The acid rinse reacidifies the organic phase before it is fed back to the contactors. The solvent needs to be reacidified before entering the contactors to prevent foaming in the extraction section. Table 19 reports the Am and Pu concentrations and total alpha activity in the IF samples.

Table 19. Activity Levels in Acid Rinse (IF)

IF Sample No.	Time, min	Plutonium Concentration, g/L	Americium Concentration, g/L	Total Alpha, dpm/ μ L
1	40	2.5E-05	3.4E-07	6.91
2 ^a	100	1.29E-05	7.07E-08	2.72
3	160	1.49E-05	9.43E-08	3.25
4	220	1.48E-05	5.76E-08	2.95
5 ^a	280	5.51E-05	6.08E-08	9.81
6 ^a	340	2.12E-05	1.10E-07	4.44
7	400	5.64E-05	1.25E-07	10.5
8	480	6.26E-05	9.99E-08	11.4
9	520	7.05E-05	1.02E-07	12.7

^a Duplicate gamma-ray counts not in good agreement.

The HP product stream (organic phase that leaves stage 20) is either pumped to the top of the alumina column or directly to the solvent reservoir, where it is bubbled through 0.1M HNO₃ to reacidify the solvent. Table 20 reports the Am and Pu concentrations and total alpha activity in the HP product samples.

Table 20. Activity Levels in the Organic Product (HP)

HP Sample No.	Time, min	Plutonium Concentration, g/L	Americium Concentration, g/L	Total Alpha, dpm/ μ L
1 ^{a,b}	40	1.2E-04	5.7E-08	21.4
2	100	5.23E-05	7.66E-08	9.46
3	160	4.17E-05	1.20E-08	7.17
4	220	4.90E-05	4.07E-08	8.62
5 ^a	280	4.01E-05	1.75E-08	6.94
6	340	4.27E-05	2.77E-07	9.35
7	400	2.04E-05	2.71E-08	3.66
8 ^a	480	1.26E-05	2.56E-08	2.34
9 ^a	520	2.76E-05	1.22E-08	4.78

^a Duplicate gamma-ray counts not in good agreement.

^b Duplicate liquid scintillation counts not in good agreement.

Most of the solvent that exited stage 20 (HP product) was run through the alumina column prior to being pumped into the solvent reservoir, where it was bubbled through 0.1M HNO₃ to reacidify. The alumina column "polishes" the solvent, removing most of the residual activity. Table 21 reports the Am and Pu concentrations and total alpha activity in the alumina column product (BC) samples.

Table 21. Activity Levels in the Alumina Column Product (BC)

BC Sample No.	Time, min	Plutonium Concentration, g/L	Americium Concentration, g/L	Total Alpha, dpm/ μ L
1	40	1.62E-05 ^a	1.25E-08	2.74
2	100	9.84E-06 ^a	b	1.67
3	160	6.7E-06 ^a	b	1.14
4 ^c	220	7.79E-06 ^a	1.24E-08	1.32
5	280	6.90E-06 ^a	b	1.17
6 ^d	340	1.95E-05 ^a	2.83E-07	3.30
7	400	3.16E-06 ^a	b	0.54
8	480	2.51E-06 ^a	b	0.43
9	520	4.04E-06 ^a	b	0.69

^a Not corrected for americium alpha activity.

^b Below detection level.

^c Duplicate gamma-ray counts not in good agreement.

^d Duplicate liquid scintillation counts not in good agreement.

The DX samples are a mixture of solvent that has been processed through the alumina column and solvent that has been pumped directly from stage 20 to the reservoir. Table 22 reports the Am and Pu concentrations and total alpha activity in the DX samples.

The Batch 3 processing is summarized in Fig. 29. The data shown in this figure are not the average over the whole run but are typical of the steady-state operation. The TRU concentration of the aqueous raffinate (DW) was approximately 1 nCi/mL, which is comparable to

Table 22. Activity Levels in the Organic Feed (DX)

DX Sample No.	Time, min	Plutonium Concentration, g/L	Americium Concentration, g/L	Total Alpha, dpm/ μ L
1	40	1.4E-04	1.4E-06	34.5
2 ^a	100	1.82E-05	3.36E-08	3.34
3	160	1.63E-05	1.95E-08	2.92
4	220	8.48E-06	1.41E-08	1.55
5	280	9.81E-06	1.59E-08	1.79
6	340	1.75E-05	1.70E-07	4.26
7 ^a	400	6.55E-06	2.86E-08	1.33
8	480	8.67E-06 ^b	c	1.47
9 ^a	520	1.20E-05	2.12E-08	2.19

^a Duplicate gamma-ray counts not in good agreement.

^b Not corrected for americium alpha activity.

^c Below detection level.

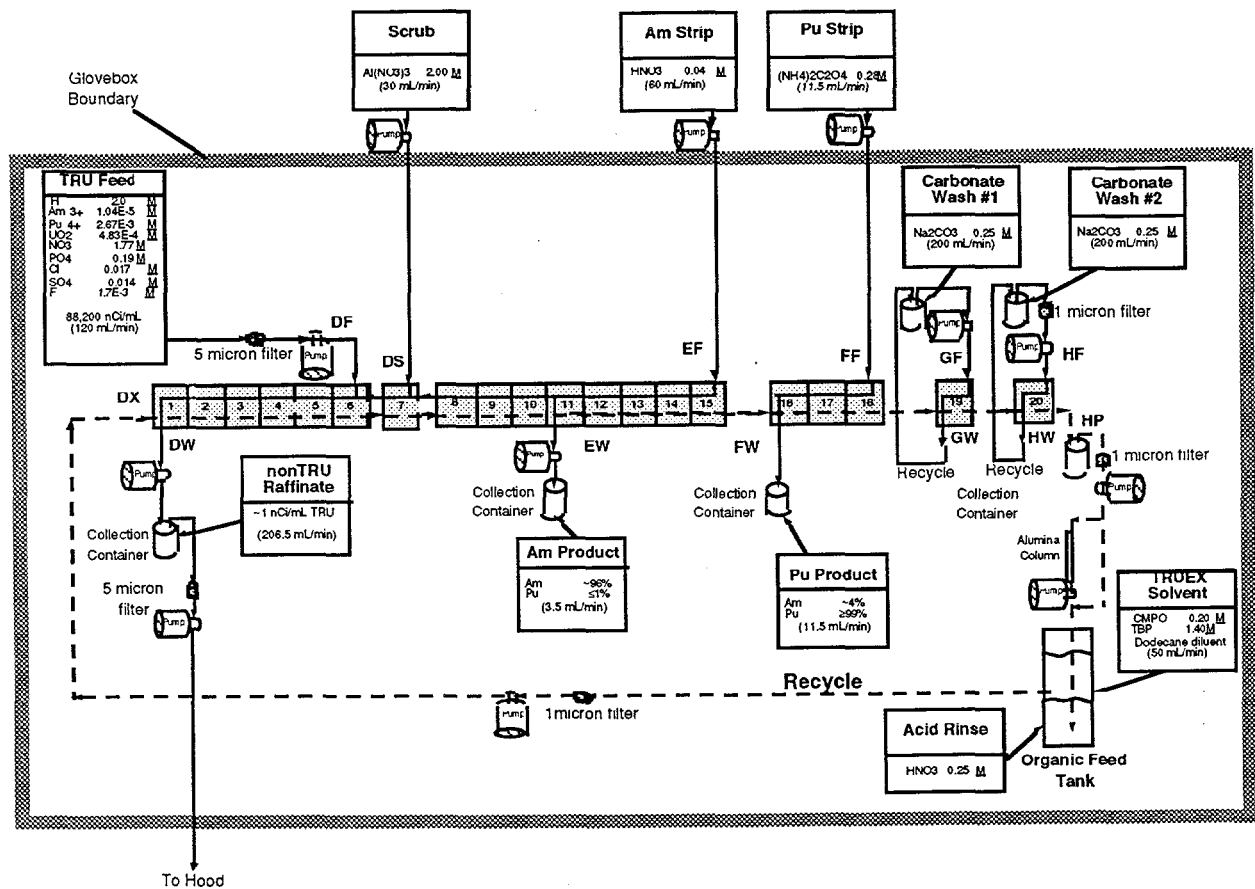


Fig. 29. Summary of Batch 3 Processing

previous batches. The americium recovery was significantly better in this run than in Batch 2. About 96% of the americium was recovered in the americium product (EW), while only 4% ended up with the plutonium (FW). Greater than 99% of the plutonium was recovered in the plutonium product.

The plutonium product generated during the processing of Batch 3 has been evaporated, calcined, analyzed, and disposed of as waste. The 36.05 g of oxide contained 30.3 g of plutonium and 5.12 g of uranium (based on ICP/AES analysis). It also contained 0.24 mg of americium-241 (based on gamma-ray spectroscopy).

The americium product from Batch 3 has been combined with the concentrated americium product from Batches 1 and 2. The combined product was then evaporated to dryness; the solids were a mixture of light yellow and white solids. After evaporation to dryness, the americium was taken back up in about 125 mL of 2M HNO₃, which formed a red brown solution. An aliquot of this solution was analyzed for americium. Based on this analysis, 140 ± 1.6 mg of americium is contained in the solution.

C. Batch 4

With the removal of Batch 3 material, preparations were made for the receipt of Batch 4. A request was issued asking for the delivery of Batch 4 on August 9, 1993. Batch 4 consists of 133 bottles contained in seven waste pails. A summary of each pail is shown in Table 23. These bottles were added to the feed tank. In addition, the acidified carbonates from processing Batch 3 were added.

Table 23. Composition of the Batch 4 Waste Pails according to ANL Waste Requisitions

Pail No.	No. of Bottles	Amount, g	
		Plutonium	235-U
287308	22	15.77	0.05
287293	22	1.95	0
288569	24	8.08	0.02
287182	22	2.06	0
288471	21	1.86	0
287152	22	4.11	0.17
Total	133	33.8	0.24 ^a

^aDoes not include U-238. Total uranium is 3.13 g.

After mixing of the feed tank, a sample was taken and analyzed by ICP/AES for U and Pu, and anion chromatography for F⁻, Cl⁻, NO₃⁻, HPO₄²⁻, and SO₄²⁻. The results of the analysis are shown in Table 24. There is a substantial difference in the quantity of plutonium reported on the waste forms (Table 23) and that determined by ICP/AES (Table 24). The difference is difficult to explain but could be because ICP/AES determination of plutonium in the presence of uranium is not that accurate. Prior to taking any action, an analysis will be done on the oxide product to determine how much material was recovered. However, additional feed analysis might be necessary.

Table 24. Feed Composition Determined by ICP/AES and Anion Chromatography for Batch 4

Component	Concentration, $\mu\text{g/mL}$	Concentration, M
U	57 ^a	2.4×10^{-4}
Pu	748 ^b	3.1×10^{-3}
F ⁻	c	c
Cl ⁻	1,210	3.4×10^{-2}
NO ₃ ⁻	161,000	2.60
HPO ₄ ²⁻	c	c
SO ₄ ²⁻	850	8.9×10^{-3}

^aFor a feed volume of 52 L, the feed contains 2.97 g of uranium.

^bFor a feed volume of 52 L, the feed contains 38.97 g of plutonium.

^cNone detected.

Batch 4 was processed over two days of operation. During the first day, total throughput was set at about 400 mL/min. However, excessive foaming was observed, and the activity in the raffinate was much higher than expected. Operation was shut down after about 10 L of feed had been processed. The total throughput was reduced to about 200 mL/min and processing resumed the next day. After the throughput had been reduced, the foaming observed the previous day was not noticed; however, the activity in the raffinate only decreased slightly. Aliquots collected during the run have been analyzed by liquid scintillation and gamma counting. Due to time constraints and lack of funding, detailed analysis of Batch 4 was not completed.

The Pu and Am product streams generated during the processing of Batch 4 have been completely evaporated. The plutonium product was also calcined, analyzed, and disposed of as waste. Analysis by ICP/AES showed that the plutonium product contained 33.0 g of plutonium and 2.5 g of uranium. Gamma-ray spectroscopy indicated that the americium product contained ~86 mg of americium-241.

V. ADVANCED EVAPORATOR TECHNOLOGY

(D. B. Chamberlain, C. J. Conner, B. Gebby, J. C. Hutter, A. Rozeveld,
D. Taylor, D. G. Wygmans, and G. F. Vandegrift)

This program in CMT consists of three efforts: (1) develop high-level waste evaporator, (2) upgrade low-level evaporator systems, and (3) develop a mobile evaporator/concentrator system.

A. Laboratory-Scale Evaporator

In 1990 a joint R&D program was established between the Chemical Technology Division (CMT) and LICON, Inc. (Pensacola, FL). The purpose of this program is to develop an evaporator that can be remotely operated to concentrate process radioactive waste and product streams such as those generated by the TRUEX process. The design of this high-level waste evaporator centered around LICON's single-effect, horizontal-tube, vacuum evaporator. Benefits of LICON's design include low height requirements, reduced scaling tendencies (because of low operating temperatures), and high decontamination factors. In March 1992, a laboratory-scale evaporator, Model C-3, was purchased from LICON for testing at Argonne. This unit is being used to study the operation of a LICON-designed evaporator, verify performance objectives (e.g., high decontamination factors), and investigate the chemistry of the evaporation process. It is being equipped with a data acquisition system to improve data collection and analysis.

The next step in this program is to collect data from a near-full-scale evaporator while processing real radioactive waste solutions. The need for a costly pilot-scale facility in CMT changed in 1992 when CMT's R&D program was combined with ANL's Waste Management's need for two replacement evaporators.

1. Data Acquisition System

A data-acquisition system (DAS) is being designed to monitor the operation of the LICON C-3 laboratory-scale evaporator. The DAS will be used to automate the data collection process, increase the measurement precision, and measure essential operational parameters. The system can be expanded later to perform mass- and heat-balance calculations.

The major flow rates, pressures, temperatures, and tank levels will be recorded by this system. Presently, most data are entered by hand into laboratory notebooks and analyzed later. However, not currently measured are some parameters needed to make heat- and mass-balance calculations, such as external cooling water temperatures. Appropriate sensors for these parameters will be added.

Figure 30 shows a schematic of the evaporator with the sensors and sample points needed to monitor the operation. The light-outlined circles in Fig. 30 indicate sensors for parameters that are currently monitored, while the bold-outlined circles indicate sensors that will monitor new parameters. Some parameters (e.g., temperatures and distillate conductivity) are currently monitored by electronic sensors whose output can be read directly by the DAS. Additional electronic sensors must be purchased for monitoring flow rates, pressures, and liquid levels. Current

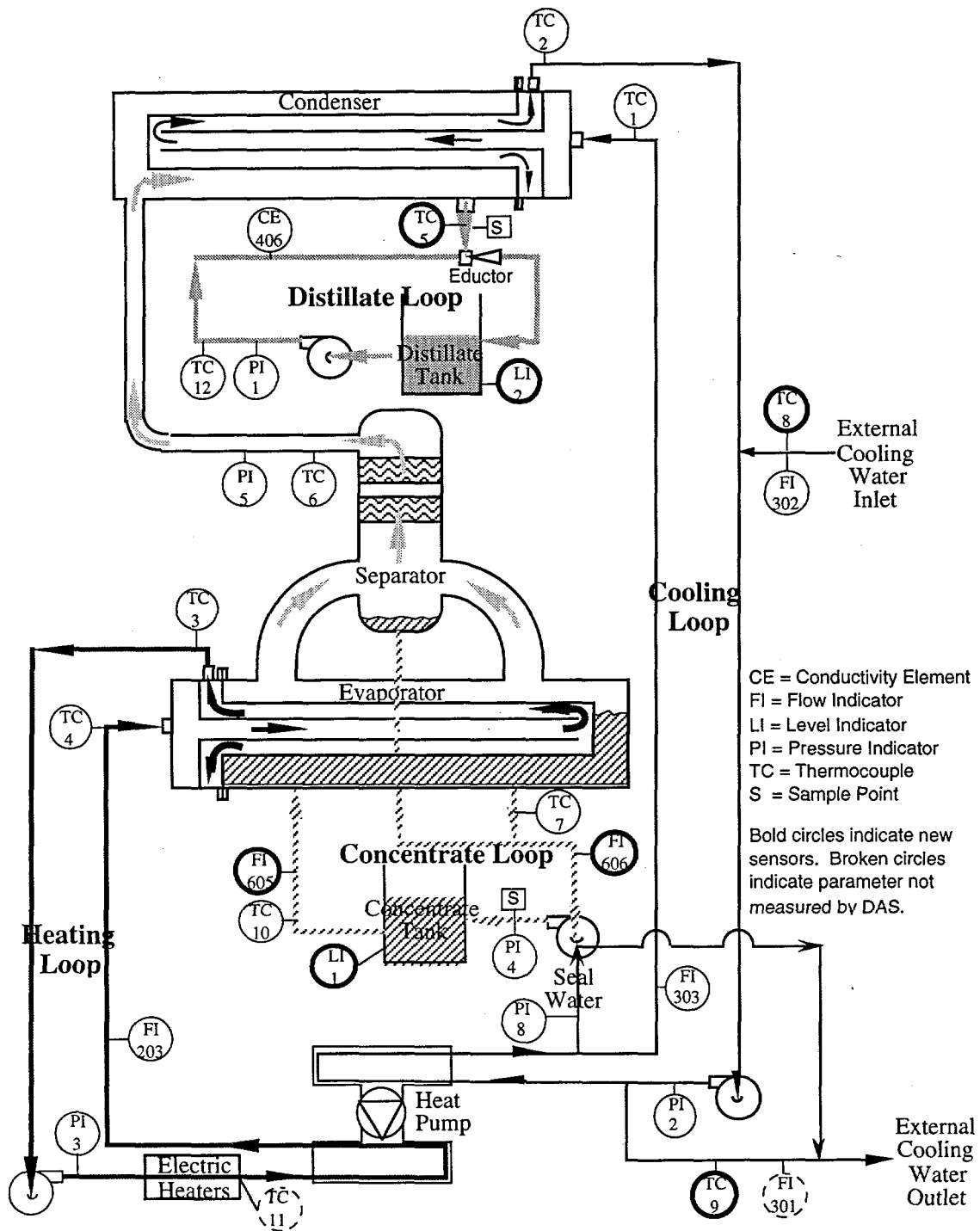


Fig. 30. Schematic of C-3 Laboratory-Scale Evaporator Showing Sensors and Sample Points

plans are to maintain the ability to visually monitor all parameters through existing sensors. Thus, as new sensors are added, the sensors in place will remain in use.

The data acquisition system will be controlled by LabVIEW software running on a Macintosh II computer. An analog-to-digital board, in conjunction with two multiplexing boards, will allow the software to monitor up to 64 channels. A variety of sensors and transducers are employed to generate the signals required to monitor the evaporator. A discussion of the components of the data acquisition system follows.

a. Software

LabVIEW software (National Instruments) was selected to control the DAS equipment. This software offers a graphical-programming environment and the ability to transfer data to Microsoft Excel spreadsheets.

b. Computer

The data acquisition system will occupy one of the NuBus slots on a Macintosh II computer. LabVIEW requires 5 MB of RAM and approximately 2 MB of hard-disk space. An external hard disk may be added to give ample room for other programs and data files. The storage of 5000 data points will require roughly 1 MB of hard disk space (32 data points requires 1 kB).

c. Data Acquisition Boards

National Instruments data acquisition boards will be used because the other supplier of Macintosh boards, Omega, does not support the LabVIEW software. The NB-MIO-16L-9 analog-to-digital converter (ADC) board, when combined with AMUX-64T multiplexing boards, will allow the computer to monitor up to 64 channels of data taken in the differential mode (two input leads per channel) with 12 bits of resolution each in under a second. The differential mode ensures greater accuracy than is attainable through the use of single-ended channels. Resistors can be placed directly on the multiplexing boards as needed to convert 4-20 mA signals to voltage signals.

d. Thermocouples

The evaporator is presently equipped with Type J thermocouples to monitor temperatures. Two additional Type J thermocouples (TC 8 and TC 9) must be added to monitor the inlet and outlet temperatures of the external cooling water. The TC 7 thermocouple will be moved so that the temperature of the concentrate leaving the evaporator shell is monitored. A new thermocouple was added to the distillate line from the condenser and named TC 5. The thermocouple on the distillate loop, previously called TC 5, was renamed TC 12. All thermocouple signals will be read by both the DAS and the thermocouple meter on the evaporator.

e. Pressure and Vacuum Sensors

The pressures within the evaporator are presently monitored using gauges at six locations. Five Omega pressure transducers will be purchased for the positive-pressure signals. Four of the transducers (PI 1, PI 2, PI 3, and PI 8) will read in the 0-60 psig (0-414 kPa) range; a fifth (PI 4, which monitors the concentrate pump) reads 0-30 psig (0-207 kPa). These transducers provide 1% full-scale accuracy and 0-5 V output. The vacuum within the evaporator will be monitored with a Cole-Parmer vacuum transducer (PI 5). This transducer reads 0-30 in. Hg (0-100 kPa) and provides 0-5 V of analog output at 0.4% accuracy.

f. Conductivity

The conductivity of the distillate is presently monitored with a Signet sensor/controller (CE 406). The conductivity measurement is an on-line indication of the quality of the distillate and controls the destination of the distillate product--either recycling unacceptable distillate back to the concentrate tank or routing acceptable distillate to a product carboy in the Vac-frame hood. The Signet meter provides an analog output of 0-5 V, which will be sent to the multiplexing boards.

g. Flow-Rate Sensors

The flow rates in the heating and cooling loops (FI 203 and FI 303, respectively) will be measured with Omega paddle-wheel transducers. The normal flow within these lines is around 15 gpm (57 L/min). The Omega sensors provide a 4-20 mA signal with 1% accuracy. Resistors placed on the multiplexing board will convert these signals to voltage signals.

The inlet flow rate of the external cooling water (FI 302) will be monitored with an Omega sensor. This sensor measures flows from 0.75 to 7.5 gpm (2.8 to 28 L/min). The output signal is 0-5 V.

The constraints on the flow-rate sensors in the concentrate loop make appropriate sensors difficult to find. The liquid in this loop will vary in color, conductivity, and density. The suspended solids in this loop may approach 5 wt%. The flow rate in the 1/2 in. (0.2-cm) lines will vary from 0.4 to 1.8 gpm (1.5 to 6.8 L/min). The accuracy of these two measurements is very important; the difference in their readings will indicate the evaporation rate. No suitable sensors have yet been found to meet these constraints.

h. Level Sensors

Ultrasonic level sensors will be employed to monitor the tank levels. These sensors (LI 1, LI 2) are manufactured by the Migatron Corp. The sensing range can be adjusted to match the liquid-height ranges in the tanks. The resolution of the sensors is about 1/32 in. (0.12 cm), representing approximately 0.1 L in the tanks. Powered by the 24-volt (DC) supply, these sensors output 4-20 mA or 0-10 V. Each sensor will be placed at the top of a PVC pipe extending down into the tanks. The pipes maintain the sensors about 12 in. (0.3 m) above the high liquid level and minimize disturbances caused by splashing in the tank.

i. Power Supply

Excitation voltage for the sensors will be provided by a Cole-Parmer power supply with a capacity of 24 volts (DC) at 625 mA. The power supply is oversized so that additional sensors may be added later. Sensors will be wired in parallel to the power supply.

2. Other Modifications

Flushing nozzles that will flush the separator and the evaporator and condenser shells with cooling water will be added during the sensor installation process. They will clean out contamination in the evaporator and dilute acids prior to disassembly of the those sections. The nozzles will be installed at the top of the columns above the evaporator and condenser, just below the sight glasses.

Transparent materials are being evaluated to replace key sections of piping in the vapor-liquid separation area. They would allow experimenters to observe two-phase flow in the vapor/liquid separation sections. Observations could help answer operational questions about what is happening, possibly leading to design changes for improving separation. Efficient vapor/liquid separation, leading to high decontamination factors, is a major goal for this project.

Four materials were evaluated to determine if they could handle the durability and temperature constraints and could be fabricated for installation on the evaporator. The materials are clear PVC, polysulfone, Teflon, and glass. For the T-shaped piping that joins the vapor uptakes to the separator, the major factors limiting the use of these materials were space, temperature, and fabrication considerations. Clear PVC cannot be used here because it would limit concentrate temperatures to below 140°F (60°C). Neither polysulfone nor Teflon can be fabricated with the separator drain line at the bottom of the T, and glass is not considered durable enough for this application. Furthermore, space in this section is very cramped, leaving very little room for flange connections for any replacement. For these reasons the search for transparent materials for the T has been abandoned.

The separator, however, is already connected by flanges, and three different-sized separators were purchased with the evaporator. A fourth separator, made of transparent PVC, could be purchased and used for low-temperature tests. This option is still under consideration; efforts at present center around finding a supplier.

3. Demonstration Runs

Twice in April, the laboratory-scale evaporator was operated as a demonstration for visitors. These runs used a chromium nitrate feed and full distillate recycle back to the concentrate tank. The 0.083M $\text{Cr}(\text{NO}_3)_3$ feed is dark blue, while the recovered distillate is clear, so high decontamination factors (DFs) attained were visually demonstrated. At the outset the DFs were expected to be quantitatively measured in concentrate and distillate samples by a spectrophotometer. Analyses of distillate samples showed a high background absorbance, but no absorbance peak was found that could be compared to the one seen in the concentrate samples. Thus, it appears that the spectrophotometer is not a useful analytical tool for this work, at least not when using a $\text{Cr}(\text{NO}_3)_3$ feed.

The distillate conductivity gradually rose during these test runs; reasons for this rise were investigated. Since a $\text{Cr}(\text{NO}_3)_3$ solution should be slightly acidic, and since some acid may have been distilled and raised the distillate conductivity, the pHs of the concentrate and distillate were measured after the second test. They were 1.7 and 5.0, respectively. The concentrate [around 0.1M $\text{Cr}(\text{NO}_3)_3$] was more strongly acidic than expected. The reason for this is not readily apparent and deserves further study. The acidity of the distillate is most likely the cause of the rise in conductivity.

B. Evaporator/Concentrator Upgrade

The existing low-level evaporator/concentrator system of ANL's Waste Management (WM) Operations is approximately 30 years old and cannot achieve the decontamination factors that are required to dispose of the on-site distillate stream. Therefore, WM decided to purchase two new evaporators to replace the existing two units; CMT personnel have been funded by WM to help design, select, and install this equipment.

1. Evaporator Design and Procurement

Waste Management personnel conducted a detailed analysis of waste generation at ANL and decided to purchase two evaporators, each capable of processing approximately 100 gal/h (378 L/h) of low-level radioactive feed. At this processing rate, WM will have enough installed capacity to treat the expected volume of waste generated each year, plus provide some additional emergency processing capacity. If two units are installed instead of one larger unit, limited processing capacity will be retained even if one unit becomes inoperable. Training, maintenance, and spare parts inventory requirements necessitate both units being the same design.

Detailed specifications were prepared for the purchase of two 1.5 gpm (5.7 L/m) evaporators. Based upon competitive bids, the contract was awarded to LICON, Inc. LICON's evaporators are Model C-90 single-effect, horizontal-tube, fully automated, vacuum units and are rated at distillate-production capacity of 1.5 gpm (5.7 L/min). This unit, except for the control scheme, is virtually identical to CMT's laboratory-scale evaporator (see Sec. V.A).

2. Concentrator Design and Purchase

Detailed specifications were also prepared for the purchase of two 0.15 gpm (0.6 L/min) concentrators. Two companies submitted bids for the WM concentrators; unfortunately, both bids exceeded our cost estimate by more than \$100,000. After discussions with CMT, WM, and Site Services Division-Procurement (SSD-PRO), the specifications were revised to reduce the cost. The following changes were made to the specifications:

- Elimination of the SCH 80 pipe and nozzle requirement for the mixed-waste concentrator.
- Elimination of the feed tank, mixer, vent condenser, and associated level instrumentation for both concentrators. The concentrate tank on the evaporator skid will be used as the feed tank to the low-level waste concentrator. Carboys or 55-gal drums will be used as feed tanks to the mixed-waste concentrator.

- Reduction of the time a service representative needs to be at ANL during installation from 5 days per unit to 2.5 days per unit (5 days total).
- Elimination of the distillate quality requirement (less than 500×10^{-6} mho/cm). Since the distillate from the concentrators will be returned to the acid waste tank for reprocessing in the evaporators, the quality of the distillate is not important.
- Reduction of the number of simulated waste solutions to be tested at vendor's site from four to one.
- Modification of the diverter valve requirement for routing rinse solutions from the product drum to simplify design and reduce cost.
- Clarification of the instrumentation section to allow the use of thermocouples.
- Reduction of the number of required manuals from 12 to 6.

Following revision, the concentrator specifications were re-issued for bidding; Artisan Industries, Inc. (Waltham, MA) was awarded the contract. Artisan's unit, called a Rototherm, is a horizontal, agitated-film unit capable of producing high-solids-content waste slurries. This unit is transportable and capable of remote operation and control. A diagram of a typical Rototherm is shown in Fig. 31.

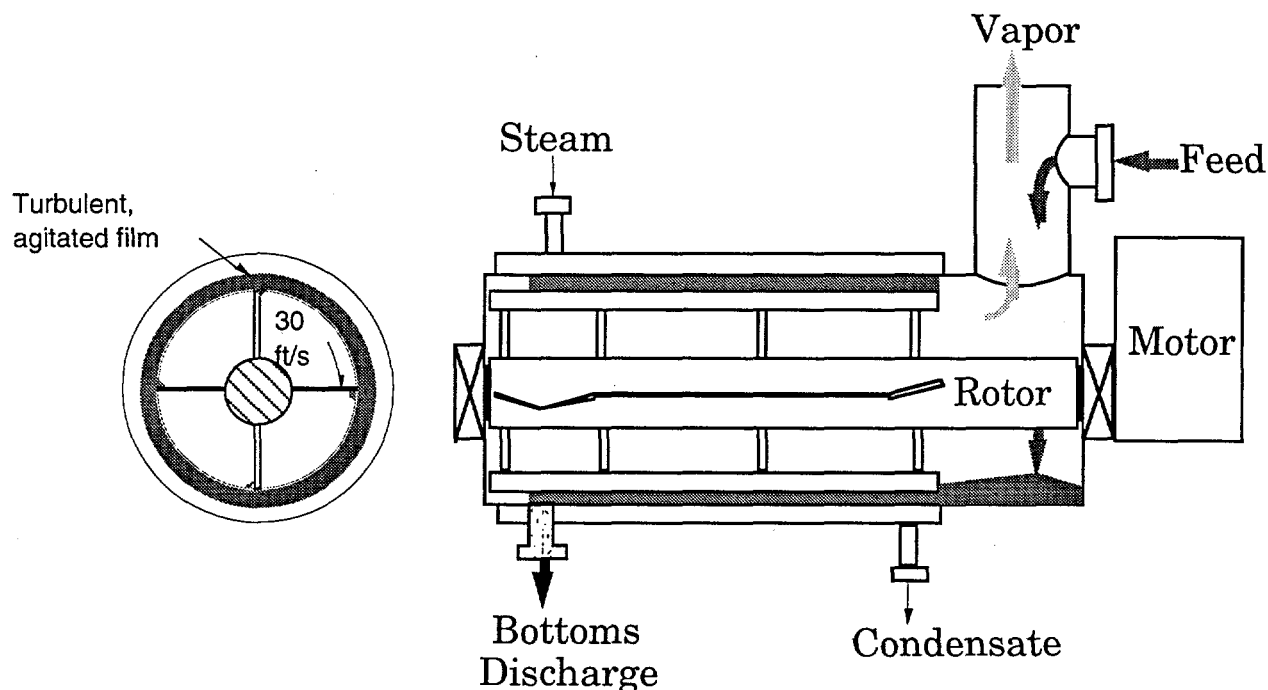


Fig. 31. Flow Diagram of an Artisan Rototherm

In an Artisan Rototherm, the agitator rotates at approximately 30 ft/s (9 m/s), which generates a thin film on the hot walls of the vessel. In this thin film, the remaining water is evaporated and passes up through the vapor duct. The concentrated slurry/solids move down the unit, where they fall from the unit through the bottoms discharge (into a 55-gal drum). In an Artisan unit, the blades do not touch the vessel walls.

3. Equipment Layout

Both new evaporators and one of the concentrators would be used to process low-level radioactive waste. The concentrate from the evaporators would then be pumped to the concentrator, where the remaining water is evaporated. The product from the concentrator, a thick slurry, is discharged directly into a 55-gal drum. The piping diagram in Fig. 32 shows how these three units are connected.

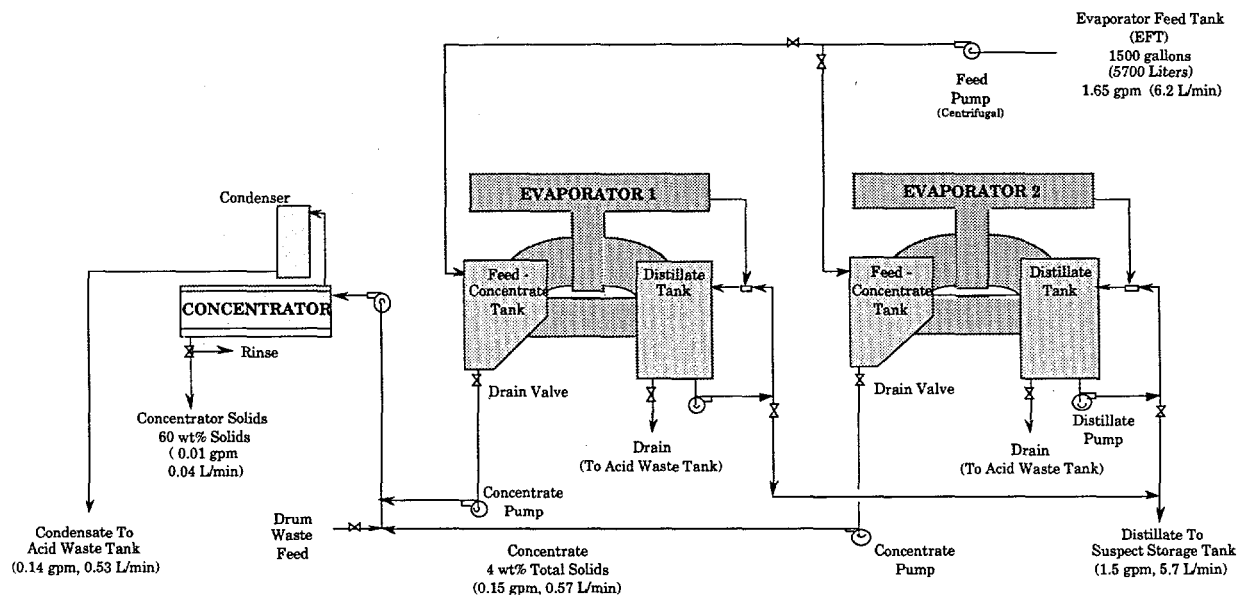


Fig. 32. Piping Schematic for the Low-Level Waste Evaporators and Concentrator

The second concentrator is being purchased to process "mixed waste," that is, waste containing radioactive and hazardous components. To simplify training and maintenance requirements, this unit will be identical to the low-level waste concentrator. Because of RCRA (Resource Conservation and Recovery Act) requirements, this unit will be operated independently of the other concentrator and the evaporators. Figure 33 is a floor plan of this facility showing the proposed location of the new equipment.

C. Transportable Evaporator Program

In April 1993, a Technical Task Plan (TTP) was submitted to DOE titled "Mobile Evaporator/Concentrator Technology Development." In this program, a mobile evaporator/concentrator system will be developed for processing waste removed from the Hanford underground storage tanks (Fig. 34). The method used for recovering waste from these tanks followed by cesium ion exchange requires the addition of a significant volume of water; a volume increase by a factor of three is anticipated. This additional water is detrimental to the envisioned organic/nitrate destruction process. An evaporator/concentrator system could be used to remove and recover this water. The decontaminated water recovered from this system can be discharged to the soil column (assuming that release criteria are met) and/or recycled to the tank waste removal process. A similar, smaller-sized unit could be used to recover nitric acid from the regenerated solution from the

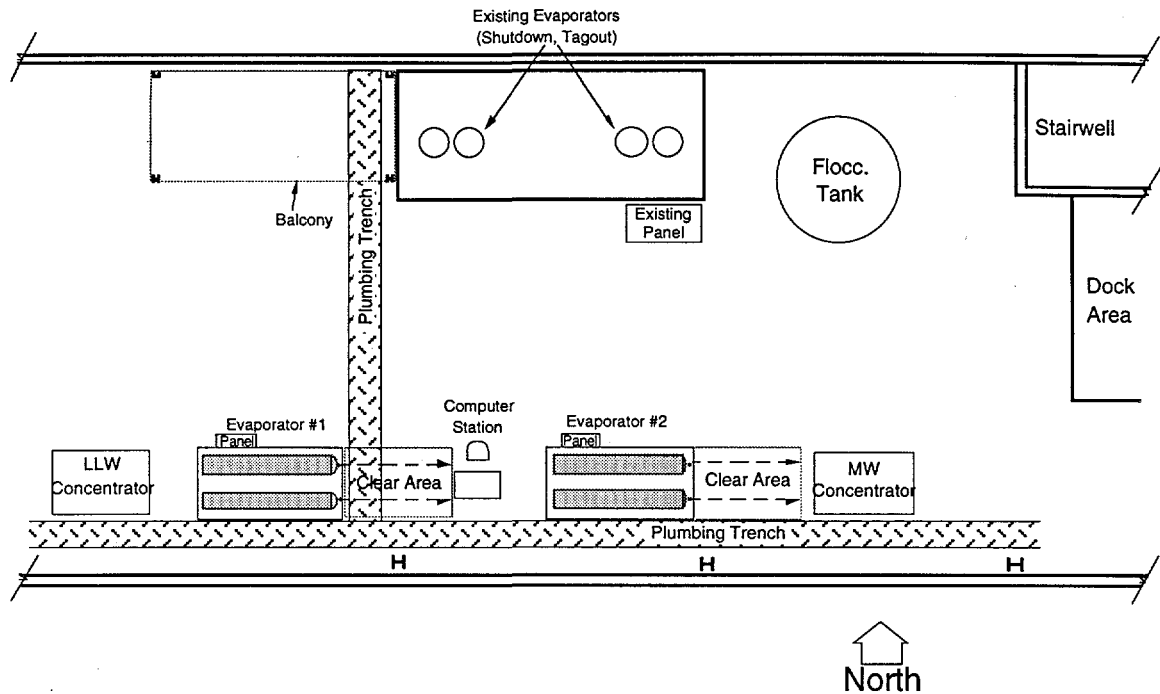


Fig. 33. Floor Plan Showing Evaporator and Concentrator Locations (MW = mixed waste, LLW = low-level waste)

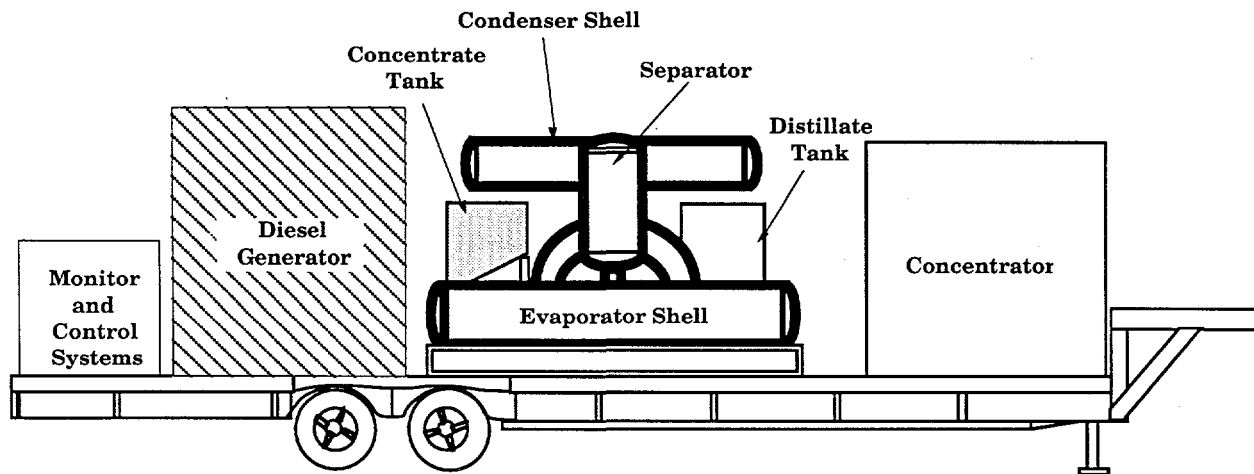


Fig. 34. Schematic of a Transportable Evaporator System

cesium ion exchange column. The Underground Storage Tank-Integrated Demonstration (UST-ID) program is currently investigating compact processes for the treatment of the Hanford storage tank wastes. Units for these compact processes would be transported and set up at the work site.

The first year of the program will be focused on proof-of-principle. In the second year (FY 1995), the evaporator/concentrator system will be designed. In the third year (FY 1996), the equipment will be fabricated, and tests with nonradioactive simulated waste will be completed. In

the fourth year (FY 1997), tests of the system with radioactive wastes will be completed, and the system will be delivered to Hanford for field testing.

Both Artisan and LICON will be directly involved in this program. Both companies have developed transportable evaporation and concentration equipment that has been installed and tested on standard-sized truck trailers. As envisioned now, a LICON evaporator will perform the initial concentration step. Their equipment is well suited for this operation because it can generate high decontamination factors. The water generated during this first operation could be returned to tank waste removal operations. The concentrated waste solution would then be fed into an Artisan concentrator. This concentrator is well suited for this operation because of its ability to handle high solids concentrations and generate a waste stream that contains little or no free-standing water.

VI. SUPPORT TO ARGONNE'S WASTE MANAGEMENT OPERATIONS

(D. B. Chamberlain, C. J. Conner, J. C. Hutter, R. A. Leonard, L. Nuñez,
J. Sedlet, B. Srinivasan, D. G. Wygmans, and G. F. Vandegrift)

We are working with ANL Waste Management (WM) Operations to develop treatment schemes for all liquid wastes stored or being generated at ANL or New Brunswick Laboratory (NBL). Liquid wastes are defined as solutions, slurries, or sludges of low-level, transuranic (TRU), or mixed wastes. The liquid phase is aqueous and/or organic. Our work for WM includes conducting studies to determine the optimum treatment schemes (including automated systems where practical), specifying treatment processes and appropriate equipment for carrying out those processes, and generating needed documentation (e.g., permit applications, safety reviews, and operations manuals).

A. Laboratory Experiments (B. Srinivasan and K. Foltz)

In the treatment of mixed wastes, laboratory experiments are an integral part of the research and development work. These experiments were done with small amounts of either actual or simulated waste solutions, including Davies-Grey waste, metal waste solutions (containing Cd, Pb, Hg, and Ag), dichromate waste, and scintillation cocktail.

1. Davies-Grey Waste Solutions (B. Srinivasan)

a. Introduction

At NBL, uranium is quantitatively determined using a titrimetric procedure known as Davies-Grey method. In this procedure U(IV) is titrated against a standard solution of potassium dichromate in the presence of a catalyst. The aqueous waste resulting from the titration is highly acidic (about 3 mol/L of phosphoric acid with smaller amounts of nitric, sulfuric, and sulfamic acids) and contains Fe, V, and Mo, in addition to U and Cr. Davies-Grey waste solutions are characterized as mixed wastes, since they contain radioactive uranium mixed with hazardous chromium in highly acidic solutions. The waste solutions are stored in several carboys, each of 5-gal capacity, awaiting treatment and disposal.

The objectives of the laboratory experiments are to neutralize the acid in the wastes by the addition of alkali and, at the same time, precipitate chromium as insoluble chromium hydroxide. The precipitate can be separated by filtration and then disposed, following regulations of the RCRA. The filtrate (in the pH range of 7 to 10, and with chromium concentration below regulatory limits) is likely to be a low-level radioactive waste if it contains uranium. It can be fed to the low-level-waste evaporators of WM. It is possible that uranium in the waste may be precipitated to a significant extent along with chromium, leaving a liquid waste stream that is suitable for direct disposal into the ANL laboratory sewer system. The alpha activity must be less than 0.07 dpm/mL for the filtrate to be eligible for sewer disposal. Note that the specific activity given above refers to cases where the alpha-emitting nuclide in the solution is unknown. The specific activity limit is, therefore, based on the most restrictive cases, by assuming the nuclide is one or

more of the transuranic nuclides such as ^{239}Pu and ^{241}Am . If it is known that the solution contains only uranium, then less restrictive limits apply.

b. Experimental Procedures

The oxidation states of Cr, Fe, and U in the waste solutions are expected to be Cr(III), Fe(III), and U(VI). It is likely that a small amount of Cr(VI) may coexist in these solutions; we were informed that small quantities of unused titrant (potassium dichromate solution) might have been disposed of in the carboys.

The neutralization and precipitation experiments with Davies-Grey waste solutions were done by titrating the waste solution in a burette against a known quantity of either a 10% calcium hydroxide slurry or a concentrated ($\sim 10\text{M}$) sodium hydroxide solution in a beaker. In some cases, the sodium hydroxide solution contained enough barium hydroxide to precipitate any sodium carbonate formed by the absorption of atmospheric carbon dioxide. Note that uranium forms soluble carbonate complexes and, therefore, may not be precipitated by the addition of alkaline solutions containing soluble carbonate. The titrations were terminated either at $\text{pH}=10$ or $\text{pH}=7$.

A separate set of experiments was done to test the completeness of chromium precipitation in solutions where chromium is known to be present in both III and VI oxidation states. These experiments were done with Davies-Grey waste solutions to which a small quantity of potassium dichromate was added. After the addition of dichromate, the waste solution was titrated against alkali (calcium hydroxide slurry or sodium hydroxide solution) directly as before. In some cases, the added $\text{Cr}_2\text{O}_7^{2-}$ was reduced to Cr(III) by the addition of Fe(II) solution before titration with alkali; enough Fe(II) was added to reduce completely the original amount of Cr(VI) present in the waste solution.

At the end of the titrations, the solutions were filtered through disposable $0.65\ \mu\text{m}$ filter assemblies. The original waste solution and the filtrate obtained after hydroxide precipitations were analyzed for Cr, Fe, Mo, V, and U by inductively coupled plasma/atomic emission spectroscopy (ICP-AES). The results are given in Table 25.

c. Discussion

The removal of Cu and U by precipitation appears to be very effective when calcium hydroxide slurry is used. Copious quantities of calcium phosphate were also precipitated, since the original Davies-Grey waste solution was rich in phosphoric acid ($\sim 3\text{M}$). The added dichromate ions did not have to be reduced to achieve effective removal of chromium. Note that the added dichromate increased the chromium concentration by a factor of two with respect to the original Davies-Grey waste solution. The rate of filtration was much lower (about 30 min to filter 30 mL) than in sodium hydroxide experiments (see below).

In sodium hydroxide experiments, the sodium phosphate formed remained in solution. Both types of sodium hydroxide solutions, that containing carbonate ions and the other free of them, were not as effective as calcium hydroxide solution in the removal of Cr and U. Titrations terminated at $\text{pH}=10$ were less effective in removing chromium than those terminated at

Table 25. Measurements of pH and Concentrations of Cr, Fe, Mo, V, and U in the Davies-Grey Waste Solution and in the Filtrate after Neutralization and Hydroxide Precipitation of the Waste Solution

Sample	pH	Conc., ppm				
		Cr	Fe	Mo	V	U
DG-0	<1	21	1200	83	69	90
DG-00	<1	39	1200	83	69	90
DG-1	10	0.12	0.023	1.4	0.007	<0.06
DG-4	6.9	0.16	0.035	1.1	0.030	<0.06
DG-5	10.2	0.12	0.032	0.24	0.017	<0.06
DG-8	6.2	0.14	0.023	1.1	<0.02	<0.06
DG-10	10	0.043	0.019	0.15	<0.02	<0.06
DG-2	10	2.3	59	19	14	20
DG-3	6.9	1.6	5.0	19	14	19
DG-6	10	2.4	44	13	10	18
DG-9	7.0	1.5	0.036	21	14	6.1
DG-11	10	3.08	48	17	13	20

Notes for Table 25

- DG-0 Original Davies-Grey waste solution
 DG-00 Original Davies-Grey waste solution + added potassium dichromate
 DG-1 DG-0 + calcium hydroxide slurry
 DG-4 DG-0 + calcium hydroxide slurry
 DG-5 DG-00 + calcium hydroxide slurry
 DG-8 DG-0 + calcium hydroxide slurry
 DG-10 DG-00 + Fe(II) to reduce added $\text{Cr}_2\text{O}_7^{2-}$ + calcium hydroxide slurry
 DG-2 DG-0 + sodium hydroxide solution
 DG-3 DG-0 + sodium hydroxide solution
 DG-6 DG-00 + sodium hydroxide solution
 DG-9 DG-0 + carbonate-free sodium hydroxide solution
 DG-10 DG-00 + Fe(II) to reduce added $\text{Cr}_2\text{O}_7^{2-}$ + carbonate free sodium hydroxide soln.

pH=7. The rate of filtration was much higher (less than 5 min to filter 50 mL) relative to calcium hydroxide experiments.

The above experiments clearly show that the preferred method of treatment of Davies-Grey waste solutions is through titrations against calcium hydroxide slurry, terminating the titration at pH values between 7 and 10. The chromium concentration after treatment (in the filtrate) is more than 10 times lower than the Toxicity Characteristic Leaching Procedure (TCLP) limit of 5 mg/L or 5 ppm. Uranium is below 60 ppb (parts per billion), which is the detection limit of the instrument used for uranium analysis. This is equivalent to <0.09 dpm/mL, calculated from the specific activity of uranium (1500 dpm/mg) by assuming that ^{238}U is in equilibrium with ^{234}U . This filtrate can be disposed of in the sewer system.

2. Simulated Waste Solutions of RCRA Metals
 (B. Srinivasan)

a. Introduction

The research and development efforts at ANL have produced waste solutions which contain radionuclides mixed with RCRA metals. The waste solutions are acidic

(pH<2) and are being stored now, by WM, in temporary facilities. The experiments were conducted with simulated acidic waste solutions containing a mixture of four RCRA metals (Cd, Pb, Hg, and Ag) but no radionuclides. The objectives are (1) to neutralize the acid in the waste solutions by the addition of calcium hydroxide and, at the same time, precipitate the RCRA metals as hydroxides (and oxides), and (2) to convert the RCRA metal hydroxides/oxides to insoluble sulfides by the addition of sodium sulfide. The precipitate containing the bulk of the RCRA metals will then be removed by filtration. The solid precipitate can then be subjected to the Toxicity Characteristic Leaching Procedure (TCLP) to decide whether it is still a mixed waste or a low-level radioactive waste.

The filtrate is expected to be free from the RCRA metals, that is, the concentrations of the metals will be below the TCLP limits (given in Table 26). The filtrate pH will be kept below 12.5, and the total sulfide ($S^{2-} + HS^{-} + H_2S$) will be kept below $1.6 \times 10^{-2}M$ (500 mg/L or 500 ppm). If all these conditions are met, then the filtrate is no longer subject to RCRA guidelines for its disposal. In the actual treatment of mixed wastes (which contain radionuclides in addition to RCRA metals), the filtrate, though free from RCRA metals, may contain some or all of the radioactivity originally present in the waste. The filtrate is then characterized as a low-level radioactive waste. In favorable circumstances, all of the radioactivity may be precipitated along with RCRA metals, thus yielding a liquid waste that is disposable as water. The solid precipitate is still a mixed waste, although the volume is significantly reduced with respect to the original waste solution. If this waste passes the TCLP test, then it is considered a low-level radioactive waste only.

Table 26. Limits for RCRA Metals in Toxicity Characteristic Leaching Procedure

Metal	TCLP Limit, ppm
Cadmium	1.0
Lead	5.0
Mercury	0.2
Silver	5.0

b. Experimental Procedure

The experimental procedure followed for the treatment of simulated waste solutions consists of the following steps: First, neutralize the acid in the waste solution by titration against 10% calcium hydroxide slurry. Usually the titration is terminated in the pH range of 7 to 1. Second, add a saturated solution ($\sim 2M$) of sodium sulfide to the neutralized waste solution to obtain an insoluble sulfide precipitate of RCRA metals. Third, separate the precipitate by filtration. Fourth, analyze the filtrate for RCRA metal concentrations.

In these experiments, the pH changes in the neutralization step will be monitored by a Ross pH electrode purchased from ORION Research. The pH electrode will be calibrated using commercially available buffer solutions.

The sulfide concentration in the solution will be monitored by a sulfide ion electrode. The ion electrode responds to S^{2-} species only, but not to HS^- and H_2S . The relative amounts of the three species containing sulfur depend upon the pH of the solution. Therefore, the proper use of the sulfide ion electrode must include studying the response of the electrode as a function of sulfide concentration in solutions at different pH. The calibration of sulfide ion electrode is described below, followed by laboratory experiments on the treatment of simulated waste solutions using the calibrated electrodes (both pH and sulfide ion electrodes).

c. Calibration of Silver/Sulfide Electrode

A silver/sulfide electrode (Model No. 94-16), a double-junction reference electrode (Model No. 90-02), and a bench-top pH/ISE (ion specific electrode) meter were purchased from ORION Research Inc. for use in our experiments. Hereafter, the silver/sulfide electrode will be referred to as the sulfide electrode, since we used it mainly to determine the sulfide concentration. The electrode could be used to measure silver concentrations if sulfide ions were absent.

The sulfide electrode was calibrated in two different ways: (1) measuring the response of the electrode (in millivolts) at constant pH (of about 13) for a suite of standard solutions of sodium sulfide and (2) measuring the response of the electrode (in millivolts) at different pH (varying between 10 and 13) for two standard solutions of sodium sulfide. The procedure followed for the first calibration was that recommended by the manufacturer of the electrode. A slight modification of the same procedure was used in performing the second type of calibration at different pH. In treating waste solutions, it is not always possible to obtain the same end value for pH in all treatments; hence, the second type of calibration is needed.

(1) Calibration of Sulfide Electrode at pH of 13.2

To derive the calibration curve of the sulfide electrode at pH of about 13, a standard sodium sulfide solution and a buffer solution were prepared as follows. For the standard sodium sulfide solution, 123.5 g of sodium sulfide ($Na_2S \cdot 9H_2O$) was dissolved in about 250 mL of deionized water. The chemical is hygroscopic, and the exact concentration of the solution was determined by titration against a standard solution of lead nitrate. The experimentally determined concentration was $1.9M$, about 8% lower than the expected value calculated from the mass dissolved and volume of the solution. It appears that, in spite of the hygroscopic nature of the chemical, sodium sulfide solutions of known concentrations can be prepared with sufficient accuracy (about $\pm 10\%$) by weighing a known amount of the chemical and dissolving it in a known volume of water. Proper care must be exercised in storing the sodium sulfide solid. It should be stored in tightly stoppered bottles and placed in the refrigerator at about $4^\circ C$.

The sulfide anti-oxidant buffer (SAOB) solution was prepared by using the recipe given in the ORION Research instruction manual for the sulfide electrode. Forty grams of sodium hydroxide, 42.5 g of disodium salt of ethylenediaminetetraacetic acid, and 18 g of ascorbic acid were dissolved in sufficient deionized water to yield a final volume of 500 mL. This solution is labeled as 100% SAOB solution. The solution is pale brown but, on standing for a few weeks, turns a darker brown. The manufacturer advises against the use of old solutions for calibration purposes. We found that up to one-week-old 100% SAOB solution may be used for

preparing calibration standards. (The SAOB reagent pack is now available from ORION Research. These packs may be purchased instead of buying the different chemicals separately.)

Seven solutions with sulfide concentrations varying in the range from 9.5×10^{-7} to 0.95M were prepared in 25% SAOB at pH of 13.2 by sequential dilution of the 1.9M standard solution. The response of the sulfide electrode was measured in each of the solutions and is shown graphically in Fig. 35. The line segment shown in Fig. 35 can be fitted into an equation of the form:

$$V = -31.4 \log [S] - 898.5 \quad (48)$$

where V = voltage in millivolts, and $[S]$ refers to total sulfide in the calibration standard. The slope is -31.4 mV per decade change in concentration; it is slightly higher than the -29.6 value expected for solutions at 25°C for the redox reaction:

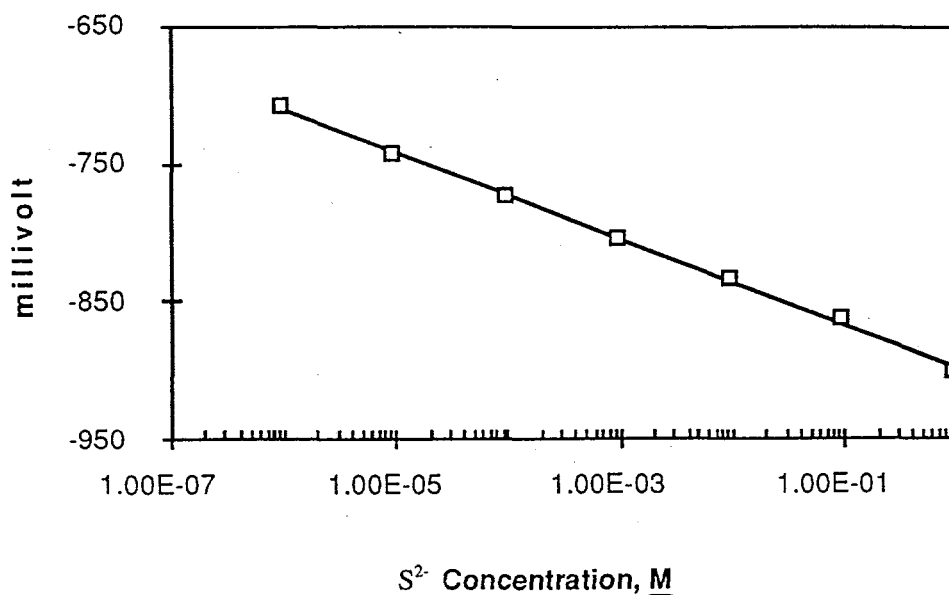


Fig. 35. Calibration of Sulfide Electrode at pH of 13.2

When the least-concentrated solution ($9.5 \times 10^{-7}\text{M}$) was used, the electrode response was quite slow. Stable readings were obtained only after waiting several minutes. With more concentrated solutions, the response was relatively quick, and steady millivolt responses were obtained usually within one minute. It appears that the electrode could be used in process control because of quick response in the region of interest ($1.6 \times 10^{-3}\text{M}$ or about 50 ppm sulfide).

The stability of three sulfide solutions (9.5×10^{-3} , 10^{-4} , and 10^{-5}M) at pH of 13.2 used for calibration was studied as a function of time. The solutions were stored at room temperature in a cardboard box (dark storage) between measurements. The millivolt

response as a function of time is shown in Fig. 36. All three solutions became increasingly darker brown with the passage of time. After four days following preparation, the response was about 5 mV more negative relative to the first day. This represents an increase of about 40% over the original concentration. This result is surprising, since oxidation of sulfide over time would decrease the S^{2-} concentration, and hence, the millivolt response would be less negative than the original solution. If high accuracy is desired in measuring the sulfide concentration, the working standard solutions have to be prepared daily. However, to classify the filtrate as a non-RCRA waste, one must ensure that the sulfide concentration is ≤ 500 ppm. It is our intent to keep the sulfide concentrations ≤ 50 ppm. Thus, even a factor of two error in sulfide measurement would not result in wrongful classification of the filtrate. Under these circumstances, an uncertainty of ± 5 mV in the response of the electrode can be tolerated. Therefore, it is sufficient to prepare sulfide calibration standards at one-week intervals instead of daily. Also, if old standard solutions are used for calibration purposes, the operator of the processing system should be made aware of the uncertainty and accuracy of sulfide measurements.

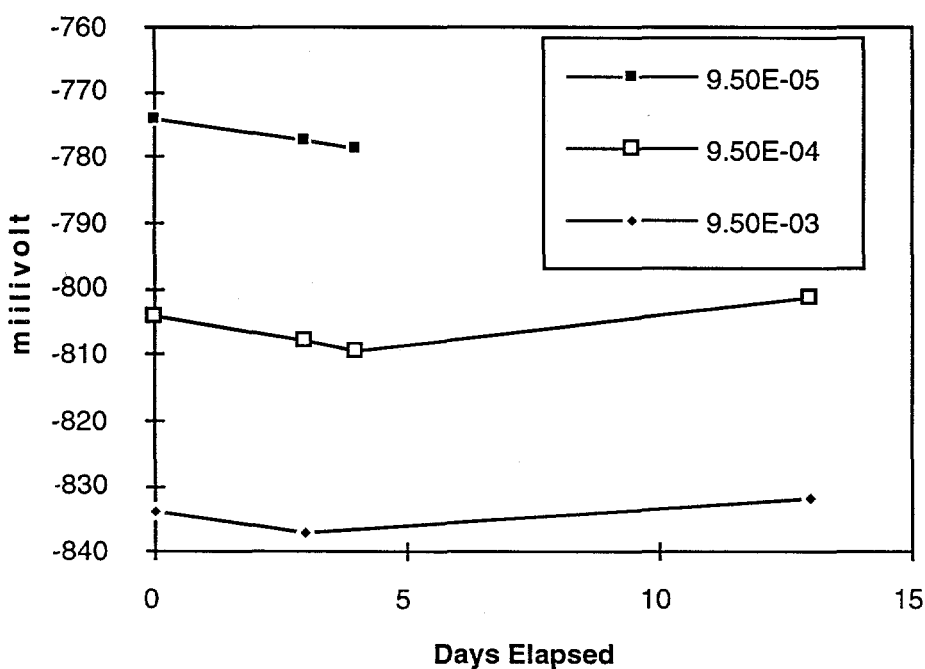


Fig. 36. Stability of Sulfide Calibration Standards as Function of Time. The concentrations of sulfide solutions in moles/liter are shown in the inset.

(2) Calibration at Different pH

Solutions containing known amounts of sulfide (60 ppm and 300 ppm) were prepared at pH values ranging from 10 to 13. The solutions were in freshly prepared 25% SAOB (pH of 13.2) and diluted with small amounts of 6M hydrochloric acid to achieve the desired pH. The millivolt response of each solution was measured with the sulfide electrode. The results are shown in Fig. 37. The two line segments in Fig. 37 can be described by the following:

$$V = (-32.6 \times \text{pH}) - 399.7 \text{ for 60 ppm sulfide} \quad (50)$$

$$V = (-33.5 \times \text{pH}) - 410.5 \text{ for 300 ppm sulfide} \quad (51)$$

The millivolt response is quite linear with respect to pH for both solutions. The two line segments are separated by about 22 mV, as expected for a factor of five change in concentration. However, the ordinate intercepts are separated by about only 11 mV because of the slight difference in the slopes and the long extrapolation involved. By using the experimental measurement as a basis, a family of curves can be constructed for any desired sulfide concentration, parallel to the two line segments shown. For example, the line segment for 50 ppm sulfide would be a line parallel to 60 ppm and displaced vertically upward by about 3 mV at every pH. A graph created along these lines is expected to be useful in determining the sulfide concentration at any end-point pH in the treatment process.

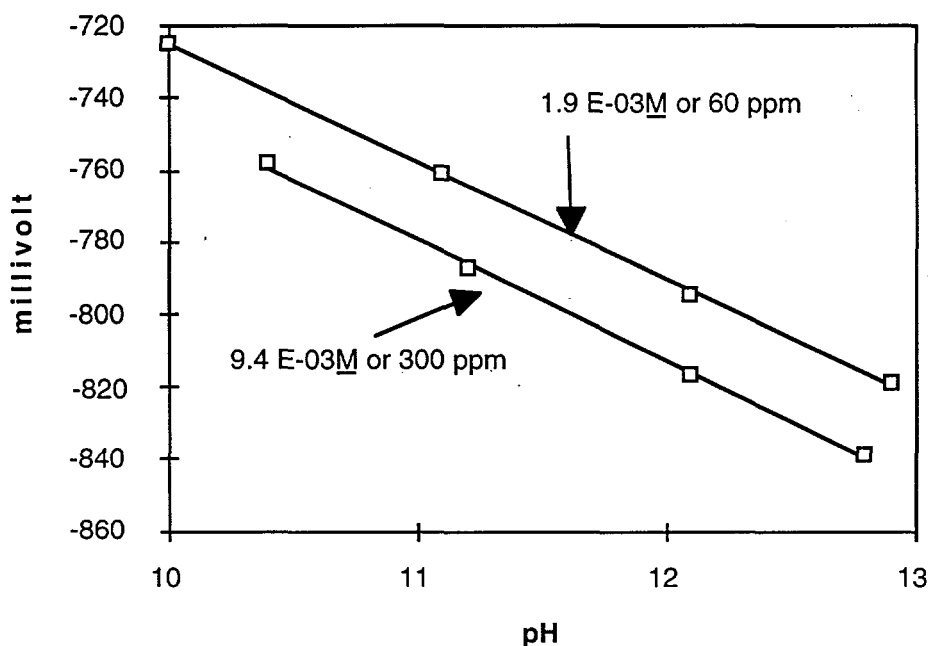


Fig. 37. Calibration of Sulfide Electrode in pH Range of 10 to 13 for Sulfide Solutions at Two Concentrations

d. Precipitation Experiments

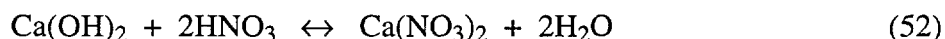
Three laboratory experiments were carried out with simulated waste solutions. The experiments were designed to provide a better understanding of both neutralization and sulfide precipitation processes. The first step in the treatment of the wastes is neutralization/precipitation by using a 10% calcium hydroxide slurry. It is followed by addition of 1.9M sodium sulfide solution to obtain the insoluble sulfide precipitate of RCRA metals by converting the hydroxides and oxides formed in the first step.

(1) Treatment of Nitric Acid

This experiment was done to study the effectiveness of neutralization of the acid by calcium hydroxide slurry and also to determine whether insoluble calcium sulfide is precipitated by the addition of sodium sulfide. Three reagents (nitric acid, calcium hydroxide, and sodium sulfide) were prepared for this study.

The 4M nitric acid solution was prepared by dilution of concentrated nitric acid (~16M). The 10% calcium hydroxide slurry was prepared by hydrolyzing 100 g of calcium oxide in deionized water to yield one liter of slurry. Note that 10% slurry refers to the amount of calcium oxide in water. Also note that the solubility of calcium hydroxide is about 1.8 g/L, and hence, most of the calcium hydroxide remains undissolved. The solution is also expected to contain insoluble calcium carbonate because of absorption of atmospheric carbon dioxide. Calcium carbonate is even less soluble (0.015 g/L) than calcium hydroxide. A 1.9M sodium sulfide solution was prepared as described earlier.

About 50 mL of 10% calcium hydroxide (pH of 12.4) was transferred to a 250 mL glass beaker, and it was titrated against 4M nitric acid in a burette. The pH of the solution was measured at periodic intervals using the pH electrode. The progress of the titration is shown in Fig. 38. The pH gradually decreased from 12.4 to about 11 and dropped sharply thereafter, even with a small addition of nitric acid, signifying the end point of the neutralization reaction. The addition of nitric acid was discontinued at a pH of 7.2. At this pH most of the calcium hydroxide was used up for neutralizing the acid, with only a very small amount of suspended undissolved matter remaining in the solution. The neutralization reaction was accompanied by evolution of heat. The chemical reaction involved in neutralization is



The pH electrode responded slowly as the neutralization progressed. At the neutralization point of 7.2, the electrode yielded a stable reading only after waiting for several minutes. At the neutralization point, there was an overshoot in the electrode response (pH was less than 7), which gradually increased and settled down to a stable value at 7.2. Therefore, it is essential that sufficient time is allowed for mixing of the reagents at or near the end point to ensure that neutralization is complete and excess unneutralized waste is not present in the treated solution.

The neutralized solution was then titrated against 1.9M sodium sulfide solution in the burette. There was a sharp increase in the pH in the initial stages, and then the change was much more gradual. The change of sulfide concentration is quite similar to the pH change. Sulfide concentration increased sharply initially, which changed to a much more gradual increase as the titration proceeded. The titration was terminated at a pH of 11.8, when the response of the sulfide electrode was -814 mV. This corresponds to a sulfide concentration of 320 ppm. Terminating the addition of sodium sulfide solution earlier, say at pH of 11.2, would have kept the sulfide concentration ≤ 50 ppm. The sulfide electrode responded quickly and yielded stable millivolt readings, usually within a couple of minutes. It appears that the sulfide electrode will function effectively as a process controller for monitoring the sulfide concentration at any given time in the treatment process.

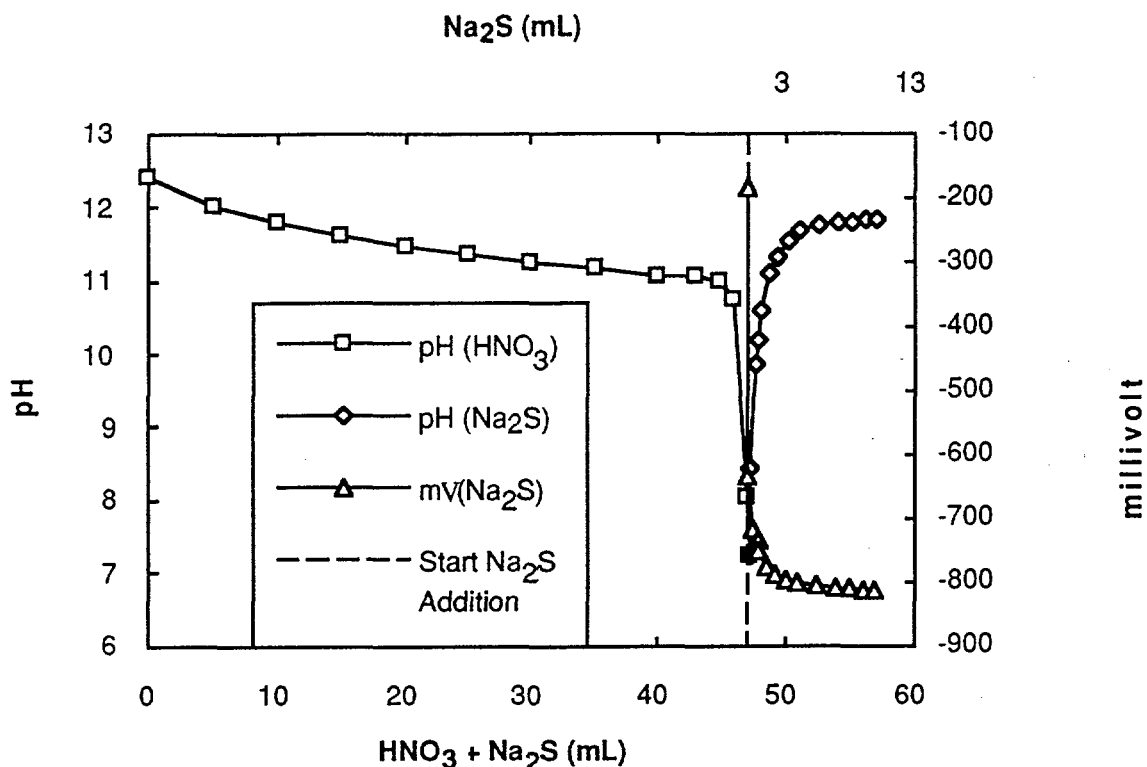


Fig. 38. Treatment of 4M Nitric Acid Using 10% Calcium Hydroxide Slurry and 1.9M Sodium Sulfide Solution. The first 47 mL of bottom abscissa represents nitric acid addition only, and the second 10 mL beyond the vertical dotted line represents sodium sulfide addition only.

The treated solution was passed through a 47-mm membrane filter with $0.45\text{-}\mu\text{m}$ pore size. The mass of the wet precipitate was about 6 g , which was reduced to 1.5 g by drying at 110°C for 2 h . The wet precipitate was green. The surface of the dried precipitate was a mixture of black and green. Freshly broken pieces were a dirty white. Even though the exact chemical composition of the precipitate is unknown, it appears to be a mixture of calcium sulfide, calcium hydroxide, and calcium carbonate. The conversion of hydroxide to sulfide appears to be incomplete. Nonetheless, the presence of calcium in the solution will aid in controlling the sulfide concentrations below TCLP limits because of the formation of solid calcium sulfide. Note that the solubility of calcium sulfide in water is about 0.23 g/L (at 18°C); it increases with temperature but decreases in the presence of hydroxide.

(2) Treatment of Copper Sulfate in Hydrochloric Acid

This experiment employed copper (a non-RCRA metal) as an analog for the four RCRA metals (Cd, Pb, Hg, and Ag). This was done to minimize the generation of RCRA wastes in the R&D activities connected with this project. The simulated copper waste solution was prepared by dissolving the appropriate quantity of copper sulfate in 4M hydrochloric acid to yield a 1M solution of copper ions. This solution was taken in a glass burette and titrated against a known amount of 10% calcium hydroxide slurry in a glass beaker to neutralize the hydro-

chloric acid. The progress of the titration was followed by measuring the pH change. Upon addition of copper sulfate solution, the calcium hydroxide slurry solution became a deep blue. As in the case of nitric acid neutralization, the pH changed gradually in the initial stages of titration and dropped sharply at the end point. The addition of copper sulfate solution was discontinued when the pH was 6.7. As in the case of nitric acid neutralization, the pH changed gradually in the initial stages of titration and dropped sharply at the end point. The addition of copper sulfate solution was discontinued when the pH was 6.7. The precipitates in the solution are expected to be a mixture of copper hydroxide, basic sulfates of copper, and calcium hydroxide (and carbonate), similar to "Bordeaux mixture."

The neutralized copper sulfate solution was then titrated against 1.9M sodium sulfide solution in the burette. Even with the addition of a few drops of sodium sulfide, the blue solution turned brownish black, indicative of insoluble copper sulfide. As before with nitric acid neutralization experiments, the pH of the solution rose rapidly at first and much more gradually with increasing addition of sodium sulfide. However, the sulfide concentration showed slightly different behavior. It changed gradually in the beginning (-200 to -300 mV) and dropped sharply at the end point, to about -700 mV. The addition of sodium sulfide was discontinued when the pH was 11.8 and sulfide concentration reached about 3 ppm, corresponding to -746 mV at pH of 11.8. The titration curve is shown in Fig. 39.

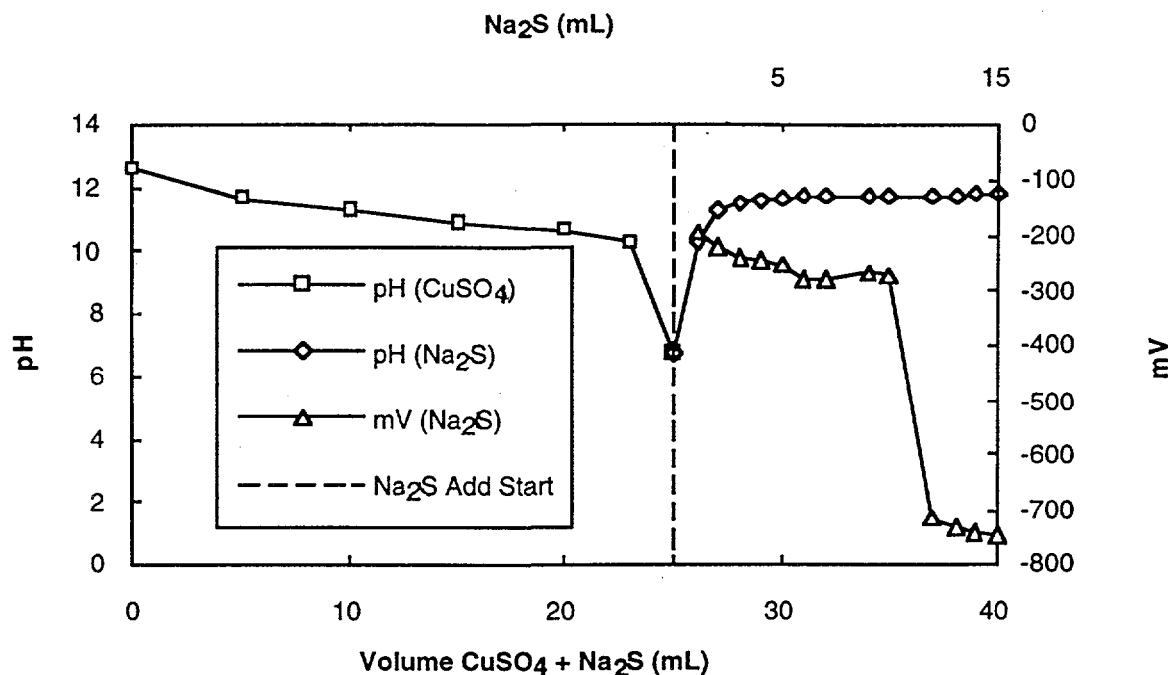


Fig. 39. Treatment of 1M Copper Sulfate in 4M Hydrochloric Acid Using 10% Calcium Hydroxide Slurry and 1.9M Sodium Sulfide Solution. The first 25 mL of bottom abscissa represents copper sulfate addition only, and the second 15 mL beyond the vertical dotted line represents sodium sulfide addition only.

The solution containing copper sulfide and other precipitates mentioned above was passed through a 47-mm membrane filter of 0.45- μm pore size. A brownish black precipitate weighing about 22 g was obtained. Upon drying at 110°C for 72 h, the mass was reduced to about 9 g. The color of the precipitate changed mostly to blue interspersed with brownish black. This is interpreted to mean that the basic copper sulfate obtained from neutralization is not completely converted to copper sulfide upon addition of sodium sulfide. Both sulfate and sulfide precipitates seem to coexist along with other insoluble calcium compounds.

(3) Treatment of Mixture of Metals in Nitric Acid

The simulated waste solution containing a mixture of Cd, Pb, Hg, and Ag (all RCRA metals) was prepared in 4M nitric acid, by diluting ~1M solutions of each of the RCRA metals to yield solutions with final metal concentrations of ~0.1M for each of the metals. The simulated solution is representative of actual mixed waste in storage, except that radionuclides are absent in the simulated solution.

The simulated RCRA metal waste solution was taken in a glass burette and titrated against a known amount of 10% calcium hydroxide slurry in a glass beaker to neutralize the nitric acid. The progress of the titration was followed by measuring the pH change. The calcium hydroxide slurry changed to yellow in the beginning, then to dark yellow and finally greenish brown. The precipitates in the solution are expected to be a mixture of RCRA metal oxides and hydroxides and calcium hydroxide (and carbonate). As in the case of nitric acid neutralization, the pH changed gradually in the initial stages of titration and dropped sharply at the end point (Fig. 40). The addition of waste solution was discontinued when the pH reached 7.4.

The neutralized waste solution was then titrated against 1.9M sodium sulfide solution in the burette (Fig. 39). The initial millivolt response of +350 mV of the sulfide electrode was more positive than in the neutralized solution of copper (see above), because of the response of the electrode to silver and possibly mercury ions in the solution. Upon addition of about 5 to 6 mL of sodium sulfide, the response dropped sharply to less positive values. The addition of sodium sulfide was terminated when the electrode response was -773 mV, corresponding to a sulfide concentration of about 60 ppm. The pH at that end point was 11.6.

The addition of sodium sulfide caused the greenish brown solution (at the end of the neutralization step) to turn black. Note that lead, mercury, and silver sulfides are black, whereas cadmium sulfide is yellow.

The mixture of metal sulfides and insoluble calcium compounds was passed through a 47-mm membrane filter of 0.45- μm pore size. A black precipitate weighing about 15 g was obtained. Upon drying at 110°C for 72 h, the mass was reduced to about 5 g. The color of the precipitate remained unchanged, in definite contrast to the previously discussed observations with calcium and copper sulfide precipitates, where noticeable color changes were observed upon drying. Nevertheless, we cannot firmly conclude that the precipitate consists of metal sulfides only.

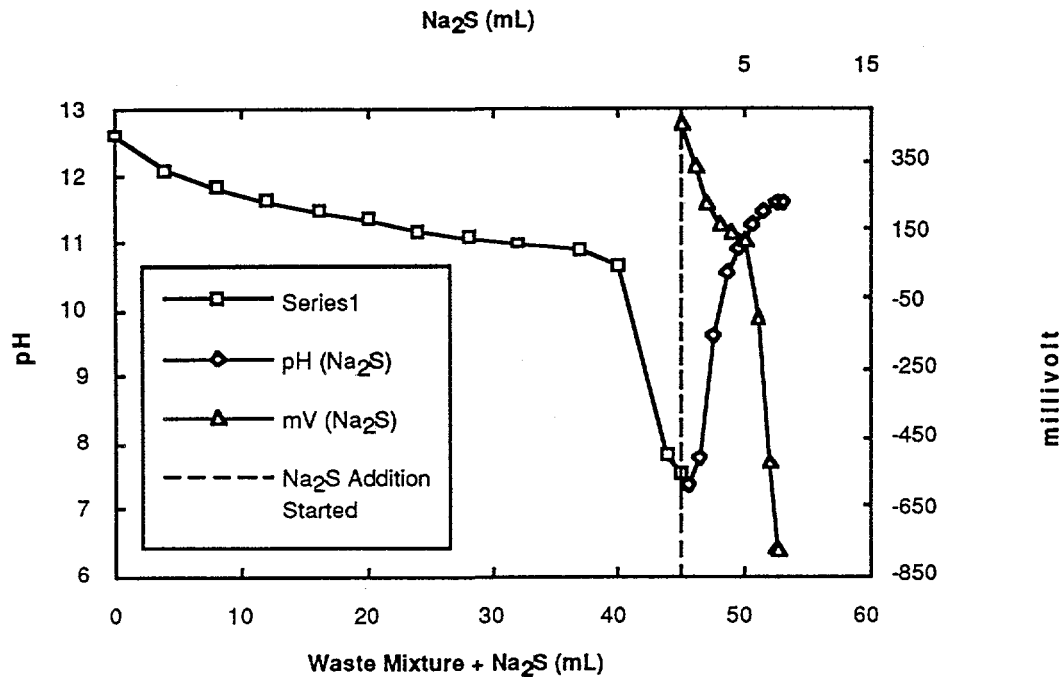


Fig. 40. Treatment of 0.1M Solution Containing RCRA Metals (Cd, Pb, Hg, and Ag) in 4M Nitric Acid by 10% Calcium Hydroxide Slurry and 1.9M Sodium Sulfide Solution. The first 45 mL of bottom abscissa represents the waste mixture addition only, and the second 8 mL beyond the vertical dotted line represents the sodium sulfide addition only.

The filtrate was clear and was analyzed for Cd, Pb, and Ag using ICP/AES and for mercury using cold vapor atomic absorption spectroscopy. As shown in Table 27, the concentrations of the metals in the filtrate, except mercury, are below TCLP limits for the four RCRA metals.

Table 27. Filtrate Concentration and TCLP Limits for Metals

Metal	Filtrate Conc., μg/mL	TCLP Limit, μg/mL
Cadmium	<0.1	1.0
Lead	<1.0	5.0
Mercury	7.1	0.2
Silver	<0.05	5.0

(4) Conclusions

Mixed waste solutions containing Cd, Pb, and Ag in acid media can be treated by neutralization and sulfide precipitation to remove the metals from the solutions until they are below TCLP limits. If mercury is present in the solutions, the above procedure is not satisfactory. Additional laboratory experiments are needed for developing a satisfactory treatment procedure for waste solutions containing mercury.

The pH electrode and the sulfide ion electrode function effectively. The electrode assemblies can be used in process control to detect the end points of neutralization and precipitation reactions.

3. Simulated Waste Solutions of Sodium Dichromate
(B. Srinivasan and K. Foltz)

a. Introduction

Mixed wastes containing chromium as one of the constituents result from R&D activities at Argonne. Another source of the waste is the chromic acid used for cleaning contaminated glassware. It appears that most of the chromium waste in storage is in acidic solution.

Chromium in the waste solutions may exist as Cr(III) and/or Cr(VI). The higher oxidation state Cr(VI), as present in sodium dichromate, is considered hazardous. However, the TCLP limit of 5 mg/L (Table 27) refers to total chromium, without regard to oxidation state.

These experiments were done with simulated acidic waste solutions of chromium containing no radionuclides. The acid in the waste solutions was neutralized by the addition of calcium hydroxide, and at the same time, the chromium was precipitated as hydroxide. The precipitate containing chromium was then removed by filtration and subjected to TCLP testing to decide whether it is still a mixed waste or a low-level radioactive waste. The filtrate is expected to be free from chromium, that is, below the TCLP limit of 5 mg/L. Also, the filtrate pH is expected to be below 12.5. If these conditions are met, then the filtrate is no longer subject to RCRA guidelines for its disposal.

In the precipitation treatment of actual mixed wastes, which contain radionuclides in addition to chromium, the filtrate may contain some or all of the radioactivity originally present in the waste. The filtrate is then characterized as a low-level radioactive waste. In favorable circumstances, all of the radioactivity may be precipitated along with RCRA metals, thus yielding a liquid waste that is disposable as water. The solid precipitate is still a mixed waste, but with significant volume reduction with respect to the original waste solution; if it passes the TCLP test, then it is a low-level radioactive waste only.

b. Principles of Laboratory Experiments

It is known that among the two oxidation states, the lower state of Cr(III) alone is capable of forming insoluble hydroxide. The higher state of Cr(VI), which exists as soluble dichromate in acid solutions, is converted to soluble chromate in alkaline medium. Furthermore, Cr(III) hydroxide is amphoteric and goes into solution with the addition of excess base.

The laboratory experiments will demonstrate that Cr(VI) in the simulated waste solutions can be reduced to Cr(III) by suitable reducing agents and then removed from the waste solutions as an insoluble hydroxide by the addition of alkali. In the experiments, reported

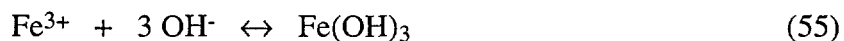
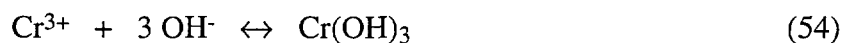
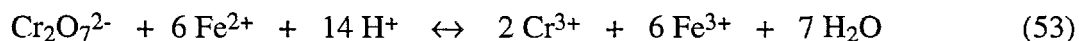
below, two different reducing agents [(Fe(II) and H₂O₂)] were tried. After reduction, Cr(III) was precipitated by using calcium hydroxide slurry.

c. Reduction of Cr(VI) Using Fe(II)

A 0.21M sodium dichromate in 1M sulfuric acid solution was used to simulate the actual waste solutions. The simulated waste solution was taken in a burette and titrated against 20 mL of 1M ferrous sulfate solution in 0.1M sulfuric acid in a beaker. The beaker also contained 5 mL of concentrated phosphoric acid and 1 mL of 0.2% solution of barium diphenylamine sulfonate, the latter serving as the redox indicator in the titration. Phosphoric acid was added to alter the electrode potential of the Fe(II)-Fe(III) couple so that the color change in the indicator coincides with the exact end point of the titration. At the end point, the indicator changed from green to blue. The same results were obtained when ferrous sulfate solution in a burette was titrated against the sodium dichromate, phosphoric acid, and indicator mixture in a beaker. In this case, the color change is from blue to green.

The simulated waste solution contained Cr(III) and Fe(III) after the reduction step. The acids present in this solution were a mixture of sulfuric and phosphoric acids. This solution was then taken in a burette and was titrated against a known quantity of 10% calcium hydroxide slurry in a beaker. The progress of the titration was followed by measuring the pH using a glass electrode. The titration was terminated at a pH of 8.2.

The calcium hydroxide neutralized the sulfuric acid and the phosphoric acid. Chromium and iron were precipitated simultaneously as a mixture of hydroxides and phosphates. The chemical equations, in ionic form, governing the reduction, precipitation, and neutralization steps are as follows:



The treated mixture was then filtered using a 0.45- μm membrane filter (47 mm size). The filtration apparatus was connected to the supply line of the laboratory vacuum system. Filtration was complete in about 15 min. The filtrate was clear and colorless. It was acidified to about pH of 1 with concentrated nitric acid and was analyzed for chromium content using ICP/AES. Shown below are the chromium concentrations in the original simulated-waste solution and in the filtrate, along with the decontamination factor achieved by the treatment:

Cr(VI) in the untreated simulated waste:	22,000 mg/L
Cr(III) in the simulated waste after reduction by Fe(II):	8200 mg/L
Chromium in the filtrate:	≤0.01 mg/L
Decontamination factor:	≥2.2 x 10 ⁶

The decontamination factor is defined as the concentration of chromium in the filtrate divided by the concentration in the original untreated waste.

Note that the treatment process has caused dilution of the original waste by a factor of about four, thereby increasing the volume of the filtrate. The concentration of chromium in the filtrate is much less than the TCLP limit of 5 mg/L. The precipitate weighed about 1.1 g and, upon drying at 110°C, was reduced to 0.8 g.

In a separate experiment, Cr(VI) was reduced by use of Fe(II), this time in the absence of phosphoric acid and the indicator. About 10% of excess Fe(II) was added to ensure complete reduction of Cr(VI). The reduced solution was then treated by using 10% calcium hydroxide slurry, as before. The precipitate obtained was a mixture of chromium and iron hydroxides only. The precipitate was removed from the filtrate by using a membrane filter (47-mm dia, 0.47- μ m pore size) and a laboratory filtration system as before. The chromium concentration in the filtrate was again ≤0.01 mg/L. This experiment clearly demonstrates that dichromate wastes can be successfully treated by using Fe(II) as reductant, and the Cr(III) and Fe(III) formed as a result can be precipitated quantitatively as hydroxides.

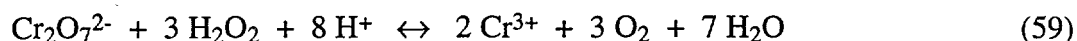
d. Reduction of Cr(VI) with H₂O₂

Again, a 0.21M sodium dichromate solution in 1M sulfuric acid was used to simulate the actual waste solutions. Twenty milliliters of the simulated-waste solution was transferred to a beaker and titrated against 0.6M hydrogen peroxide in a burette. The electrode potential of the titrated solution was measured following additions of known volumes of the titrant. This measurement was made with a combination electrode, hereafter referred to as the ORP (oxidation-reduction potential) electrode, consisting of a platinum sensor electrode and a reference electrode. The ORP electrode response was sluggish throughout the titration; long waiting periods, usually greater than 5 to 10 min, were required after each addition of titrant was made and before the millivolt readings stabilized. The end point was characterized by a sharp change in the electrode potential. Beyond the end point the ORP electrode responded quickly.

The progress of the titration between dichromate and hydrogen peroxide could be easily followed by noting the color change. The dichromate solution, originally orange/yellow, changed to brown, then to green, and finally to blue at the end point. The appearance of blue color coincided with the sharp change in potential of the titrated solution.

The treated solution, now containing Cr(III) only, was then titrated against a known quantity of 10% calcium hydroxide as before. The titration was terminated at a pH of 8.3. The calcium hydroxide neutralized the sulfuric acid in the waste solution. The chromium was pre-

precipitated as hydroxide. The chemical reactions, in ionic form, governing the reduction, precipitation, and neutralization steps are as follows:



As before, the precipitate was removed by filtration using a 0.45- μm membrane filter. The filtrate obtained this time was light yellow, in contrast to the colorless filtrate obtained with Fe(II) reductant. The filtrate was analyzed for chromium content by ICP/AES. The results of the analysis are

Cr(VI) in the untreated original waste:	22,000 mg/L
Cr(III) in the waste after reduction by H_2O_2 :	4,500 mg/L
Chromium in the filtrate:	92 mg/L
Decontamination factor:	240

Note that the treatment process has caused dilution of the original waste by a factor of about six, thereby increasing the volume of the filtrate. Despite the dilution, the concentration of chromium in the filtrate remained about 18 times higher than the regulatory limit of 5 mg/L. Hence, the hydrogen peroxide reduction method is not suitable for treating dichromate wastes.

The high chromium concentration of 92 mg/L in the filtrate appears to be CrO_4^{2-} , as revealed by the yellow filtrate. In basic solutions hydrogen peroxide can oxidize Cr(III) to CrO_4^{2-} , according to the following equation:



e. Conclusions

Acidic waste solutions containing dichromate ions can be treated successfully through a two-step process: a reduction step using Fe(II), followed by a precipitation step using calcium hydroxide slurry. The base also neutralizes the acid in the wastes.

In the actual treatment of mixed wastes, the Cr(VI) content of the wastes can be determined independently by drawing a small aliquot from the waste and titrating the aliquot against standard ferrous sulfate solution in the presence of phosphoric acid and barium diphenylamine sulfonate, the latter serving as a redox indicator. It will be necessary to train the operator(s) of the waste treatment process on the use of this titrimetric method to determine the Cr(VI) content.

The titration result could then be used to calculate the quantity of ferrous sulfate required to effect complete reduction of Cr(VI) in the waste. Alternatively, analytical chemists in the CMT Division will be able to determine Cr(VI) in the original waste solution. After the Cr(VI) content is known, the reduction reaction may be performed in a vessel separate from the one that will be used for precipitation of Cr(OH)₃.

Hydrogen peroxide is not recommended as a reducing agent in the treatment of dichromate wastes. It is an effective reducing agent for Cr(VI) in acidic solutions but acts as an oxidizing agent in basic solutions to re-oxidize Cr(III) to CrO₄²⁻.

4. Scintillation Cocktail (B. Srinivasan)

Scintillation cocktail wastes arise as a result of the use of liquid scintillators in determining radioactivity. The wastes consist of a mixture of organic compounds: some of them are hazardous and others are environmentally safe. However, upon addition of radionuclides, the waste produced is considered either a mixed waste or simply a low-level radioactive waste, depending upon whether or not hazardous chemicals are present in the waste solutions. The wastes are now in storage at temporary WM facilities. A part of the waste is now being shipped to the Hanford site for long-term storage and eventual disposal when a suitable disposal technology becomes available. In the interim, ANL itself is interested in developing a separation technology with which the mixed waste could be treated to separate the radioactive components with a concomitant reduction in volume of the total waste.

The objectives of the separation method are as follows: First, release the radioactive constituents in the organic cocktail wastes into aqueous solutions. The laboratory studies will be confined to removal of transuranic nuclides (mainly Am and Pu) only. Second, treat the separated aqueous phase to obtain a low-volume, low-level radioactive waste which is not characterized as TRU waste, that is, the alpha specific activity is <100 nCi/g. Third, the organic part of the waste, now stripped of radioactivity, becomes an ordinary waste or a hazardous waste, depending upon the absence or presence of hazardous chemicals. The previous statement is strictly true only if de-minimus levels are defined to acknowledge the absence of radioactivity in these wastes. If no radioactivity is present, then the organic chemical can be disposed in a suitable manner with due consideration to RCRA and other EPA regulations.

The first set of laboratory experiments is based on the solvent extraction principle of the distribution of radioactivity between the organic cocktail phase and an aqueous salt phase. If the aqueous phase contains a complexing agent, it may aid in a more efficient removal of the radionuclide.

Some preliminary experiments were conducted using concentrated solutions of sodium oxalate (up to 0.28M) or aluminum nitrate (up to 1M) as the aqueous phase. "Ultima gold" cocktail mixed with trace quantities of ²⁴¹Am in nitric acid solution constituted the organic phase. Equal volumes (3.5 mL each) of the organic phase and aqueous phase were mixed in a culture tube, and allowed to stand overnight. The sodium oxalate solutions separated into two clearly distinguishable phases, whereas the aluminum nitrate showed much less-clear separation. However, upon centrifuging for a period varying from 30 to 105 min with maximum speed in a clinical cen-

trifuge, the phases separated clearly in all cases. The radioactivity in the separated phases was counted to assess the efficiency of the separation method. It appears that ^{241}Am was extracted much more effectively by sodium oxalate than aluminum nitrate. The preliminary study was not quantitative. Nonetheless, the results are encouraging enough to pursue work toward establishing a treatment scheme for liquid scintillation cocktail wastes.

B. Equipment for Alkaline Sulfide Precipitation
(C. J. Conner and J. C. Hutter)

The treatment process as described earlier is an alkaline sulfide precipitation in which the acidic waste is added to a slurry of calcium hydroxide until a pH of 10 is achieved. This will precipitate the majority of the toxic metals as hydroxides. The process is completed by metering a near saturated solution of sodium sulfide into the treatment vessel until the total free sulfide reaches 10 ppm. Addition of sulfide converts the metal hydroxides into metal sulfides, which in general are much more insoluble than hydroxides. In addition to being more insoluble, metal sulfides form a crystalline precipitate that is easier to filter than a gelatinous hydroxide sludge. Equipment to carry out the above process was purchased and installed in WM (Building 306). This equipment is described below.

1. Treatment Hood

An existing hood in the WM building was modified to allow treatment of mixed waste. Modifications included removal of existing equipment from the hood, installation of a stainless steel well in the floor of the hood, mounting of a control panel for instrumentation on the side of the hood, and fabrication of a drip pan for the floor of the hood. The layout of the hood and control panel is shown in Fig. 41.

2. Treatment Vessel

The vessel is polypropylene and therefore resistant to both acids and bases. It is 36 cm in diameter and 69 cm high and has a usable capacity of 50 L. The vessel is contained in the stainless steel well in the floor of the treatment hood.

3. Mixing

Mixing is accomplished by using a 45° pitched blade turbine with a diameter $\sim 1/3$ that of the vessel and is operated at low speeds (30-60 rpm). The impeller has a low solidity ratio (ratio of impeller projected area to impeller swept area), which allows a high flow rate at low shear. Since the tank is not baffled, the impeller is inserted into the tank at an angle of $\sim 15^\circ$ from the vertical axis of the tank. Flow through the impeller is downward, as this is the most efficient way to operate this impeller as a blending device.¹²

4. Process Control

The process has two control loops, one for pH and one for sulfide. The pH control loop consists of the pH electrode, pH proportional controller, and a diaphragm metering pump. The controller actuates the diaphragm metering pump for addition of feed. Above the proportional

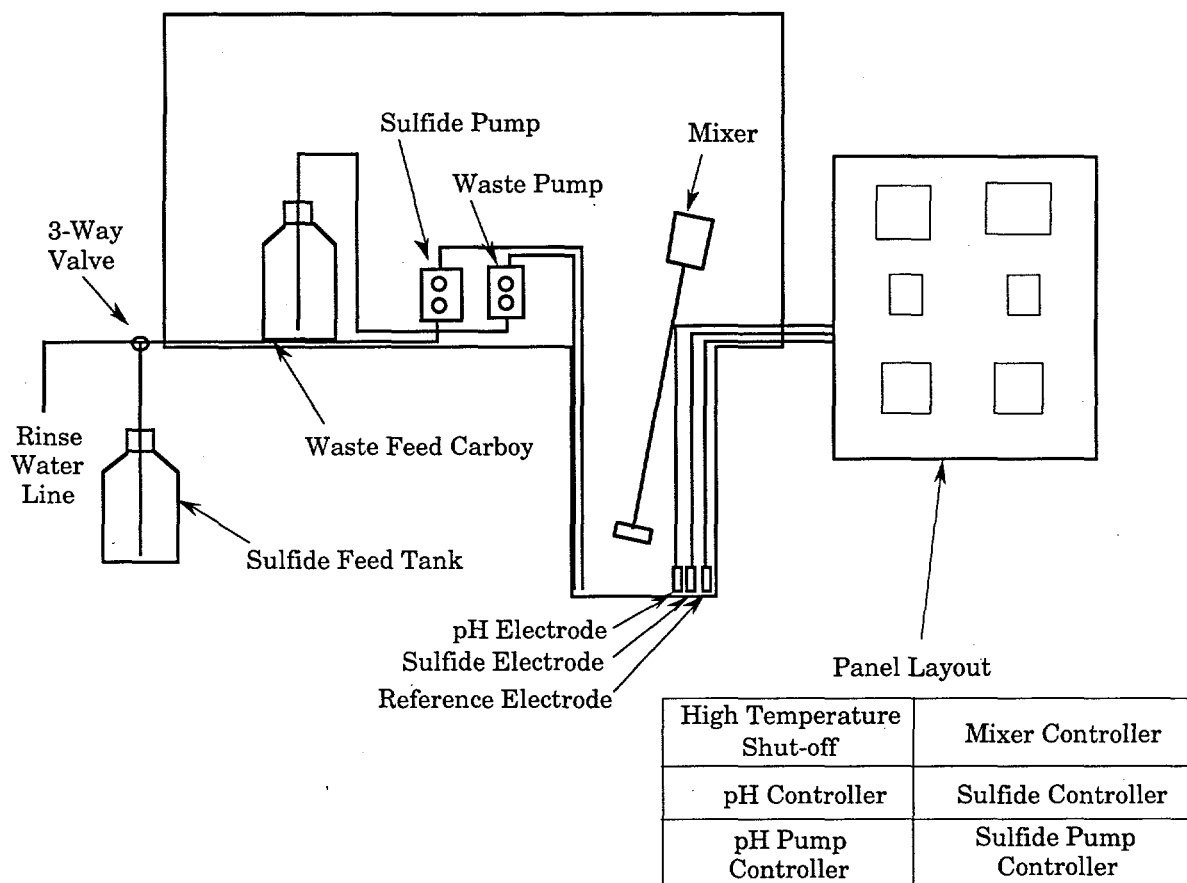
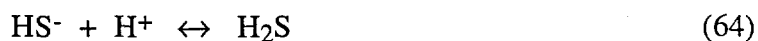


Fig. 41. Equipment for Alkaline Sulfide Precipitation

control region the pump runs at maximum flow rate. In the proportional control range the flow rate is proportional to the difference between the actual pH and set point pH. The pH proportional control action is set to start 1 pH unit away from the set-point pH; this allows rapid addition of feed to the tank while minimizing overshoot.

The sulfide control loop consists of a sulfide specific electrode, mV proportional controller, and a diaphragm metering pump. The controller actuates the diaphragm metering pump to feed sulfide until the desired concentration of free sulfide is achieved. For this controller the proportional control region is set 100 mV greater than the set point. However, determination of the set points for this controller is not straightforward. The sulfide specific electrode senses only S^{2-} ; both HS^- and H_2S are also present in varying amounts, depending on the pH, according to the following equilibria:



Real-time measurements and control of total sulfide ($S^{2-} + HS^- + H_2S$) are possible if the pH and the sulfide specific electrode potential are known. The pH and the quantity of S^{2-} present in the solution are measured, and the quantity of HS^- and H_2S can be determined from the

chemical equilibrium given in Eqs. 63 and 64 to determine total free sulfide. Alternatively, a table showing the desired total sulfide concentration as a function of pH has been prepared (shown in Table 28). If the table is used, the potential for the corresponding pH is entered into the controller. Sulfide addition stops when that potential is reached.

Table 28. Calibration Data to Adjust Sulfide Set Points

pH	Low Current Set Point, mV	High Current Set Point, mV	Maximum Potential for Sulfide at 300 ppm, mV
10.0	-707	-607	-746
10.5	-724	-624	-763
11.0	-740	-640	-779
11.5	-757	-657	-796
12.0	-773	-673	-813
12.5	-790	-690	-830

5. High Temperature Shutdown

Neutralization reactions are fairly exothermic. The high temperature shutoff (Fig. 41) stops the process in the event of excessive heating ($T > 80^{\circ}\text{C}$). The polyethylene tank used for the treatment vessel has a glass transition of $\sim 110^{\circ}\text{C}$,¹³ which is well above the high-temperature shutdown point.

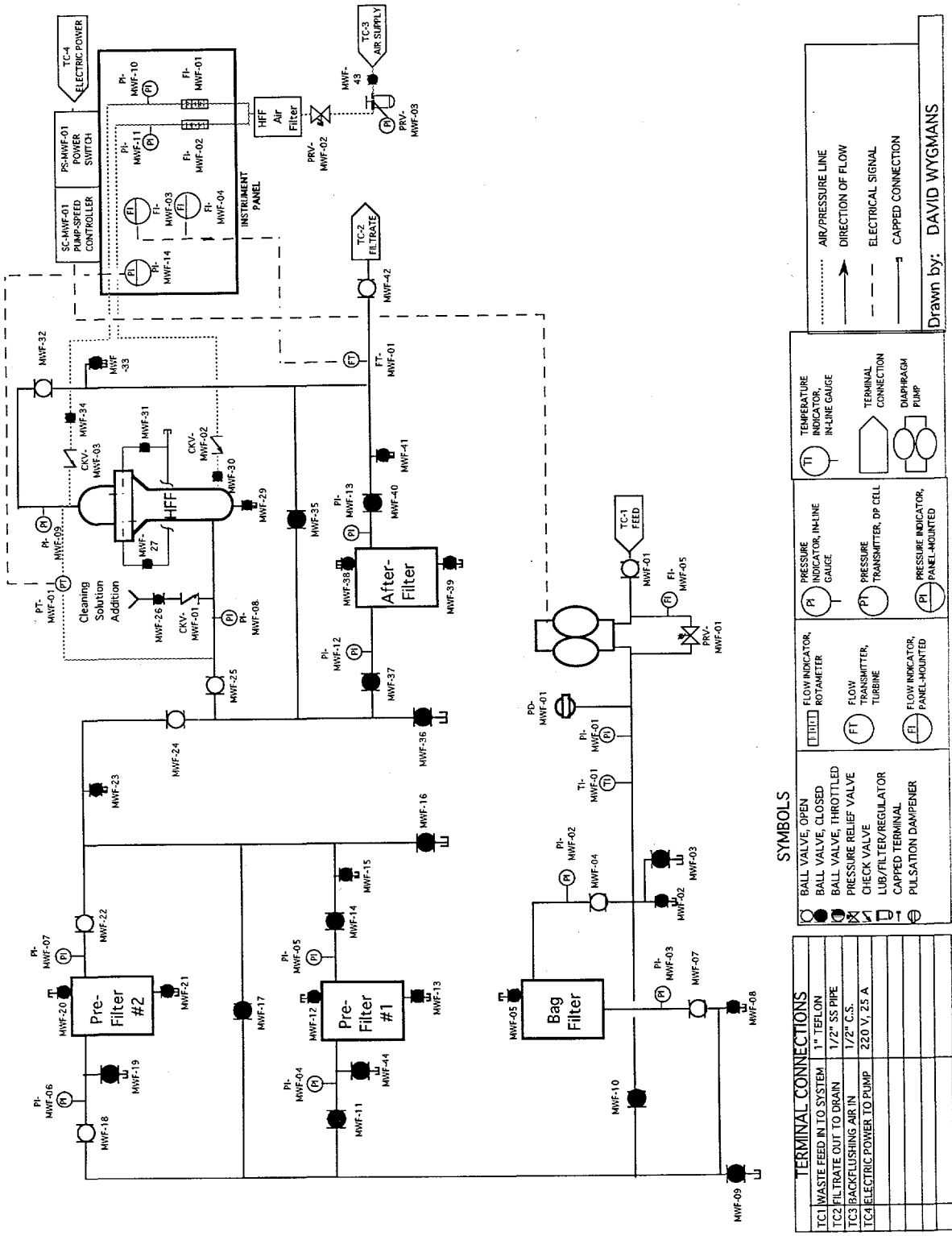
6. Transfer Pump

A peristaltic pump (not shown in Fig. 41) is used to pump waste from the treatment vessel into a transport tank. The transport tank can then be moved from the treatment room to the filter skid for separation of the solids from the liquid.

C. Development of Filter Skid (D. Wygmans)

A portable filtration skid had been designed for use in filtering a wide variety of mixed waste streams, including the one generated in the alkaline sulfide precipitation process, and an overview of the design was given in the previous report.¹⁴ Fabrication of the skid is close to completion. A current piping and instrumentation diagram for the filtration skid is shown in Fig. 42. As fabrication and testing of the skid proceeded, a number of design changes were necessary. Most of these modifications are outlined below.

The pressure relief valve originally installed on the system bypassed a considerable amount of flow at lower pressures, so that the design flow of 5 gpm (19 L/min) at 100 psig (0.69 MPa) could not be attained. A suitable relief valve was purchased, which would protect the system against pressures above 120 psig (0.83 MPa) yet allow a flow of 5 gpm (19 L/min) through the system at 100 psig (0.69 MPa).



Drawn by: DAVID WYGMANS

SYMBOLS

TERMINAL CONNECTIONS	1" TEFLON
TC1 WASTE FEED IN TO SYSTEM	
TC2 FILTRATE OUT TO DRAIN	
TC3 BACKFLUSHING AIR IN	
TC4 ELECTRIC POWER TO PUMP	

○	BALL VALVE, OPEN
●	BALL VALVE, CLOSED
⊘	BALL VALVE, THROTTLED
⊘	PRESSURE RELIEF VALVE
⊘	CHECK VALVE
⊘	LUB/FILTER/REGULATOR
⊘	CAPPED TERMINAL
⊘	PULSATION DAMPENER

⊘	FLOW INDICATOR, ROTAMETER
⊘	FLOW TRANSMITTER, TURBINE
⊘	FLOW INDICATOR, PANEL-MOUNTED

⊘	PRESSURE INDICATOR, IN-LINE
⊘	PRESSURE TRANSMITTER, DP CELL
⊘	PRESSURE INDICATOR, PANEL-MOUNTED

⊘	TEMPERATURE INDICATOR, IN-LINE GAUGE
⊘	TERMINAL CONNECTION
⊘	DIAPHRAGM PUMP

⊘	AIR/PRESSURE LINE
→	DIRECTION OF FLOW
---	ELECTRICAL SIGNAL
⊘	CAPPED CONNECTION

A front-end strainer was needed to protect the pump from large particles. The manufacturer states that the diaphragm pump can handle particles up to about 1/16-in. dia without plugging the reed valves. Given that the feed stream is waste, which may contain rubbish (e.g., paper, pipette tips), the presence of particles larger than 1/16-in. is likely. A suitable strainer is being sought.

A considerable amount of organic material was found in the piping system during startup tests. This material is apparently Teflon "pipe dope" used on the pipe threads during fabrication. Some of this organic material apparently dissolves or becomes suspended in the water being pumped through the system, leaving a slippery film on wetted parts. Also, dollops of the material were flushed out when the filter housings were drained and when the sample valves were opened. The material is apparently denser than water; it was found in low points in the system, where sedimentation had apparently deposited it. Since organics will wet the pores of the hollow-fiber filter and plug them, this organic material must be eliminated from the system before the filter skid is operated. A search for appropriate cleaning agents is underway. Teflon tape will be used instead of pipe dope during any future modifications made on the system.

During testing, the prefilter housings initially installed would not hold the prefilter elements that were purchased. The housings were purchased under the verbal understanding that industry-standard cartridges would fit into the housings, but the housings did not meet this specification. Suitable replacement housings were purchased from another manufacturer and installed on the skid.

Flow rate vs. pressure drop data across the hollow-fiber filter (HFF) were taken. They indicated that the HFF is a hydrophobic membrane. HPD, Inc., who manufactured the filter in 1988, now manufactures a hydrophilic model in its place. The data also indicated that the membrane is in good condition and has not been damaged by drying out.

Conversations held with HPD, Inc., uncovered that, after much field experience, HPD now recommends a crud-loading limit of 10 grams per square meter of HFF area. Previous specifications used the pressure drop across the element as the sole indicator of the need for cleaning. The new specification attempts to limit the amount of solids trapped on the filter so that back flushing can be effective. The HPD found the new specification necessary because the pressure drop indicator alone did not ensure that effective back flushing could be attained. For WM's 10 m² hydrophobic-membrane unit, the new specification means that no more than 100 g of suspended solids between the sizes of 0.1 and 10 μ m should be fed to the unit before a back-flushing cycle should be initiated. The import of this new specification has yet to be determined.

To limit disposal of spent filter elements, the piping system was modified so that both pre-filters could be back-flushed.

An operations manual for the filtration skid was compiled. This manual includes general information, equipment descriptions and layout, operating and maintenance procedures, and individual component information. Start-up testing procedures for the skid were written. A safety analysis report for the filtration skid was also prepared, reviewed, and adopted.

After a hydrostatic test of the piping system showed that the system was free of leaks, start-up testing was completed. The purpose of this testing was to verify proper operation of the major

system components. The testing verified that most of the components on the skid operate as expected, while some components need work. Most of the problems found are noted above and have been remedied. The written operating procedures were also tested and modified as necessary during the start-up testing. Once all modifications are complete, another hydrostatic test will be performed.

D. Regulatory Permits

Before processing of mixed wastes can begin, documentation and permitting are required under the National Environmental Policy Act (NEPA) and the Resource Conservation and Recovery Act (RCRA). The NEPA regulates work done by government agencies. The RCRA, which is mandated by the federal government but controlled at the state level, regulates the handling, treatment, shipment, etc., of hazardous wastes.

A NEPA application was first submitted on July 23, 1993, requesting that the mixed-waste treatment system (chemical treatment, filtration, and concentration) be covered under existing Categorical Exclusions (CX). This request was rejected because of lack of clarity regarding whether the system was to be used for long-term processing or for treatability studies. [If the system is to be used for long-term processing, an Environmental Assessment (EA) may be required; treatability studies, by definition, are limited in scope and duration and may be covered under a number of CX's already in place.] Re-submittal was made on September 13, 1993, requesting a CX for treatability studies. After sufficient data have been gathered to prove the principle of the treatment system, another NEPA application will be filed to determine if an Environmental Assessment is needed.

Since the treatment system will be used to treat mixed wastes (i.e., containing a hazardous component and a radioactive component), the system must be permitted under the RCRA. The permitting process involves two parts. Part A is an informational, interim step whereby notification is given of the intent to handle hazardous wastes. Once a Part-A permit has been granted, 1000 kg of material (~four drums of liquid) can be processed under the category of treatability studies. Part B of the permitting process, to be completed during the interim period, requires considerably more documentation.

Since WM is already under a Part A permit, an informational overview of the system is all that is necessary before treatability studies can be undertaken. A letter, with an informational overview attached, was sent on September 9, 1993, from the Argonne Area Office to the Illinois EPA (IEPA) notifying them of our intent to conduct treatability studies on mixed waste. A 45-day notification period is required following the issuance of the letter before treatability studies can begin.

Treatability studies are subject to a number of constraints, including the following:

1. No more than 1000 kg of hazardous waste can be treated under a particular study. This limit may be extended to 1500 kg by the state under certain conditions.

2. No more than 250 kg of "as received" hazardous waste is subjected to initiation of treatment in all treatability studies in a single day. This constraint requires coordination of all treatability studies at ANL.
3. Accurate records are kept for all samples stored and treated under the study. These records must include information about daily storage and treatment and must be kept on file for at least three years.
4. A report needs to be submitted to the state by March 15 of each year detailing plans regarding treatability studies for the coming year as well as detailed records for the past year.

The above is a general summary of the requirements. Full requirements are specified under the RCRA (40 CFR Ch.1, §261.4) and under 35 Illinois Adm. Code 721.

E. Cesium Removal from Wastewater

(D. B. Chamberlain, C. J. Conner, D. G. Wygmans, and G. F. Vandegrift)

1. Resin Studies

As part of our ad hoc technical support to WM, methods were investigated for treating two sources of wastewater that contained radioactivity in excess of the laboratory-site discharge limits. One source consists of 4,000 gal (15 m³) of water in a Suspect Waste Tank (SWT). The other source is ~14,000 gal (~53 m³) of water in High Level Waste Vault (HLWV). Initial analysis of the samples indicated that most of the activity in both water samples was due to ¹³⁷Cs. The Analytical Chemistry Laboratory (ACL) in CMT confirmed the presence of ¹³⁷Cs; results of ACL's radiochemical analysis are shown in Table 29. The cationic compositions of these two water samples were also measured by ACL and are shown in Table 30.

Table 29. Activity (in pCi/L) of Radiochemical Analysis of SWT and HLWV Samples

Sample	Cs-137 ^a	Co-60 ^a	Cs-134 ^a	Alpha	Beta
SWT	8.53x10 ⁴	1.14x10 ³	3.31x10 ³	1.58x10 ³	9.37x10 ⁴
HLWV	1.99x10 ⁵	1.70x10 ²	—	1.24x10 ³	3.26x10 ⁵

^aDetermined by gamma-ray spectroscopy; because Cs-137 and Cs-134 also release β-rays during decay, they also contribute to the total beta activity in the samples.

Table 30. Concentration (ppm) of the Cations in Water Samples

Sample	Mg	Fe	Ca	K	Na
SWT	2.9	0.49	5.4	54	1200
HLWV	19	<0.02	57	13	16

Batch distribution tests were performed to determine the effectiveness of several ion-exchange resins at removing the cesium contamination. First, general-purpose ion-exchange resins were tried, and results for these tests are reported in Table 31. (PUROLITE C-105 is a sodium-form weak-acid resin, and IONAC CFP-110 is a hydrogen-form strong-acid resin.) The

Table 31. Measured Distribution Ratios for ^{137}Cs with General-Purpose Ion-Exchange Resins

Sample	g Resin per mL Feed	K_d , ^a mL/g	
		PUROLITE (C-105)	IONAC (CFP-110)
SWT	0.01	32	85
	0.05	12	203
	0.10	20	385
HLWV	0.01	59	560
	0.05	63	b
	0.10	79	b

^aCalculated using the 662 keV (Cs-137) gamma-ray.

^bCould not be calculated; the 662 keV gamma-ray was below detection limits.

distribution ratios (K_d) for these resins were not large enough to effectively treat the wastewater. For favorable treatment, K_d values should be >1000 ; for effective treatment they should be $>10,000$. The batch distribution ratios (K_d) are determined from

$$K_d = \frac{\text{CPM}_{[\text{Initial}]} - \text{CPM}_{[\text{Equilibrated}]}}{\text{CPM}_{[\text{Equilibrated}]} * \frac{\text{g Resin}}{\text{mL Solution}}} \quad (65)$$

where CPM = counts per minute.

A single-column test was also completed with the DOWEX AG 50W-X8 resin (strong acid, converted from hydrogen form to sodium form). Since the DOWEX resin and the IONAC resin are both strong-acid forms, they should behave similarly. The column used was 10-cm high by 1-cm dia, and the flow rate through the column was 22.5 gal/(ft²-h), which is equivalent to nine column volumes (CV) per hour. Results from the analysis of the column effluent from this test are shown in Fig. 43.

A breakthrough of 1% occurred at less than 1 CV; between 1 and 10 CV the breakthrough rose from 4% to 6%. Thus, the column at this high flow rate was not very effective. Improvements could be made to this system by using a lower flow rate (≤ 3 CV/h) and using a resin in the hydrogen form rather than in the sodium form. In the hydrogen form, the resin would remove the sodium from solution in the top of the column, leaving the bottom of the column to remove ^{137}Cs . For this test, the column was converted to the sodium form to better simulate the PUROLITE resin, which was recommended by the vendor. Based on the results of these laboratory tests, a cesium-specific resin is required because of the large difference in concentrations between ^{137}Cs and the other cations in solution. Two cesium-specific resins are available: (1) CS-100, manufactured by Rohm & Haas, and (2) resorcinol, available from Savannah River Site (SRS).

Samples of the CS-100 and resorcinol resins were obtained, and batch distribution ratio studies were completed. Initial tests with CS-100 resin (Table 32) showed little promise.

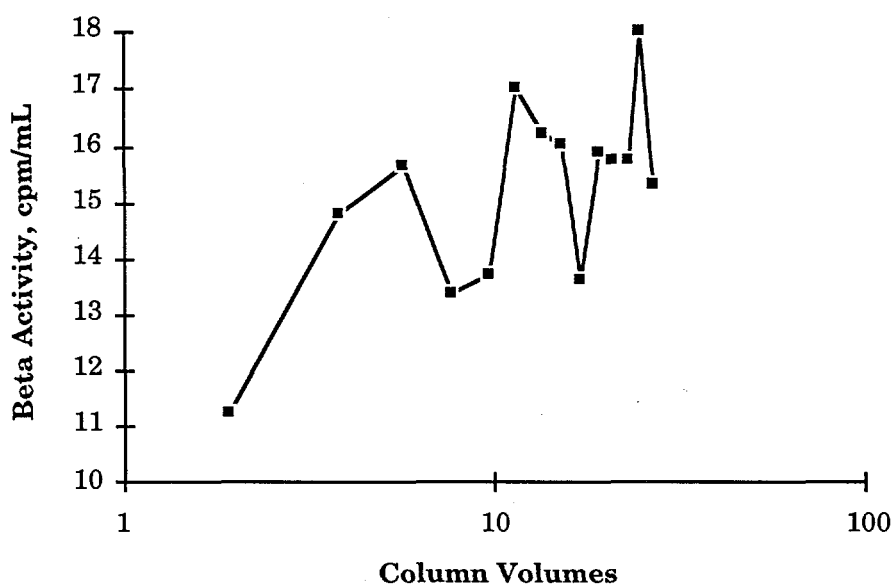


Fig. 43. Results from Analysis of Column Effluent Using DOWEX AG 50W-X8 Resin (beta activity in feed = 260 cpm/mL)

Table 32. Batch Distribution Ratios for Cesium-Specific Resins

Sample	g Resin per mL Feed	pH	Cs-137 Dist. Ratios, ^a mL/g			
			Resorcinol (AT Sample ^b)	Resorcinol (AM Sample ^c)	Resorcinol (BT Sample ^d)	R&H (CS-100)
SWT ^e	0.01	8-9	—	—	—	8
	0.05		—	—	—	278
HLWV ^e	0.0002	7-8	—	—	—	33
	0.001		—	—	—	74
	0.01		156	135	100	23
	0.05		355	455	109	10
HLWV ^f	0.001	10	—	660	—	—
	0.01		—	1672	—	72
	0.05		—	—	—	117
HLWV ^f	0.01	12	—	1212	—	—
HLWV ^{f,g}	0.001	10	—	16,320	—	—
	0.01		—	16,463	—	—

^aCalculated using the 662 keV (Cs-137) gamma-ray.

^bSample from Drum A Top portion.

^cSample from Drum A Middle portion.

^dSample from Drum B Top portion.

^eThe pH was not adjusted.

^fThe pH was adjusted by using 0.1M NaOH.

^gAfter sample was pH adjusted, it was treated with 0.1 g/mL of PUROLITE (C-105) resin. Then it was treated with the resorcinol resin. The K_d values reported are for the overall resin treatment.

Therefore, effort was concentrated on the resorcinol resin. (Resorcinol resin is manufactured in the potassium form, but it was converted to the hydrogen form for our distribution studies.) Resorcinol is reported to be the best cesium-specific resin available. Two drums of the resorcinol resin were obtained from Jane Bibler (SRS). The quality of the resin in the two drums was different. Therefore, three samples were taken for testing: one from the top of the first drum (drum A), one from the middle of drum A, and one from the top of the second drum (drum B). Drum B was wet inside and contained about 2 in. (5 cm) of standing water on top of the resin, making sampling difficult and messy, so only one sample was taken. Initial results with the resorcinol resin were lower than expected. However, the resin was designed to work at much higher pH (10-14). Therefore, batch tests were completed by using HLWV water that had been adjusted to pH 10 and 12 with 0.1M NaOH. This significantly increased the K_d values, but they were still lower than expected. We thought that the significant quantity of Ca and Mg present in the HLWV might interfere with cesium removal. Therefore, a sample of the HLWV was treated with the PUROLITE resin to remove Ca and Mg prior to treatment with the resorcinol resin. This improved the K_d values from marginal to excellent. Even so, Bibler did not think that Ca and Mg would interfere with the resorcinol resin, so the large increase cannot be explained at this time.

A small column was set up with the same hydrodynamic characteristics as the column purchased by WM (see Sec. VI.E.2). The test column was loaded with 80% resorcinol resin (potassium form) on the bottom, and the remaining 20% at the top was filled with PUROLITE resin (sodium form). Inactive cesium chloride was added to a sample of HLWV water to increase the cesium concentration by a factor of 500, as calculated from the ^{137}Cs concentration. This was done in an effort to load the column with a small volume of solution so breakthrough could be observed. The sample was also pH adjusted with 0.1M NaOH to increase the pH to 10. Approximately 1000 CV of solution was run through the column at a flow rate of 9 CV/h. No ^{137}Cs was detected in the effluent before the experiment was terminated due to lack of solution; therefore, no breakthrough curve could be generated. Thus, the column that has been set up (as discussed below) with the PUROLITE and resorcinol resin combination should be effective for treating the HLWV water at a flow rate of 9 CV/h.

2. Setup of Resin Column

Two identical vessels were purchased by WM from Environmental Dynamics Corp. (EDC) for use in ion-exchange treatment of the SWT and HLWV wastes. A schematic of these vessels is shown in Fig. 44. The vessel, a 14-in. (35-cm) dia x 64-in. (162-cm) high (not including end caps) cylinder, is made of fiberglass, and the main plumbing components are PVC. Given those dimensions, the column should have a capacity of about 6 ft³ (0.17 m³). The EDC recommends filling the column with about 4 ft³ (0.11 m³) of resin to allow for expansion, which may occur as the resin changes form during processing. Unfortunately, the design of these columns does not allow for resin regeneration. The resin must be disposed of once it is spent. The EDC also sells a column that is capable of a regeneration cycle. However, these columns will be considered for future efforts only.

The column is charged with resin using the eductor. Laboratory water or deionized water flows in the charging-water inlet and out the charging-water outlet or the process water outlet. (It is important to take into account the change in form that may occur in the resin as it is

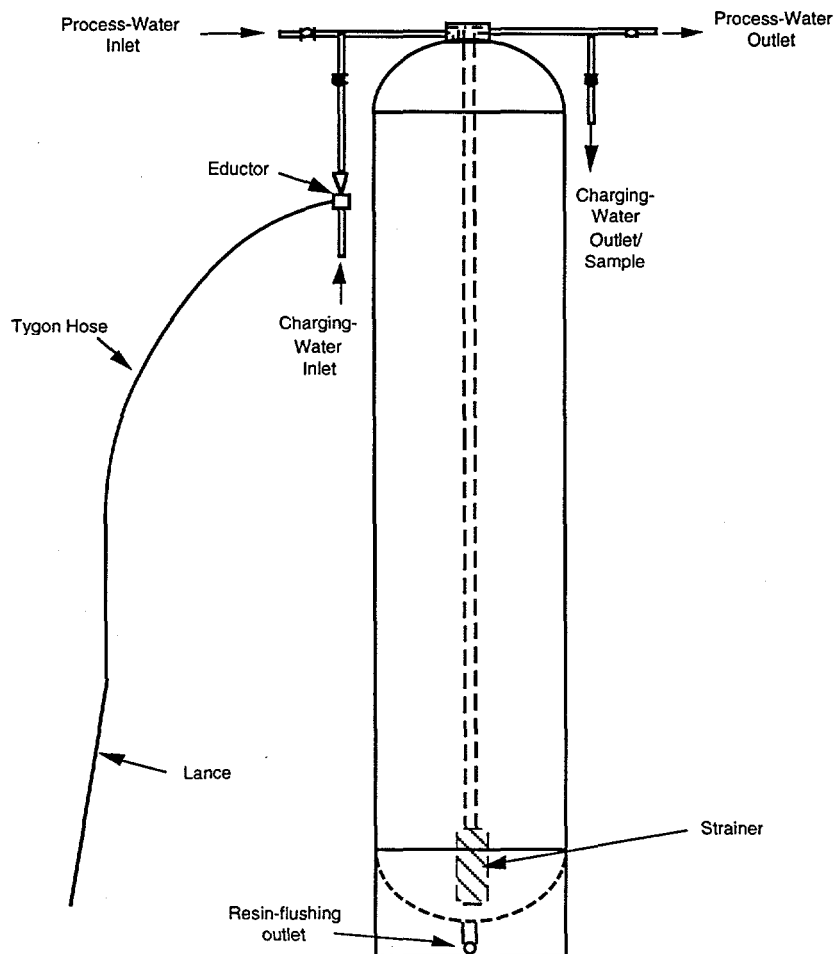


Fig. 44. Schematic of Ion-Exchange Vessel

contacted with the charging water.) As water flows through the eductor, a pressure differential is generated by the eductor, and low pressure will be seen at the lance. The lance is then used to suck a stirred resin slurry (~50% mixture) into the vessel. The resin is trapped at the strainer and held in the column. For processing, the process-water inlet and outlet valves are opened, and all other valves are closed. Water flows into the manifold at the top of the column, is dumped into the vessel, and flows through the strainer and then the outlet. Resin is discharged from the column by opening the resin-flushing outlet valve at the bottom of the column and running water into the column while the other outlet valves are dead.

The resin studies (Sec. VI.E.1) indicate that the best results are attained when a combination of PUROLITE and resorcinol resins is used, with the PUROLITE contact as a pre-treatment step. Because the resorcinol (which has a very small particle size) would be in contact with the strainer (which is a plastic cylinder with ~250-300 μm slits), a quick test was performed to determine if resin particles would pass through the strainer. Results showed that some resin did pass through, while other particles got stuck in the slits. Therefore, the strainer was covered with a 30 μm bag filter. The column was then loaded with about 3.3 ft^3 (0.09 m^3) of resorcinol resin,

followed by 1 ft³ (0.02 m³) of PUROLITE; the eductor and laboratory cold water were used as the charging water.

During the loading of the resorcinol, the resin had to be flushed with water before the flushing water was free of a dark material (either dissolved or colloidal) which could not be retained on a filter. Since this material could complex cesium and carry it through the filter, the resin bed had to be flushed of this material before the bed could be used to process contaminated water. About 130 gal of laboratory water was run through the bed after charging had been completed. The water effluent at the end of this flushing was fairly clear.

Flow rate vs. pressure drop data for the resin bed (Table 33) were taken while the pump on the filtration skid was used to pass water through the resin bed. The instruments on the skid were used for the pressure and flow-rate measurements. That the last two data points shown in Table 33 are conflicting may be due to packing of the bed during the test. Both pairs of readings were taken with the pump speed set for 100%, and there was an unrecorded time lag (probably about 10 min) between readings, during which the flow was continuous. However, a problem with the pressure relief valve on the filtration skid was also noted shortly after the test (as noted below), and the discrepancy between the two readings may be associated with this problem.

Prior to running any of the HLWV water through the ion-exchange column, a variance for the laboratory-site discharge limits was obtained. Therefore, no water was processed through the column but was discharged directly.

Table 33. Results of Pressure-Drop Test on Resin Bed

Flow Rate, gpm (L/min)	Pressure Drop, psi (kPa)
0.04 (0.15)	15 (103)
0.8 (3.0)	20 (138)
1.8 (6.8)	22 (83)
2.9 (11)	30 (113)
4.7 (18)	35 (132)
4.6 (17)	40 (151)

VII. MAGNETICALLY ASSISTED CHEMICAL SEPARATIONS

(L. H. Nuñez)

We are developing a process for the treatment of radioactive and hazardous sludge or supernatant from the Hanford waste tanks. Transuranic (TRU) waste is of considerable concern, due to the longevity of its potential hazard resulting from the long half-life of its radioactive components. Our process for treating this waste is based upon magnetically assisted chemical separation (MACS). The process combines the selective and efficient separation afforded by chemical sorption with the magnetic recovery of ferromagnetic beads.

Many DOE sites have aqueous radioactive, mixed, and hazardous wastes stored in tanks awaiting treatment and ultimate disposal. The sludge and supernatants in the underground storage tanks at Hanford contain Cs, Sr, and, in some cases, TRU elements (low concentrations) that must be removed to dispose of this stream as grout. For the remediation efforts at Hanford and other DOE sites, this project will develop a compact, economic, in-tank or near-tank process for the removal of contaminants from solution.

The process uses magnetic beads coated with (1) a selective ion-exchange material (e.g., silicotitanates, resorcinol), or (2) an organic complexant-containing solvent for Cs and Sr removal, or (3) solvents for selective separation of TRUs (e.g., from the TRUEX process). Organic solvents can be adsorbed onto the polymeric surface by contacting the beads with a solution of the solvent in a volatile diluent and removing the diluent by evaporation. These coatings selectively separate the contaminants onto the beads by their chemical nature, and the beads can be recovered from the tank using a magnet. After removal, the contaminants can be either left on the loaded beads and added to the glass feed slurry, or stripped into a small volume of solution to regenerate the extracting beads. (For example, the TRUEX solvent can be washed from the beads with alcohol, which diminishes the extraction power of CMPO and TBP, and stripped of activity by dilute acid. The alcoholic solution can then be evaporated to regenerate the beads.) The greatest benefit of the process is the simple separation of radionuclides from waste in a cost-efficient and compact manner without the production of large waste streams. Also, this process is applicable to many liquid TRU waste streams of DOE.

The technical progress reported here covers (1) coating of magnetic particles, (2) particle morphology and its effect on the TRU partitioning, (3) TRU separation capabilities in acid media, (4) cesium removal from Hanford tank supernatant, and (5) effects of gamma-irradiation damage on magnetic particles.

A. Particle Morphology (C. Bradley and L. H. Nuñez)

The MACS process is being developed using both partition coefficient (Eq. 65) determinations and transmission electron microscopy (TEM) data to identify the particle types most suitable for nuclear waste remediation. Figure 45 shows three TEM micrographs that were used to eliminate particle types that inhibit the chemisorption of the CMPO/TBP extractants. Figure 45a shows that the dark magnetite particles (<10 nm) are aggregated on the polymeric surface; this particle type showed the poorest chemisorption of the extractants. Figure 45b shows magnetite encapsulated within the polymer coating, which resulted in larger K_d values than those obtained from



(a)

(b)

(c)

Fig. 45. Transmission Electron Micrographs of (a) Bright Field Image of Polyacrolein/Magnetite Particles, (b) Magnetite-Encapsulated Particles, and (c) Charcoal-Cross-Linked N,N,Methylene Bis-acrylamide with Irregular Polymer Shape and Magnetite Particles

particles illustrated in Fig. 45a. Figure 45c illustrates charcoal-type particles with irregular shape and large surface area for sorption of the extractants. The magnetite particles are distributed in the inner core and the surface of the polymer. Our analysis results indicate that particles with hard, smooth surfaces or all the magnetite distributed on the surface did not adsorb the extractants.

B. Particle Coating Process

(M. D. Kaminski and L. H. Nuñez)

The sorption process was evaluated by systematically varying physical parameters (volume, temperature, time) and determining the partition coefficient K_d . The particles used for coatings are mixtures of a cross-linked polyacrylamide (N,N-methylene bis-acrylamide), charcoal, and magnetite (Fe_3O_4) in a 1:1:1 weight ratio. The CMPO concentrations were 0.6-1.5M dissolved in TBP. All partitioning tests used ^{241}Am tracer in 2M HNO_3 at 25°C. As shown in Table 34, the most sensitive parameter was the temperature of the coating process, and an annealing procedure will be developed to obtain maximum TRU partitioning.

Table 34. Partition Coefficient Dependence on Ethanol Volume, Initial Temperature, and Particle Separation Time. (CMPO concentration, 1.36M; coating thickness, 1.4 μm)

K_d , mL/g	Ethanol Volume, mL	Initial Temperature, °C	Particle Separation Time
1157	30	85	30 min
1096	30	85	30 min
1030	15	85	18 h
790	15	65	30 min
780	30	65	30 min
686	15	85	30 min

C. Transuranic and Cesium Separation Capabilities

(L. H. Nuñez, B. A. Buchholz, and M. D. Kaminski)

To compete with other separation techniques, a batch process such as MACS must yield large partition coefficients for TRU elements. Large partition coefficients for both Am and Pu were measured with CMPO/TBP-coated magnetic particles in nitric acid of various concentrations (Fig. 46). The ^{238}Pu experiments yielded K_d values of 5800 for a 2M HNO_3 solution, while K_d values of the particles without any extractant are between 0 and 33. As shown in Fig. 46, the K_d values for both Am and Pu increased slowly up to 1M HNO_3 , then decreased at the higher nitric acid concentrations. The K_d values fall between 10 and 4000 for americium and between 100 and 46,000 for plutonium. This result suggests that the process can be applied in a batch mode for a wide range of nitric acid concentrations.

Currently, ANL and Bradtec, Inc., are developing magnetic particles with resorcinol, silicotitanate, clinoptilolite, and transylvanian volcanic tuff (TVT) to be evaluated for the separation of cesium from a basic supernatant similar to the composition of some Hanford tanks (indicated in Table 35).

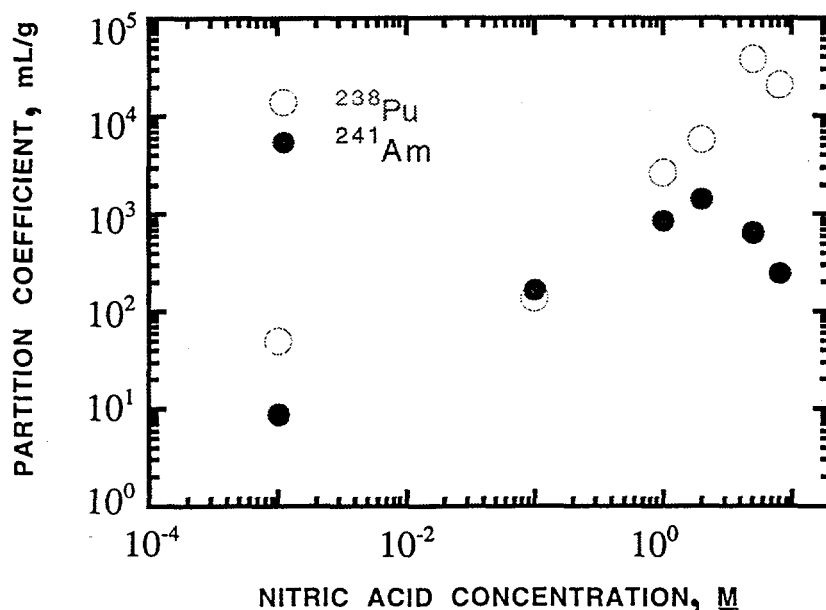


Fig. 46. Dependence of Partition Coefficients for ^{241}Am and ^{238}Pu on Nitric Acid Concentration (CMPO/TBP coatings on magnetic particles at 25°C)

Table 35. Composition of Simulated Tank Supernatant for Cesium Removal

Major Components	Component Charge	Concentrations, mol/L
Na	1	8.83E+00
K	1	9.35E-02
Cs	1	4.88E-05
OH	-1	6.54E+00
NO ₃	-1	1.09E+00
NO ₂	-1	8.09E-01
Al(OH) ₄	-1	2.06E-02
CO ₃	-2	2.22E-01
CrO ₄	-2	4.37E-03
PO ₄	-3	8.00E-04

D. Gamma-Irradiation Studies (B. A. Buchholz)

The irradiation of magnetic micro-particles in a ^{60}Co cell began recently. The particles in various irradiation solutions (Table 36) were sealed in quartz vials and rotated while being irradiated. Upon completion of irradiation, the samples were recovered and K_d values were measured. The approximate doses to the particles (equivalent to 10, 100, and 2000 cycles of use) were calculated based upon the composition of waste solutions and the physical characteristics of the particles. The particles for TRU removal receive most of their radiation dose from the α -decay of Am and Pu, while the particles designed for ^{137}Cs removal receive their dose from β -decay and γ -rays.

The dose is deposited through the ionization of target atoms when the emitted alpha or beta particles pass through them. Preliminary indications are that the K_d values of the TRU-coated particles decreased as the acid concentration of irradiation solutions increased from 0.1 to 5M. Also, the K_d values appeared to decrease as dose increased. More detailed results will be given later.

Table 36. Irradiations of Magnetic Microparticles

Particles	Dose, Mrad/cycles	Irradiation Solutions
TRU Removal	0.013/10	Deionized Water
	0.13/100	0.1M HNO ₃
	3.1/2000	2.08M HNO ₃
		5M HNO ₃
		PFP Simulant ^a
Cs-137 Removal	0.6/10	SST Supernatant Simulant ^b
	6.0/100	

^aPFP = Plutonium Finishing Plant.

^bSST = Single-Shell Tanks.

VIII. MOLYBDENUM-99 TARGET PROCESSING

(J. Hutter, C. Srinivasan, and G. F. Vandegrift)

Molybdenum-99 is a precursor of ^{99m}Tc , which is used in several medical applications. Since ^{99}Mo is not naturally abundant, it must be produced by one of two types of controlled nuclear reactions. In one method, ^{99}Mo is produced by neutron bombardment of ^{98}Mo , and the ^{99}Mo is generated by the following nuclear reaction: $^{98}\text{Mo}(n,\gamma)^{99}\text{Mo}$. This method is not amenable to full-scale production because its product has a low specific activity.¹⁵ In several parts of the world, ^{99}Mo is being produced by the fission of ^{235}U , i.e., $^{235}\text{U}(n,f)^{99}\text{Mo}$. The ^{99}Mo is recovered by dissolving the irradiated target and purifying to ^{99}Mo from the dissolved solution. This process has many variations, but its common feature is that the ^{235}U is contained in high-enriched uranium (HEU) targets.

Recent legislation in the United States requires that the export of HEU be curtailed to prevent nuclear weapons proliferation. To meet these new requirements, production of ^{99}Mo must proceed with low enriched uranium (LEU). The Reduced Enrichment Test Reactor (RERTR) was established to develop LEU reactors and reactor fuels. We are developing processes to produce ^{99}Mo from LEU targets instead of HEU targets. The two most promising new LEU targets contain uranium metal or uranium silicide. These new targets can be substituted for the HEU UO_2 or various UAl_x alloys now in use. Like the UO_2 -based process, an acid dissolution scheme is being developed for ^{99}Mo recovery. For various UAl_x alloys, both acid and basic dissolution schemes are being used. The uranium silicide is more amendable to a basic dissolution procedure.

A. The Cintichem Process

The Cintichem process^{16,17} is now used to produce ^{99}Mo from the fission of 93% enriched UO_2 . The Cintichem target is shown in Fig. 47.

The HEU fuel containing UO_2 as the target is constructed of 304 stainless steel with an electroplated coating of the target material on the inside walls of the tube. Electroplating is done from an aqueous solution of $0.042\text{M } \text{UO}_2(\text{NO}_3)_2 \cdot 6\text{H}_2\text{O}$ and $0.125\text{M } (\text{NH}_4)_2\text{C}_2\text{O}_4 \cdot \text{H}_2\text{O}$ at pH of 7.2. The physical characteristics of the cylindrical fuel element are given in Table 37.

Table 37. Characteristics of Cintichem Fuel Element

Volume of the fuel element	231.33 cm ³
Density of UO_2	≤ 10.96 g/cm ³
Mass of UO_2	22.6 g
Thickness of UO_2	0.0068 cm
Length of UO_2	38.1 cm

Targets are typically irradiated at a neutron flux of 3×10^{13} n/cm²•s for about 100 h. The target is designed to withstand temperatures up to 500°C; it will reach 330°C under the conditions of irradiation.

Upon completion of the irradiation, the target is cooled and then moved to a hot cell. Before the UO_2 dissolution, all gases released during the cool down are vented to a liquid nitrogen

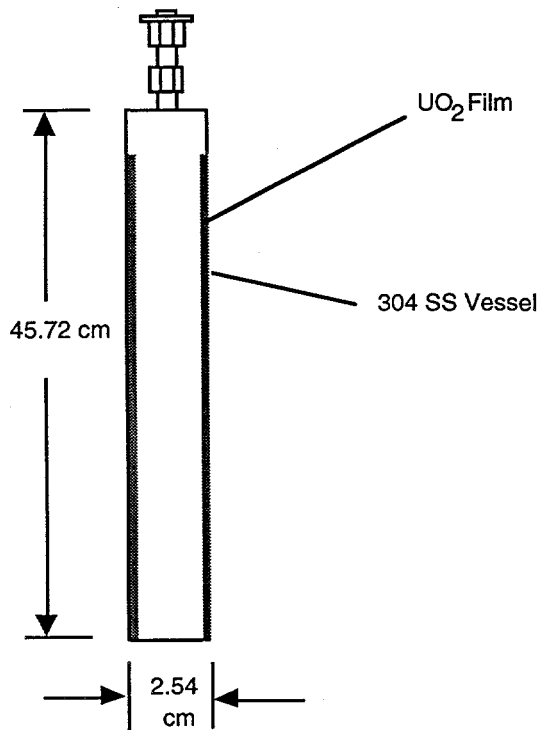


Fig. 47. Schematic of Cintichem Target

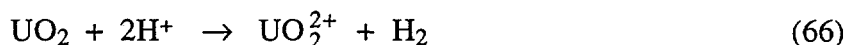
cold trap to recover radioactive isotopes of Xe and I. The UO_2 in the cylindrical target is then dissolved in a mixture of 0.83M HNO_3 and 1.86M H_2SO_4 pumped through a feed line. The ^{99}Mo is recovered from the dissolved liquid through a chemical separation process. The material balance for the dissolution procedure is shown in Table 38.

Table 38. Material Balance for Dissolution of UO_2 Reported for Cintichem Process (from Ref. 17)

	Initial Mass, g (mol)	Final Mass, g (mol)	Difference, g (mol)
^{235}U	18.5 (0.078)	-	-
U	19.9 (0.084)	-	-
HNO_3	4.536 (0.072)	0.421 (0.0067)	-4.115 (-0.065)
H_2SO_4	15.68 (0.16)	6.287 (0.064)	-9.393 (-0.096)
H_2O	77.44 (4.302)	72.04 (4.002)	-5.40 (-0.300)
UO_2SO_4		30.73 (0.084)	30.73 (0.084)
Total Liquid	97.66	109.4	11.7
Volume, mL	86	87	1
Density, g/mL	1.135	1.135	-
Head Space Volume, mL	145.33	144.26	-1.07
Temperature, $^{\circ}\text{C}$	20	94	74
Pressure, ^a atm	2.36	9.50	7.14

^aPressurized initially with helium gas.

The products of chemical reactions that accompany the dissolution of the UO_2 in acid have not been characterized. The following reaction is likely to occur:

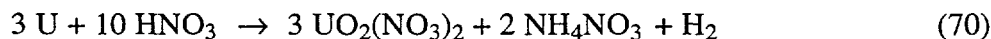
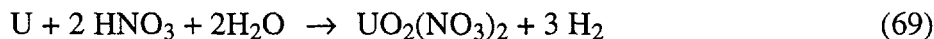


The UO_2^{2+} thus formed will produce complexes with nitrate and sulfate anions in the acid mixture. The solution containing uranium and the fission products, including molybdenum isotopes, is then subjected to a precipitation/chromatographic separation to isolate the molybdenum. Details of the separation procedure are given in Ref. 17. It is anticipated that the dissolved solution resulting from uranium metal foils will be processed in a similar manner as the Cintichem targets to recover the ^{99}Mo .

B. Use of Uranium Metal Foil or Uranium Silicide Fuels

It is proposed to use uranium metal foil instead of UO_2 and uranium silicide instead of U-Al alloys as target materials in the LEU fuel designs. If the use of these new materials is adopted, the dissolution of the target material and ^{99}Mo separation procedures will have to be changed.

Uranium metal can be dissolved by nitric acid alone; sulfuric acid does not readily react with it.¹⁸ The reactions are complex and several different products are possible, depending on the concentration of nitric acid.¹⁸ At low acidities, 8M or less, nitric oxide is the primary gaseous product. At higher acidities, nitrogen dioxide is the primary gaseous product. Even ammonia may be formed, but in nitric acid solutions it will be converted to the nitrate salt. Possible reactions for the dissolution of uranium in nitric acid are



It appears that the dissolution of uranium metal is likely to produce more heat and more gas release than the dissolution of UO_2 . We are in the process of verifying which of these reactions are important in the dissolution of uranium metal targets.

Uranium silicide targets can be dissolved by the action of alkaline hydrogen peroxide.¹⁹ It appears that unirradiated targets as well as targets irradiated to a very low burnup ($\ll 0.1\%$) dissolve readily in this mixture. The rates of dissolution, the products of reaction, and the heat released during the reaction have not been studied. Our immediate need is to obtain a better understanding of the dissolution reaction using unirradiated targets, and then proceed with the dissolution of a mini-plate uranium silicide target with about 40% burnup. This irradiated target, which

has been cooled for several years, contains no ^{99}Mo , but other stable molybdenum isotopes (^{95}Mo , ^{97}Mo , ^{98}Mo , and ^{100}Mo) formed from the precursor isobaric fission fragments.

A schematic of the laboratory dissolver is shown in Fig. 48. The dissolver is constructed from a 1000 mL glass round-bottom flask. Procedures to test the proposed alkaline peroxide dissolution procedure are being developed. The molybdenum isotopes will be recovered using chromatographic separation procedures¹⁹ and will be analyzed by ICP/AES to determine the efficiency of the separation procedure.

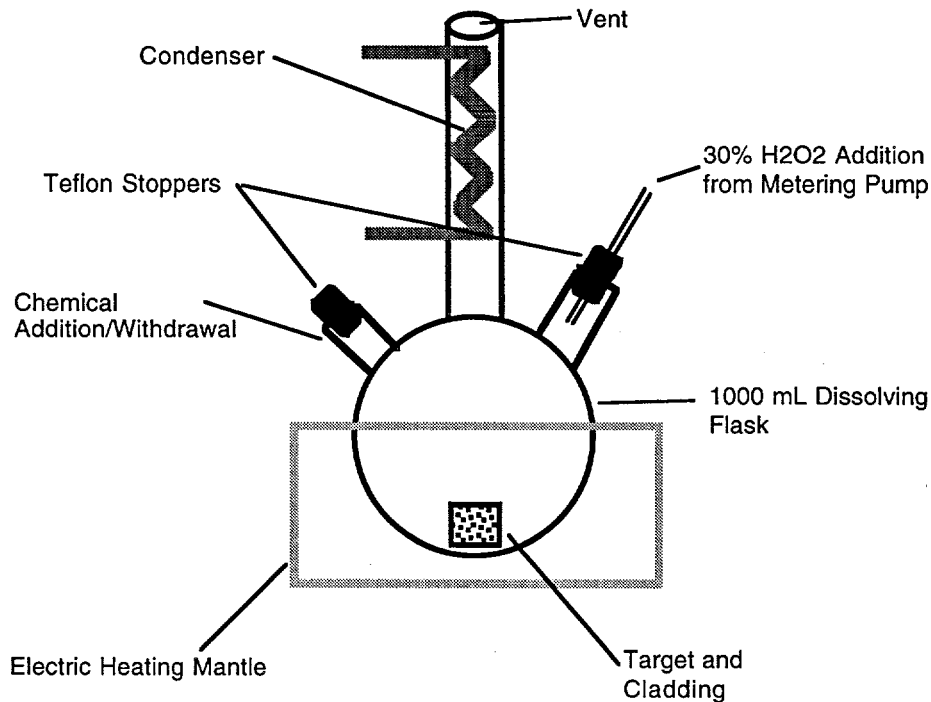


Fig. 48. Schematic Drawing of the Dissolver Flask

REFERENCES

1. B. Carnahan, H. A. Luther, and J. O. Wilkes, *Applied Numerical Methods*, John Wiley and Sons, New York (1969).
2. G. J. Lumetta and J. L. Swanson, *Pretreatment of Neutralized Cladding Removal Waste Sludge: Status Report*, Pacific Northwest Laboratory Report PNL-8558 (1993).
3. J. L. Swanson, *Initial Studies of Pretreatment Methods for Neutralized Cladding Removal Waste (NCRW) Sludge*, Pacific Northwest Laboratory Report PNL-7716 (June 1991).
4. S. Kotrly and L. Sucha, *Handbook of Chemical Equilibria in Analytical Chemistry*, John Wiley and Sons, New York (1985).
5. James A. Murphy, "Determination of the Zirconium Fluoride Stability Constants by Direct Measurement of Equilibrium Hydrofluoric Acid Using the Amperometric Response of Titanium and Hafnium Electrodes," Ph.D. Thesis, University of Idaho (April 1991).
6. W. H. Furman, Ed., *Scott's Standard Methods of Chemical Analysis*, 6th ed., Vol. 1, D. Van Nostrand Co., Princeton, NJ, p. 201 (1962).
7. R. H. Perry et al., Eds., *Perry's Chemical Engineer's Handbook*, 6th ed., McGraw-Hill, New York, pp. 5-63 to 5-66 (1984).
8. Dennis Benker and Kevin Felker, Private Communication, Oak Ridge National Laboratory (March 11, 1993).
9. C. J. Mandleberg, K. E. Francis, and R. Smith, in *Plutonium Handbook*, Vol. 1, Gordon and Breach, New York, pp. 371-372 (1967).
10. G. A. Burney and J. A. Porter, "Solubilities of Pu(III), Am(III), and Cm(III) Oxalates," *Inorg. Nucl. Chem. Lett.* 3, 79-85 (1967).
11. K. L. Nash, R. C. Gatrone, G. A. Clark, P. G. Rickert, and E. P. Horwitz, "Hydrolytic and Radiolytic Degradation of O₂D(iB)CMPO: Continuing Studies," *Sep. Sci. Technol.* 23, 1355-1372 (1988); P.-K. Tse, L. Reichley-Yinger, and G. F. Vandegrift, "TRUEX Process Solvent Cleanup with Solid Sorbents," *Sep. Sci. Technol.* 25, 1763-1775 (1990).
12. James Y. Oldshue, *Fluid Mixing Technology*, McGraw-Hill, New York (1983).
13. R. H. Perry et al., Eds., *Perry's Chemical Engineer's Handbook*, 6th ed., McGraw-Hill, New York (1984).
14. G. F. Vandegrift et al., *Separation Science and Technology, Semiannual Progress Report, October 1992-March 1993*, Argonne National Laboratory Report ANL-95/4, p. 50 (1995).

15. A. A. Sameh and H. J. Ache, "Production Techniques of Fission ^{99}Mo ," in *Fission Molybdenum for Medical Use*, International Atomic Energy Agency Report, IAEA-TECDOC-515, pp. 47-64 (1987).
16. A. Hirofumi, F. J. Cosolito, K. D. George, and A. K. Thorton, "Preparation of a Primary Target for the Production of Fission Products in a Nuclear Reactor," U. S. Patent No. 3940318 (February 24, 1976).
17. "Flowsheet for the Production of Mo-99," Merrick and Co., Los Alamos, NM, Contract No. C-LT2-N1569-1 (January 1993).
18. R. P. Larsen, "Dissolution of Uranium and its Alloys," *Anal. Chem.* 31(4), 545-549 (1959).
19. G. F. Vandegrift et al., "Preliminary Investigations for Technology Assessment of ^{99}Mo Production from LEU Targets," in *Fission Molybdenum for Medical Use*, International Atomic Energy Agency Report IAEA-TECDOC-515, pp. 99-113 (1987).

Distribution for ANL-95/43Internal:

D. B. Chamberlain	E. P. Horwitz	S. A. Slater
C. Conner	J. J. Laidler	M. J. Steindler
J. M. Copple	R. A. Leonard	G. F. Vandegrift (5)
H. Diamond	C. J. Mertz	R. D. Wolson
D. W. Green	L. Nunez	D. G. Wygmans
J. E. Harmon	J. Sedlet	TIS Files
J. E. Helt		

External:

DOE-OSTI (2)
 ANL-E Library
 ANL-W Library
 Manager, Chicago Operations Office, DOE
 J. C. Haugen, DOE-CH
 A. L. Taboas, DOE-CH
 Chemical Technology Division Review Committee Members:
 H. U. Anderson, University of Missouri-Rolla, Rolla, MO
 E. R. Beaver, Monsanto Company, St. Louis, MO
 D. L. Douglas, Consultant, Bloomington, MN
 R. K. Genung, Oak Ridge National Laboratory, Oak Ridge, TN
 J. G. Kay, Drexel University, Philadelphia, PA
 R. A. Osteryoung, North Carolina State University, Raleigh, NC
 G. R. St. Pierre, The Ohio State University, Columbus, OH
 B. A. Buchholz, Lawrence Livermore National Laboratory, Livermore, CA
 L. Chen, Naperville, IL
 M. K. Clemens, Lisle, IL
 M. Dinehart, Los Alamos National Laboratory, Los Alamos, NM
 D. Dong, Owens-Corning Science and Technology Center, Grandville, OH
 K. Foltz, University of Illinois at Urbana-Champaign, Urbana, IL
 C. W. Frank, USDOE, Office of Science and Technology, Washington, DC
 B. Gebby, Ohio State University, Columbus, OH
 L. Holton, Pacific Northwest Laboratory, Richland, WA
 J. C. Hutter, Marmora, NJ
 S. C. T. Lien, USDOE, Office of Technology Development, Germantown, MD
 G. J. Lumetta, Pacific Northwest National Laboratory, Richland, WA
 C. P. McGinnis, Oak Ridge National Laboratory, Oak Ridge, TN
 A. C. Muscatello, LATO Office, Rocky Flats Plant, Golden, CO
 A. L. Olson, Lockheed Idaho Technology Company, Idaho Falls, ID
 M. Palmer, Los Alamos National Laboratory, Los Alamos, NM

G. Pfennigworth, Martin Marietta Energy Systems, Oak Ridge, TN
M. C. Regalbuto, Amoco Oil Company, Naperville, IL
A. Rozeveld, Eaton Rapids, MI
B. Srinivasan, Woodridge, IL
I. R. Tasker, Waste Policy Institute, Gaithersburg, MD
D. W. Tedder, Georgia Institute of Technology, Atlanta, GA
M. Thompson, Westinghouse Savannah River Company, Aiken, SC
T. A. Todd, Lockheed Idaho Technology Company, Idaho Falls, ID
S. Yarbrow, Los Alamos National Laboratory, Los Alamos, NM